TAMPEREEN TEKNILLINEN YLIOPISTO
TAMPERE UNIVERSITY OF TECHNOLOGY

Bobin George Abraham

Fluorescent Protein Toolbox:
Protein Engineering Broadens the Range of *in vitro and in vivo* Applications of Fluorescent Proteins

Julkaisu 1351• Publication 1351

Tampere 2015

Tampereen teknillinen yliopisto. Julkaisu 1351
Tampere University of Technology. Publication 1351

Bobin George Abraham

Fluorescent Protein Toolbox:

Protein Engineering Broadens the Range of *in vitro* and *in vivo* Applications of Fluorescent Proteins

Thesis for the degree of Doctor of Science in Technology to be presented with due permission for public examination and criticism in Festia Building, Auditorium Pieni Sali 1, at Tampere University of Technology, on the 4th of December 2015, at 12 noon.

Tampereen teknillinen yliopisto - Tampere University of Technology
Tampere 2015

Supervisors: Professor Matti Karp
Professor Nikolai V Tkachenko

Department of Chemistry and Bioengineering
Tampere University of Technology
Tampere
Finland

Reviewers: Professor Pekka Hänninen

Laboratory of Biophysics
Department of Cell Biology and Anatomy
University of Turku
Turku
Finland

Professor Marko Virta

Department of Food and Environmental Sciences
University of Helsinki
Helsinki
Finland

Opponent: Docent Vesa Hytönen

BioMediTech
University of Tampere
Tampere
Finland

ISBN 978-952-15-3635-9 (printed)
ISBN 978-952-15-3655-7 (PDF)
ISSN 1459-2045

ABSTRACT

In the last two decades, fluorescent proteins have become one of the most widely studied and exploited protein in biochemistry and cell biology. Fluorescent protein is a protein that upon excitation at low wavelength light emits fluorescence at higher wavelength. Its ability to generate high intracellular visibility together with the stable internal fluorophore and non-invasive measurement technologies made it the finest tool to monitor cellular processes and molecular events in living cells at its normal physiological conditions. Protein engineering and identification of novel fluorescent proteins have resulted in the development of color variants ranging from the blue to near-infrared region of the spectrum. Protein engineering has also lead to the development of highly stable fluorescent proteins with improved photochemical properties and sensing abilities.

The fluorescent proteins have made a strong impact in cell biology research due to its ability to participate in energy transfer interactions, such as Fluorescence resonance energy transfer (FRET) and thus allowing to measure and study molecular-scale distances and dynamics through changes in fluorescence. Development of novel FRET based techniques, FRET sensors and FRET pairs will provide opportunity to understand the cellular processes and dynamics with high precision at nano-scale level. This thesis focusses on FRET studies by developing novel FRET based sensor, novel FRET pairs and analyzing intramolecular FRET. The study also focuses on analyzing the potential of fluorescent proteins in sensing applications outside the cell environment, an area which has not yet been exploited. This was accomplished by protein engineering of fluorescent proteins with specific objectives followed by steady-state and time-resolved fluorescence spectroscopy measurements.

In one of the specific objective, intramolecular FRET in fluorescent proteins was studied by demonstrating FRET between fluorescent protein and conjugated chemical fluorophores whereby FRET occurs from inside to outside of the protein and vice versa. For this study, novel FRET pairs MDCC−Citrine and Citrine− Alexafluor 568 was generated. FRET analyzed using steady-state and ultra-fast time-resolved spectroscopy measurements revealed strong intramolecular FRET with high efficiencies. To my knowledge, this is the first and only study on bidirectional FRET between fluorescent protein and conjugated chemical labels. This study was made possible by genetically engineering Citrine to incorporate cysteine residues on the surface of the protein and this enabled site-specific bioconjugation of the labels to the fluorescent protein.

The surface exposed cysteine on the fluorescent protein was also exploited in this study to generate self-assembled monolayer (SAM) of Citrine on the surface of etched optical fibers (EOF). The conjugation of Citrine to the surface of EOF demonstrated a proof-of-concept for the use of this bio-conjugated protein in *in vitro* bio-sensing applications. To the best of our knowledge, this is the first and only study on the formation of fluorescent protein SAM on EOF. Steady-state and fluorescence lifetime measurements confirm the formation of SAM on EOF and revealed that the bioconjugation is site-specific and covalent in nature. The study also demonstrates that the proteins retains its photochemical properties on bioconjugation and are stable at physiological conditions.

The engineered surface exposed cysteine was further used in this study for the development of a FRET based redox sensor. This was developed aiming to overcome the disadvantages of the current FRET based redox sensors which includes low FRET efficiency and dynamic range, and to monitor the redox status in bacteria. For the sensor development, fluorescent proteins Citrine and Cerulean were genetically engineered to expose reactive cysteine residues on the protein surface. The proteins were fused using a biotinylation domain as a linker to generate the FRET sensor. The redox titrations and the fluorescence measurements confirmed the redox response and reversibility of the sensor. The FRET sensor exhibited high FRET efficiency and dynamic range in intensity based measurements. Intracellular studies with *Escherichia coli* revealed the capability of the FRET sensor in detecting real-time redox variations at single cell level.

In the final study, novel FRET pairs were developed aiming at improved fluorescence lifetime dynamic range and high FRET efficiency for the use in fluorescence lifetime imaging microscopy (FLIM) studies. The fluorescent protein with the longest reported fluorescence lifetime NowGFP was used as a FRET donor and various red-fluorescent protein variants were screened for the optimal FRET acceptor. Among the FRET pairs screened, NowGFP-tdTomato and NowGFP-mRuby2 were found to be superior FRET pairs with high lifetime dynamic range and FRET efficiency. NowGFP-tdTomato pair was found to have the highest reported Förster radius and fluorescence lifetime dynamic range for any fluorescent protein based FRET pairs yet used in biological studies.

In summary, we have developed novel FRET based tools and *in vitro* techniques using fluorescent proteins which can assist in deepening the knowledge on intracellular environment and dynamics, and also in developing novel fluorescent protein based sensors which can be used outside the cellular environment.

ACKNOWLEDGEMENTS

This thesis is based on the research conducted at the Department of Chemistry and Bioengineering (KEB), Tampere University of Technology (TUT), Finland. LasKeMo (Graduate School of Computational Chemistry and Molecular Spectroscopy), TUT Graduate School, Biomedical Image Quantification/University Alliance Finland, and Academy of Finland are acknowledged for financial support.

Several people have helped me during my years at the Department of Chemistry and Bioengineering and deserve to be acknowledged. Foremost, I would like to express my sincere gratitude to my supervisor Professor Matti Karp for believing in me and sharing your unparalleled knowledge inside and outside the field of science. Thank you for being there when times are bad and for your support and motivation. I would like to extend my sincere gratitude to my second supervisor Professor Nikolai Tkachenko for introducing me to photochemistry, for your valuable suggestions and help in fluorescence measurements. Also for your generosity in giving me complete freedom to work in your lab and for the help with LasKeMo. I also thank my co-supervisor Adjunct Professor Ville Santala for the guidance and for the troubleshooter as you are never short of ideas. I am grateful to my co-authors Alexey Veselov and Karen Sarkisyan for the fruitful collaboration.

I own my gratitude to all my co-workers in lab and other personnel at the department. Special thanks to the past and present members of "Matti's group": Alessandro Ciranna, Anniina Virtanen, Suvi Santala, Nina Virolainen, Anna-Liisa Välimaa, Joanna Alanko, Katariina Tolvanen, Noora Männistö, Matti Kannisto and Tapio Lehtinen for the enjoyable lab atmosphere, advice, friendship and support. Thank you to Dr. Vladimir Chukharev for the help in spectroscopy laboratory and Asst. Prof. Meenakshisundaram Kandhavelu for the scientific discussions. I extend my thanks to all my friends in Tampere, especially Rahul Krishnan Mangayil for the years of friendship and support, Rajasekaran Andiappan for the good weekends, and Dhanesh Rajan for the friendship during my early days in Tampere.

Above all I would like to thank my parents and siblings for the unconditional love and endless support. I am grateful to my God Jesus Christ for all the blessings. Last but not least, my better half Reeja for the love and support. Thank you for being my editor, proofreader and above all my best friend. Finally to my daughter Evelyn who missed me the most and taught me that working is important but not the only thing in life.

- Bobin George Abraham

TABLE OF CONTENTS

LIST OF PUBLICATIONS

This thesis is based the following original publications, hereafter referred by their Roman numerals in the thesis.

I. Abraham, B.G., Tkachenko, N.V., Santala, V., Lemmetyinen, H., Karp, M. (2011). Bidirectional Fluorescence Resonance Energy Transfer (FRET) in Mutated and Chemically Modified Yellow Fluorescent Protein (YFP), *Bioconjugate chemistry*, Vol. 22(2), pp. 227-234.

II. Veselov, A.A.*, Abraham, B.G.*, Lemmetyinen, H., Karp, M., Tkachenko, N.V. (2012). Photochemical properties and sensor applications of modified yellow fluorescent protein (YFP) covalently attached to the surfaces of etched optical fibers (EOFs), *Analytical and Bioanalytical Chemistry*, Vol. 402(3), pp. 1149-1158.
*Equal contribution

III. Abraham, B.G., Santala, V., Tkachenko, N., Karp, M. (2014). Fluorescent protein-based FRET sensor for intracellular monitoring of redox status in bacteria at single cell level, *Analytical and Bioanalytical Chemistry*, Vol. 406(28), pp. 7195-7204.

IV. Abraham, B.G., Sarkisyan, K.S., Mishin A.S., Santala, V., Tkachenko, N., Karp, M. (2015). Fluorescent protein based FRET pairs with improved dynamic range for fluorescence lifetime measurements, *PLOS ONE*,10(8): e0134436.

AUTHORS CONTRIBUTION

I Bobin George Abraham wrote the paper and is the corresponding author. He planned and conducted the experimental work and interpreted the results.

II Bobin George Abraham and Alexey Vaselov contributed equally to the publication. BGA and AV planned and executed the work. The proteins were engineered and prepared by BGA and AV prepared the solid surfaces and both contributed equally in wet lab experiments, data analysis, interpretation of results and manuscript writing.

III Bobin George Abraham wrote the paper and is the corresponding author. He planned and conducted the experimental work and interpreted the results.

IV Bobin George Abraham wrote the paper and is the corresponding author. He planned and conducted the experimental work and interpreted the results.

The planning and experimental work was conducted under supervision of Prof. Matti Karp, Prof. Nikolai V Tkachenko and Adjunct Prof. Ville Santala.

ABBREVIATIONS

A.D	Anno Domini
AF468	Alexa fluor 568
BFP	Blue fluorescent protein
BiFC	Bimolecular fluorescence complementation
BRET	Bioluminescence resonance energy transfer
CFP	Cyan fluorescent protein
EOF	Etched optical fiber
FLIM	Fluorescence lifetime imaging microscopy
FLIP	Fluorescence Loss in Photobleaching
FRET	Förster resonance energy transfer or fluorescence resonance energy transfer
FRAP	Fluorescence Recovery After Photobleaching
GFP	Green fluorescent protein
HEPES	4-(2-Hydroxyethyl)piperazine-1-ethanesulfonic acid
IPTG	Isopropyl β-D-1-thiogalactopyranoside
J(λ)	Spectral overlap integral
KO	Kusabira orange
MDCC	7-Diethylamino-3-((((2-Maleimidyl)ethyl)amino)carbonyl) coumarin
ORF	Open reading frame
OD_{600}	Optical density (absorbance) at 600 nm wavelength
PBS	Phosphate-buffered saline

RFP	Red fluorescent protein
ROI	Region of interest
R_0	Förster radius
SAM	Self-assembled monolayer
TCSPC	Time correlated single photon counting
UV	Ultraviolet
YFP	Yellow fluorescent protein

This page intentionally left blank

1. INTRODUCTION

The fascination of mankind to glowing objects in nature can be traced back to the first century A.D. from the comments by roman natural philosopher Pliny the Elder in A.D.77 referring glowing jellyfish (Pulmo marinus) in the Mediterranean Sea.

"*If wood is rubbed with the pulmo marinus, it will have all the appearance of being on fire; so much so, indeed, that a walking-stick, thus treated, will light the way like a torch*." (translation of Pliny the Elder from John Bostock, 1855).

The research on florescent proteins started in 20th century with the isolation of glowing protein from jellyfish and in this 21st century, this glowing fluorescent protein is lighting the way like a torch to unravel the mysteries inside living cells and organelles.

The discovery of Green fluorescent proteins (GFP) change the way cell biologists study molecular processes. The scientists were able to fuse fluorescent proteins to different protein and enzyme targets. This enabled visualization and studies on molecular processes in living cells without perturbing its natural physiological environment. The modifications in fluorescent proteins resulted in the development of sensors to monitor cellular biochemical and physiological condition inside live cells and organelles. Mutagenesis and protein engineering of GFP and isolation of novel fluorescent proteins from different species have resulted in the development of a variety of visible fluorescent proteins with emission ranging from the blue to the red region of the spectrum. This, along with the advancement in microscopy and imaging techniques enabled multicolour imaging and Fluorescence Resonance Energy Transfer (FRET) based techniques with sub-nanometer spatial resolution.

The knowledge on molecular interactions and the precise locations of events inside living cell is crucial in understanding the molecular events. These interactions occur in a space of few nanometers. FRET with fluorescent protein provides opportunity to visualize this interaction with high precision. This made FRET a molecular scale to monitor events happening in 1-10 nm, a distance in which most cellular molecular interactions occur. Furthermore, FRET based sensors are developed with fluorescent protein to analyze biochemical molecules inside the cells and organelles. Development of novel tools for using fluorescent proteins and FRET is necessary to widen the applications of fluorescent proteins which help us to untangle the complex cellular biochemistry and interactions. The focus of this thesis is on development of novel tools using fluorescent proteins and FRET aiming to deepen the knowledge on cellular

processes. Additionally, this study also aims at the development of *in vitro* techniques to expand the applications of fluorescent protein beyond the field of cell biology.

This thesis reviews the development and applications of fluorescent protein variants with more focus on FRET based applications. The structure of this thesis is divided into 8 chapters. Chapter 2 describes the history and important timelines in the development of fluorescent proteins. Chapter 3 focuses on fluorescent protein structure and its variants. Chapter 4 describes FRET phenomenon and its fluorescent protein based applications. The hypothesis and aims of this thesis are described in Chapter 5 followed by materials and methods employed in papers **I**-**IV** in Chapter 6. Chapter 7 and 8 summarize the results and discussion from the papers with the concluding remarks.

2. FLUORESCENT PROTEINS – A BRIEF HISTORY

Although, the first mention of fluorescent protein was in A.D.77 by Pliny the Elder, the formal discovery of fluorescent protein was from jelly fish *Aequorea victoria* in 1962 by Osamu Shimomura when he observed a protein in the jelly fish extract exhibiting bright green fluorescence under ultraviolet (UV) light illumination (Shimomura et al. 1962). Later in the 1970's, Shimomura with his colleagues purified, crystalized and partially characterized the protein responsible for bright green fluorescence – 'Green Fluorescent Protein' (GFP) and demonstrated energy transfer between aequorin and GFP (Morise et al. 1974). Shimomura further continued his studies with GFP, and in 1979 he reported the structure of the GFP chromophore (Shimomura 1979).

The applications of GFP remained an enigma for biologists to almost three decades after its discovery, until the GFP gene was cloned and sequenced (Prasher et al. 1992). Its potential to be used as a molecular probe was first demonstrated by Chalfie et al., when they used GFP as a marker for gene expression (Chalfie et al. 1994). Mutagenesis of the GFP resulted in the generation of a wide variety of visible fluorescent proteins with varying spectral properties (Cubitt et al. 1995). Red fluorescent proteins were also isolated and cloned from non-bioluminescent reef corals (Matz et al. 1999), making fluorescent proteins to cover the whole range of visible spectrum from blue to red. Within few years after its cloning, GFP and its variants become one of the most studied proteins in the field of cell biology and biochemistry (Tsien 1998).

Besides mutations which affect the spectral properties, various modifications in the genetic level has resulted in improved brightness, protein folding, higher photostability and fluorescence lifetime, increased solubility, and also showed better expression at 37^{o}C in organelles (Davis & Vierstra 1998; Kremers et al. 2006; Griesbeck et al. 2001). GFP was modified to act a molecular sensors and its potential in labeling specific proteins inside live cells replaced the use of exogenous synthetic or antibody labelled fluorescent tags (Day & Davidson 2009; VanEngelenburg & Palmer 2008; Hanson et al. 2002; Hanson et al. 2004). The discovery of photosensitive and photoswitchable fluorescent proteins further increased its application in real-time monitoring of cellular events inside living cells (Ando et al. 2002). The development of photoactivatable proteins whose fluorescence can be controlled by irradiating the protein with light of a specific wavelength, intensity and duration provides new possibilities in labeling and tracking of cells, organelles and intracellular molecules. The timeline of important events in the development of green fluorescent protein is depicted in Figure 2.1. These

events together with the new tools developed using fluorescent proteins (which includes FRET and BiFC) facilitates the study of protein-protein interactions, protein localization, protein conformational changes and signaling events in the normal physiological conditions inside intact live cells. This also enabled the study of biochemical events, and physicochemical conditions inside live cells, in its natural environment.

Together with the advances in fluorescent protein research, the astonishing advances witnessed in the last decade in live-cell imaging technologies and microscopy techniques further ushered and extended the applications of fluorescent proteins in the field of cell biology and medicine. The development of super-resolution imaging techniques and the use of fluorescent proteins as probes for super-resolution imaging have driven fluorescent protein development tremendously. The super-resolution imaging enabled video-rate movies of intracellular environment with resolution of below 50 nm and efforts are underway to reach the goal of video-rate imaging of live cells with 1–5 nm resolution (Fernández-Suárez & Ting 2008). The area of fluorescent protein research continues by developing improved fluorescent protein variants and novel fluorescent protein based sensors aiming to understand and unravel the biological mysteries at molecular, cellular and organism level. The improvement in fluorescent proteins is opening up new application areas which include *in vitro* sensors, solar cells and lasers (Veselov et al. 2012; Chuang et al. 2009; Gather & Yun 2011).

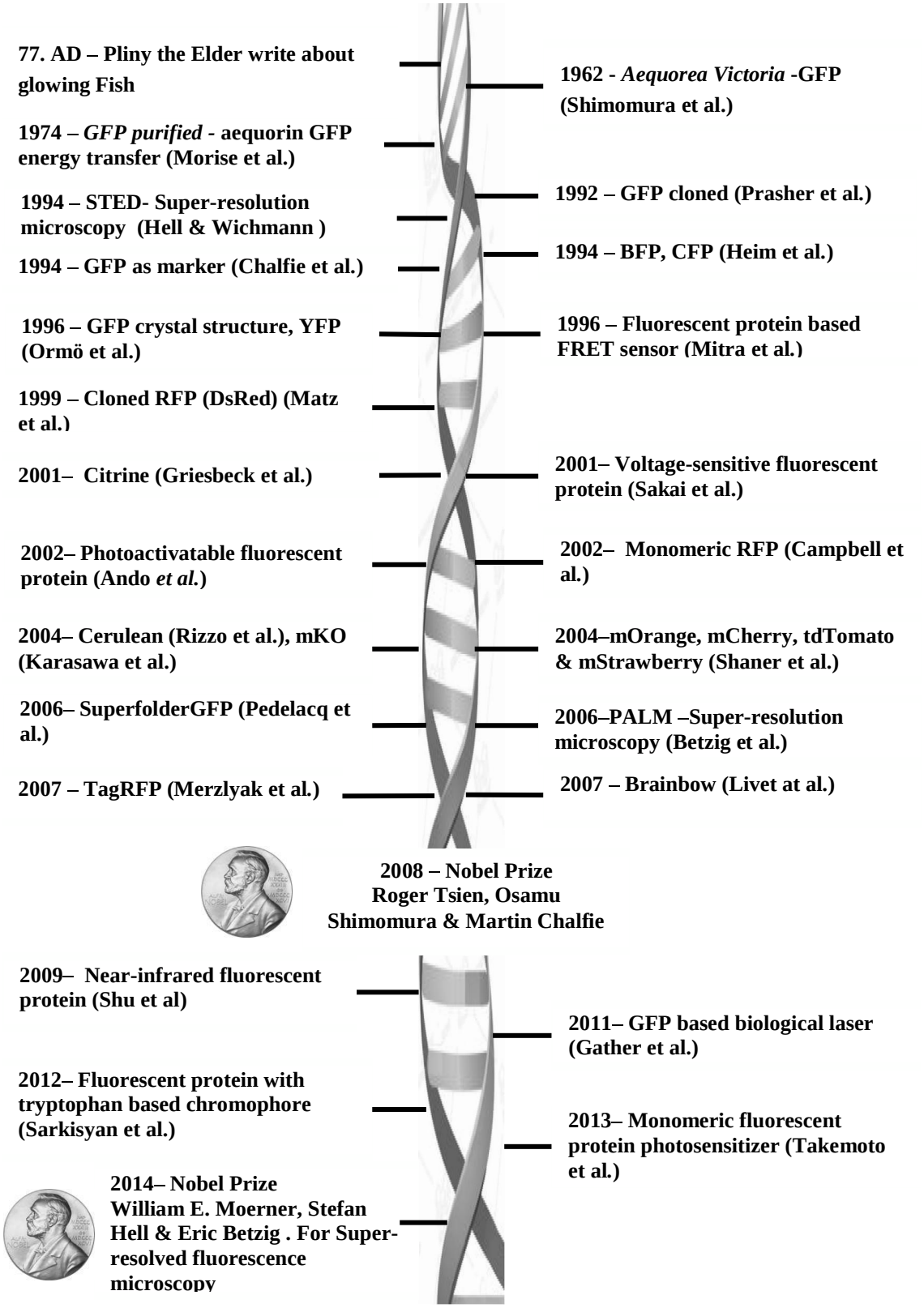

Figure 2.1 Timeline showing major achievements in the field of fluorescent protein technology.

This page intentionally left blank

3. FLUORESCENT PROTEINS

3.1. Structure and chromophore formation

The jelly fish *A. victoria* derived Green fluorescent protein from which the other fluorescent variants are developed is a 27 kDa protein (Shimomura 1979). The primary structure of GFP composed of 238 amino acid residues (Prasher et al. 1992). Though a minimum of 2-232 amino acids are essential for the development and maintenance of fluorescence, the principle fluorophore is derived from just 3 amino acids: Ser65, Tyr66, Gly67 (Dopf & Horiagon 1996). The remaining amino acids in the GFP forms a remarkably stable barrel structure which consists of 11 antiparallel β-strands from a single β-sheet folded into a cylindrical structure with an α-helix running through the central axis of the cylinder (Figure 3.1) (Ormö et al. 1996; Yang et al. 1996a). The chromophore is attached to the α-helix and it is located at the center of the cylindrical structure which is often referred to as "β-can" (Phillips Jr. 1997). Apart from the α-helix at the axis, the barrel structure with β-strands has small α-helix at the amino terminal and has a long flexible ends which enables the tagging by a fusion protein of interest at either ends. As the chromophore is located in the center of the barrel structure, it is protected from contact with solvents and outside environment by the surrounding β-

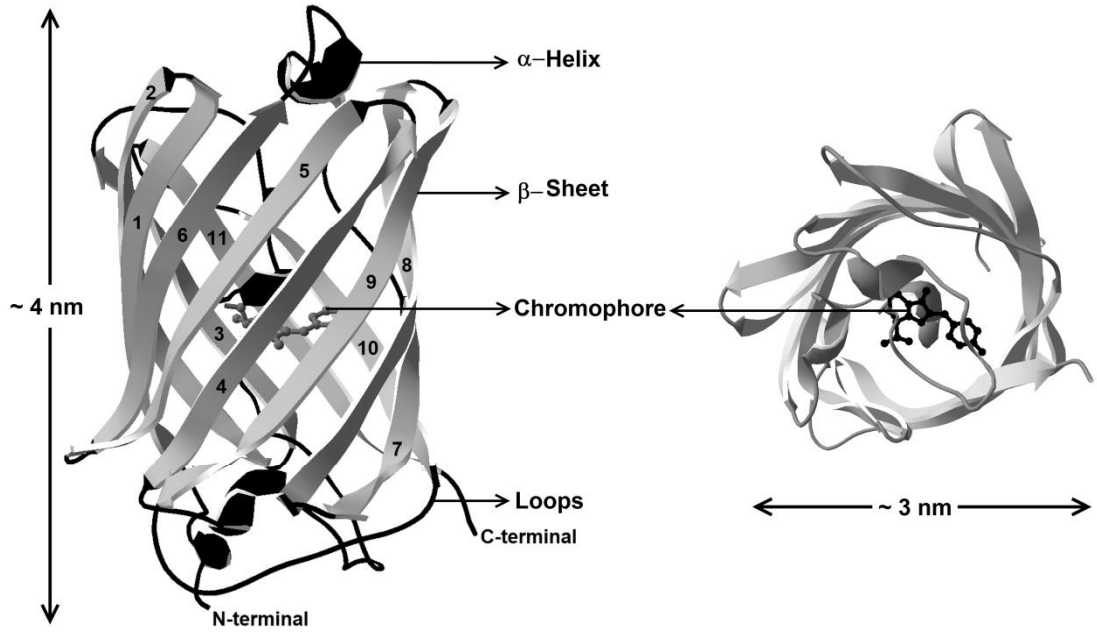

Figure 3.1 Structure of GFP showing the β-can structure. The β-sheets are marked with the strand numbers. The chromophore can be observed in the center of the can. The protein model is made using Swiss-PdbViewer from the X-ray diffraction structure of EGFP (PDB ID: 2Y0G).

sheets. Additionally, the β-barrel is stabilized by multiple non-covalent interactions which offers resistance to proteolysis and delivers high stability to thermal and chemical denaturation (Chudakov et al. 2010).

The *A. victoria* GFP structure has a tendency to oligomerize and exists in an equilibrium mixture of monomeric and dimeric state. The degree of dimerization is determined by the protein concentration, salt concentration and composition of the medium (Barbieri et al. 2001). The first X-ray diffraction structure of wild type GFP showed the dimeric nature of GFP (Yang et al. 1996a). The dimerization was a result of the hydrophobic patch from Ala206, Leu221 and Phe223 from each of the two monomers together with few hydrophilic contacts between the monomers (Yang et al. 1996a). At high salt condition, the hydrophobic associations dominate and favor dimerization (Barbieri et al. 2001). Similar to GFP, oligomerization is common for most of the GFP-like red fluorescent proteins which includes DsRed (Matz et al. 1999). Monomeric variants of fluorescent proteins can be developed by eliminating the dimerization property by point mutations (Chudakov et al. 2010; Zacharias et al. 2002; Shaner et al. 2004).

The chromophore of GFP composed of three aminoacids -Ser65, Tyr66, Gly67 (Cubitt et al. 1995; Ormö et al. 1996). While the amino acids Tyr66 and Gly67 is conserved in among all natural GFP- like proteins, the amino acid at position 65 can vary in different fluorescent proteins. The wild-type GFP which has Ser65 at the chromophore was not strongly fluorescent. The fluorescence excitation spectrum of wild-type GFP had only a minor peak at the green region and had a bigger peak below 400 nm which makes it glow better under UV light. Mutagenesis of the chromophore, especially S65T accentuated the visible peak at the green region and removed the peak at the UV region (Heim et al. 1995). This mutation also made the protein more stable and this variant of the GFP is commonly used for further improvements and other applications. Further substitution of amino acids of the chromophore or around the chromophore region could generate different color variants of the fluorescent protein (Tsien 1998).

The GFP fluorescence due to its p-hydroxybenzylideneimidazolinone chromophore formed by a unique post translational modification involving spontaneous cyclization and oxidation of three amino acids located at the center of the β-can -Ser65 (or Thr65), Tyr66, Gly67 (Cubitt et al. 1995). Figure 3.2 shows the mechanism of chromophore formation in GFP. The first step in the formation of the chromophore from the primary structure involves the folding of the amino acids by placing the carboxyl group of Tyr65 in close proximity to the amide of Gly67 (Reid & Flynn 1997). The maturation process is initiated by the cyclization. This involves the nucleophilic attack of the amino group of Gly67 on the carbonyl group of Ser65 to form a five membered ring. This is followed by dehydration to form an imidazoline-5 one intermediate (Cubitt et al. 1995). The cyclisation is assumed to be promoted by Gly67 due to the steric constrains imposed by

the β-barrel shape. Glycine is the best nucleophile in cyclization due to its minimal steric hindrance. Moreover, Gly67 is conserved in all the mutants of GFP and this supports the above argument (Tsien 1998).

The next and the final step in the chromophore maturation is the oxidation of hydroxybenzyl side chain of Try66 by molecular oxygen from the outside environment leading to the formation of the matured chromophore which is fluorescent (Cubitt et al. 1995). This oxidation process will release hydrogen peroxide molecule for each mature GFP (Zhang et al. 2006). The release of hydrogen peroxide can result in cytotoxic effect in case of GFP overexpression. Alternative pathways and time constants for chromophore maturation have also been proposed in which the maturation process follows cyclization – oxidation – dehydration process (Rosenow et al. 2004) rather than cyclization – dehydration - oxidation.

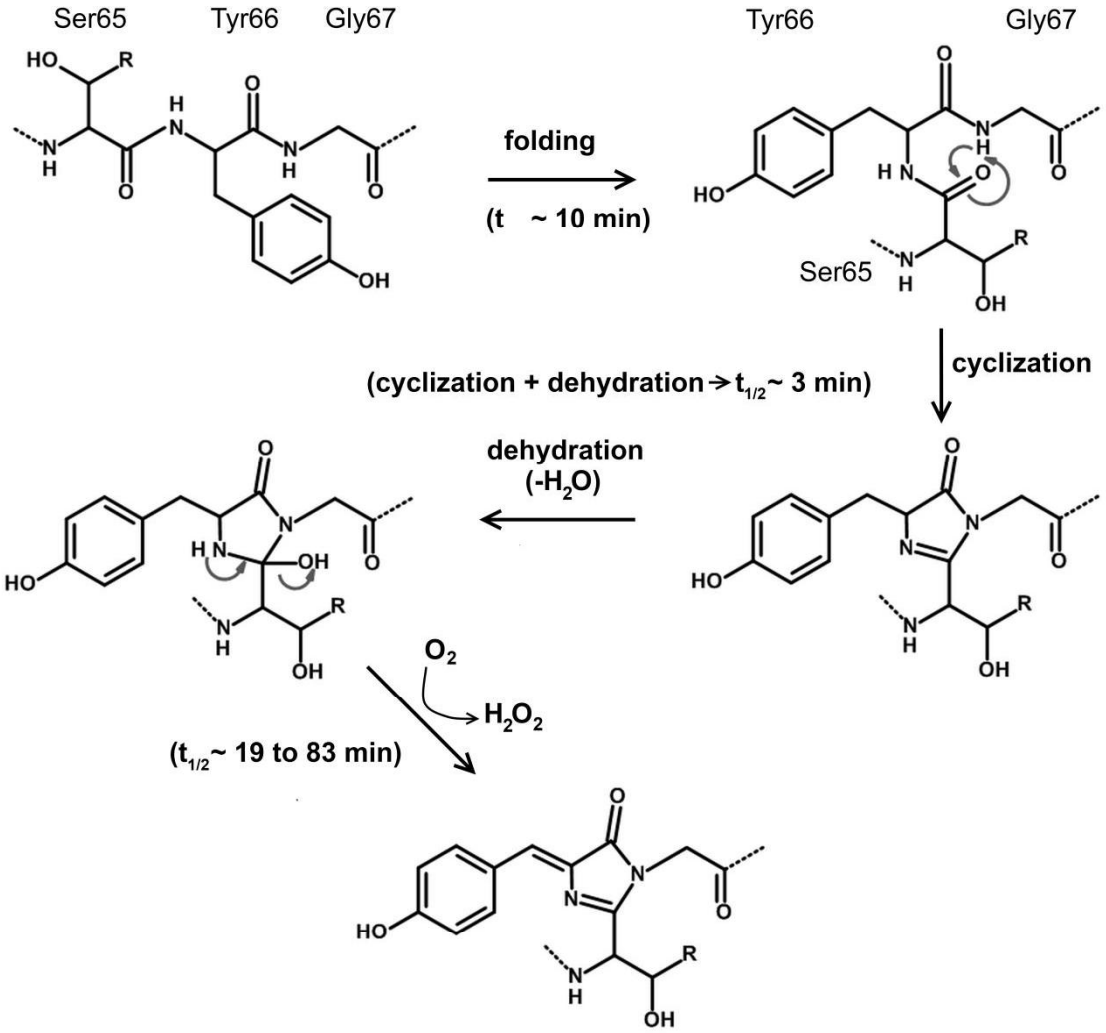

Figure 3.2 Mechanism of chromophore formation in GFP as proposed by Cubitt *et al.*, 1995. The figure is modified from (Cubitt et al. 1995; Tsien 1998). Chemical structure is drawn using Accelrys Draw 4.1.

3.2. Fluorescent protein variants

The enormous potential of GFP in cell biology research came into light when it was used as a marker for gene expression by Martin Chalfie in 1994 (Chalfie et al. 1994). Following this, protein engineering of the wild type GFP and search for novel fluorescent proteins from other organisms have resulted in the discovery and development of wide variants of fluorescent protein with different spectral and chemical properties. The mutagenesis of *Aequorea* GFP facilitated the development of fluorescent proteins in the visible region from blue to yellow. However, mutagenesis failed to create a stable and bright red version of GFP. This drives the search for novel fluorescent proteins in other organisms with fluorescence beyond yellow region of the spectrum. Search for new fluorescent proteins in other species revealed the presence of fluorescent proteins in the class Anthozoa, which can be tuned to develop wide variants of fluorescent proteins. The Anthozoa derived fluorescence proteins are improved to generate fluorescent protein ranging from blue to far red region of the spectrum. Additionally, fluorescent proteins are developed from bacterial phytochromes which have emission in the near-infrared region of the spectrum enabling fluorescent proteins to cover the whole range of visible spectrum. As the search for novel fluorescent proteins in organisms continues, the search for improving the current versions of fluorescent proteins is also underway. Aside from the various color variants, fluorescent proteins which are also photoactivable, photoconvertable, photoswitchable and fluorescent timers has also been developed (See reviews Tsien 1998; Day & Davidson 2009; Chudakov et al. 2010; Shcherbakova et al. 2012; Shaner et al. 2005). With the development of novel fluorescent proteins and imaging techniques, novel applications also arise increasing the popularity of these magnificent proteins. The fluorescent protein variants and the development of the fluorescent protein variants are discussed below. The fluorescence and structural properties of the most significant variants of fluorescent proteins are listed in Table 3.1.

3.2.1. Green variants of fluorescent protein

The wild type *A. victoria* GFP has the broad excitation peak with the excitation maximum at the ultra violet region close to 380 nm which can result in the damage of the cells and this hinders its application in live cell imaging. By mutagenesis at S65T, the excitation maximum of the protein is shifted to 488 nm and with this mutation GFP emerged as an important reporter molecule in gene expression (Cubitt et al. 1995; Heim et al. 1995; Chalfie 1995). The GFP was further improved to increase the fluorescence intensity by mutation F64L to generate GFPmut1 (Cormack et al. 1996). This version of GFP displayed greater solubility and improved protein folding in bacteria (Yang et al. 1996b). The GFPmut1 was codon optimized for enhanced expression in human cells to increase the sensitivity of the reporter protein. The codon optimization give rise to the

most popular variant of GFP, the enhanced GFP (EGFP; (Yang et al. 1996b)). EGFP was the most photostable and brightest Green fluorescent protein variant when it was developed. Moreover, the excitation spectrum of EGFP overlays with the 488 nm argon-ion laser line and can be imaged using the commonly available filter sets designed for fluorescein (Day & Davidson 2009). This made EGFP popular, and till date it is the most widely used *Aequorea* green variant for cell imaging studies. Further mutagenesis of GFP lead the development of green variants with improved brightness or folding properties and this includes T-Sapphire, Emerald and TagGFP (TagGFP was modified from GFP-like protein isolated from *Aequorea macrodactyla*) (Day & Davidson 2009; Zapata-Hommer & Griesbeck 2003; Xia et al. 2002). However, the engineered green variant which is getting more popular than EGFP recently is the "superfolder" GFP (Pedelacq et al. 2006). This monomeric version of GFP is brighter than EGFP, has improved folding kinetics, offers greater resistance to chemical denaturant and can fold even when fused to insoluble proteins (Pedelacq et al. 2006; Cava et al. 2008). This is a thermostable fluorescent protein and the only fluorescent protein known to be expressed in thermophiles (Cava et al. 2008). With fluorescence lifetime imaging getting popular, a novel mutant of GFP - WasCFP with tryptophan based chromophore was developed which has double the fluorescence lifetime of EGFP (Sarkisyan et al. 2012). The modified version of WasCFP was developed with improved stability and fluorescence property and it was named NowGFP (Sarkisyan et al unpublished). The NowGFP is used in paper **IV** of this thesis. Clover is a different bright fluorescent protein which has excitation and emission maxima of 505 and 515 nm, respectively between EGFP and EYFP. This protein was demonstrated to be a good FRET donor, which displays large FRET dynamic range when coupled to mRuby2 (red fluorescent protein) (Amy et al. 2012).

Aside from *A. victoria* GFP, many green variants of fluorescent proteins have been isolated form reef corals, sea anemones and copepods. aceGFP is one popular version developed by random mutagenesis of a colorless chromoprotein isolated from *Aequorea coerulescens* (Gurskaya et al. 2003). The aceGFP has high molar extension coefficient, quantum yield and brightness similar to EGFP and the humanized codon optimized versions are available commercially from Clontech (AcGFP1) and Evrogen (AceGFP). GFP isolated form copepod *Pontellina plumata* (Arthropoda; Crustacea; Maxillopoda; Copepoda) is resistant to pH changes and ~ 30% brighter than EGFP and is named ppluGFP2 (Commercially available from Evrogen under the names CopGFP) (Shagin et al. 2004). CopGFP is further engineered by mutagenesis to develop TurboGFP which is known to maturate faster, and hence useful in studies involving cell and organelle labeling, tracking the promoter activity, and to monitor rapid and/or transient events in gene regulation (Evdokimov et al. 2006). Search for GFP from reef corals lead to the isolation of Azami Green from stony coral, *Galaxeidae* (Karasawa et al. 2003) and ZsGreen from *Zoanthus* sp. reef coral (Matz et al. 1999). The isolated Azami Green was

tetramer, but it was modified to a monomer which is comparable to EGFP, though it has only less than 6% sequence the sequence homology to EGFP. Although, many green variants of fluorescent proteins are isolated, most of them are natively dimeric or tetramers and are not characterized in detail. This makes the *A. victoria* GFP variant still the most popular green variant choice for cell imaging applications.

3.2.2. Blue variants of fluorescent protein

Soon after the cloning of wtGFP, scientists discovered that the mutagenesis of GFP can be used to alter the spectral and fluorescence property of the fluorescent protein. The substitution of amino acid Y66H at the center of the chromophore of wtGFP resulted in the generation of the first reported blue fluorescent protein with excitation maxima at 382 nm and emission maxima at 448 nm (Heim et al. 1994). This blue variant had low quantum yield and brightness and further mutagenesis to improve the fluorescence property resulted in the enhanced variant EBFP (wtGFP with mutations F64L, S65T, Y66H and Y145F) (Yang et al. 1998). Though it was an improved version, the EBFP was not as bright as EGFP and had poor photostability. Apart from the drawback in fluorescence properties, the requirement for excitation with near-UV light, which is toxic to cells, restricts the interest in developing improved blue versions of fluorescent proteins for a long time. However, in 2006, Mena *et al.*, reported an engineered BFP variant known as 'Azurite' with enhanced quantum yield, reduced pH sensitivity and a 40-fold increase in photobleaching half-life (Mena et al. 2006). This was followed by the development of SBFP2 (strongly enhanced BFP) (Kremers et al. 2007), mKalama1 and EBFP2 (Ai et al. 2007). Among this, EBFP2 is the most photostable and the brightest BFP variant know, and the most popular blue variant of fluorescent protein.

Instead of Y66H, Y66F can also be used to generate BFP. Y66F followed by random mutagenesis of the amino acids surrounding the chromophore region resulted in the development of a variant named 'Sirius'. This variant is highly photostable and insensitive to changes in pH, but not as bright as EBFP2 (Tomosugi et al. 2009). Another promising blue variant is the TagBFP which is created by a combination of site-specific and random mutagenesis of TagRFP derived from sea anemone *Entacmaea quadricolor* (Subach et al. 2008; Merzlyak et al. 2007). TagBFP has higher molar extinction coefficient, higher quantum yield and exhibits 1.8-fold brighter fluorescence on comparison with the most popular BFP variant EBFP2 (Subach et al. 2008). Even though significant progress has been made in the recent years in generating better versions of BFP, the development of a BFP variant, with similar or improved fluorescence and physicochemical properties, comparable to EGFP still remains as a challenge.

3.2.3. Cyan variants of fluorescent protein

Mutation of *A. Victoria* GFP at Y66W resulted in the generation of the first cyan fluorescent protein variant. This cyan version was less soluble and had low yield when expressed in *E. coli* cells. Furthermore, the excitation spectrum was contaminated with autofluorescence from the intact cell making it unsuitable for cell imaging applications (Heim et al. 1994). This mutant was further engineered to develop ECFP with more refined spectrum and improved photo-stability (Cubitt et al., 1999). However, the complex fluorescence lifetime profile and the lower brightness (on comparison with EGFP, 60% less bright than EGFP) of ECFP limited its use as a probe in cell biology applications. The applications of CFP variants as a probe and as a FRET pair widened with the development of Cerulean fluorescent protein (ECFP with mutations -S72A, Y145A and H148D) (Rizzo et al. 2004). Cerulean is 2.5 times brighter than ECFP, has high quantum yield and higher extinction coefficient on comparison with ECFP. Moreover, the fluorescent lifetime of CFP is best fit by a single exponential model, made it a good choice for FRET (Rizzo et al. 2004). All these advantages made Cerulean as a popular choice of FRET donor with YFP variants (Citrine or Venus) (Day & Davidson 2009; Yano et al. 2010; Sarkar et al. 2009; Abraham et al. 2014). Cerulean is used as FRET donor in paper **III** of this thesis. Another CFP variant which known to be an excellent FRET pair with YFP variant is CyPet (Nguyen & Daugherty 2005). This monomeric version was generated by random mutagenesis of ECFP and offers improved fluorescence properties compared to ECFP, but will not outperform Cerulean. However, Cerulean is further modified recently to generate ‘mCerulean3’ which is 20% brighter than Cerulean, has high quantum yield (0.87) and longer fluorescence lifetime (4.10 ns) (Markwardt et al. 2011). This version is expected to replace Cerulean in cell imaging applications in near future.

Introduction of mutations to improve protein folding resulted in the development of an improved CFP named ‘SCFP3A’ (Kremers et al. 2006). The main mutations which plays role in improving protein folding in *Aequorea* fluorescent protein variants are S72A and A175G. The SCFP3A had higher quantum yield (0.56) and was 9 times brighter than ECFP when expressed in *E. coli*. This variant had a higher lifetime (3.2 ns) on comparison to ECFP (3.0 ns) but lower than that of Cerulean (3.3 ns). Though SCFP3A has shown to be an excellent FRET pairs with YFP variants (Kremers et al. 2006), the Cerulean fluorescent protein still remained as the most popular version of CFP before the introduction of mCerulean3 and mTurquoise. The mTurquoise is developed by introducing only a single mutation to SCFP3A. The single mutation T65S improved the brightness to 50% than its predecessor, has a quantum yield of 0.84 and exhibits monoexponential decay (Goedhart et al. 2012). The mTurquoise was further improved by a combination of site-directed mutagenesis and fluorescence lifetime-based screening to yield mTurquoise2. This brightest CFP version maturates faster, has

high photo-stability and longer mono-exponential lifetime among the CFP variants. Additionally, mTurquoise2 has the highest quantum yield (0.93) measured for a monomeric fluorescent protein making it the best CFP variant till date (Goedhart et al. 2012).

The improved version of Anthozoan species derived CFP's are also commercially available for cell imaging and FRET applications, although they are not as popular as *Aequorea* derived CFP's. The most popular among Anthozoan CFP's are AmCyan1 and MiCy. AmCyan1 (originally amFP486) is modified from protein isolated from reef coral *Anemonia majano*, exhibits similar brightness and has better resistance to photobleaching than *Aequorea* CFP (Matz et al. 1999). This protein forms tetramers, and this limitation hampers its use as in FRET sensors or as a fusion tag. MiCy is improved version of protein isolated form *Acropara* stony coral species, and has been used as a FRET pair with Oranges fluorescent protein (mKo) to monitor the activity of caspase 3 during apoptosis (Karasawa et al. 2004). MiCy is a dimeric protein and this hinders its application as a FRET pair. Monomeric version of MiCy known as mMiCy1 is commercially available from Amalgaam Co., Ltd. (Japan), but to the best of my knowledge, no application for this version is published till now.

3.2.4. Yellow variants of fluorescent protein

The mutagenesis of amino acids at the chromophore of GFP resulted only in blue shifted spectral versions, but not the red shifted variants. Structural analysis of GFP revealed that an amino acid replacement at T203 with an aromatic amino acid can result in π-stacking interactions between the chromophore and the highly polarizable phenol, leading to a shift in spectral properties towards the red region. Based on this notion, amino acid Threonine (T203) was substituted by aromatic amino acid Tyrosine (T203Y) and this resulted in the development of Yellow fluorescent protein (Wachter et al. 1998). Latter, EYFP was developed from EGFP with mutations L64F, S65G, S72A and T203Y (Llopis et al. 1998). This variant was sensitive to pH, chloride ions and had poor photo-stability on comparison with other fluorescent protein variants making it unattractive as a fusion tag or for FRET sensors. However, these disadvantages of YFP was exploited to develop biosensors for determining intracellular pH (Llopis et al. 1998) and measuring concentrations of intracellular chloride ions (For a review see (Bregestovski et al. 2009)). Efforts to reduce to environmental sensitivity of YFP led to the development of the most popular yellow variant named 'Citrine' (GFP with S65G, V68L, Q69M, S72A and T203Y) (Griesbeck et al. 2001). The mutation Q69M decreased the pH sensitivity (pK_a - 5.7) on comparison with EYFP (pK_a - 7.1) (Griesbeck et al. 2001; Llopis et al. 1998). Citrine had better resistance to chloride ions, has twice the photo-stability and offers better expression at 37 °C and in organelles (Griesbeck et al. 2001). All these advantages made Citrine one of the best yellow

fluorescent protein variant and the most popular acceptor for FRET based sensors (Griesbeck et al. 2001; Yano et al. 2010; Abraham et al. 2014; Abraham et al. 2011). The Citrine fluorescent protein is used in papers - **I**, **II** and **III** of this thesis. In another attempt to reduce the pH and chloride sensitivity of EYF, Nagai *et al.*, developed Venus yellow fluorescent variant (EYFP with F64L, M153T, V163A and S175G). The mutation F46L accelerates the maturation at 37°C, while the other mutation played role in reducing the acid and chloride sensitivity (Nagai et al. 2002). But the limited photo-stability (75% less photostable than EYFP) upsets its performance in studies which needed long-term imaging.

YPet is another yellow variant developed to be used as a FRET pair with CFP variants. YPet has lower pH sensitivity (pK_a - 5.63) and has demonstrated to be an excellent FRET pair with CyPet exhibiting 20-fold ratiometric FRET signal change (Nguyen & Daugherty 2005). Recently, YPet is also used in a BRET pair with bioluminescent protein (Nanoluc, Nluc) to develop a homogenous insulin assay (Shigeto et al. 2015).

Apart from *Aequorea* GFP modified variants of YFP, an yellow protein fluorescent protein was isolated from *Phialidium* jellyfish and was named – PhiYFP (Shagin et al. 2004). Ironically, this protein bears striking similarity in some key positions to the engineered variants of *Aequorea* GFP. This protein naturally had leucine at position 64 (F64L improved protein folding in EGFP) and tyrosine at position 203 (T203Y converted EGFP to yellow fluorescent protein). phiYFP was further modified by random mutagenesis to generate phiYFPv, which exhibits faster and complete maturation in bacteria (Pletneva et al. 2013). Another enhanced version of PhiYFP is TurboYFP, which brighter and maturates faster in mammalian cells on comparison with other PhiYFP versions (Shagin et al. 2004). All these PhiYFP versions are dimeric and this limits its application as a fusion tag. The non-*Aequorea victoria* derived monomeric version which is commercially available is the TagYFP (modified from GFP-like protein isolated from jellyfish *Aequorea macrodactyla*) (Xia et al. 2002). Though TagYFP is intended for protein labeling in protein localization and interaction studies, the presence of better monomeric version from *Aequorea victoria* derived YFP (eg: Citrine) hinders its applications.

3.2.5. Orange and Red variants of fluorescent protein

With the progression in imaging techniques, the need for red-emitting fluorescent proteins become crucial for multicolor imaging and for generating new FRET based sensors emitting at longer wavelengths. Moreover, moving to the red region of spectrum offers many advantages which include: decreased cellular autofluorescence, low light-scattering, reduce phototoxicity at longer wavelengths and allows deeper biological tissue imaging making it a good choice for visualizing fusion tags in whole-body

imaging of live animals (Shcherbakova et al. 2012; Shcherbo et al. 2009). Search for red-emitting fluorescent protein by engineering of *Aequorea*-based fluorescent proteins has not yielded promising results. The search for red fluorescent proteins from corals and other *Anthozoa* species lead to the development of the wide range of red fluorescent protein currently available. The red fluorescent proteins can be divided based on their spectral properties into orange fluorescent proteins (emission at 550-570 nm), red fluorescent proteins (emission at 570-620 nm) and far-red fluorescent proteins (emission over 620 nm) (Shcherbakova et al. 2012).

In the Orange region of spectrum, one of the first protein isolated is Kusabira orange (KO), isolated from *Fungia concinna* (mushroom coral) (Karasawa et al. 2004). Cloning of amino acid encoding KO to *E. coli* cells did not yield fluorescent protein. Therefore, it was engineered to attach 10 amino acids at the N-terminus resulting in an orange fluorescent protein. Further mutagenesis of KO resulted in the development of the monomeric version mKO, which was displayed as a good FRET acceptor with cyan and green variants (Karasawa et al. 2004; Tsutsui et al. 2008). The most promising orange fluorescent protein as a FRET acceptor comes from *Discosoma sp.*, known as mOrange (Shaner et al. 2004). mOrange is the brightest orange monomer of fluorescent protein and is employed in paper **IV** of this thesis. The main disadvantage of this protein is the low photostability, and to overcome an improved version mOrange2 is developed. The mOrange2 was 25-fold more photostable than its ancestor, but the brightness and quantum yield got reduced on comparison with mOrange (Shaner et al. 2008).

Most of the red fluorescent proteins in the emission range from 570-620 nm are modified versions of DsRed isolated form sea anemone *Discosoma striata* (Matz et al. 1999). The monomeric version from DsRed was obtained by random and directed mutagenesis totaling 33 substitutions, to generate the first monomeric red fluorescent protein variant mRFP1 (Campbell et al. 2002). mRFP1 is now obsolete with the development of a modified version ‘mCherry’ which offers superior photostability (Shaner et al. 2004). Both of these monomeric versions generated from DsRed is approximately 5 times less brighter than DsRed and this remained as a drawback for mCherry. However, another photostable DsRed variant tdTomato which is a tandem dimer (contains two copies of the gene encoded in a single ORF), is 38% brighter than DsRed and this version is used for FRET sensors and as a fusion tag (Shaner et al. 2004; van et al. 2008). The tdTomato is used in paper **IV** of this thesis. The other less popular monomeric red fluorescent variants modified from DsRed includes mStrawberry, mHoneydrew, mTangerine and mBanana (Shaner et al. 2004).

After the discovery of red fluorescent protein from *D. striata*, the search in more organisms for red variants yielded a positive result by the isolation of proteins from *Entacmaea quadricolor* (commonly called bubble-tip anemone) yielding red and far-red

variants (Shcherbo et al. 2007). The prevalent red fluorescent proteins derived from *E. quadricolor* are TagRFP, mRuby and mRuby2. The TagRFP which has emission wavelength of 584 nm is approximately 3 times brighter than DsRed derived mCherry making it the brightest monomeric red fluorescent protein when it was developed (Merzlyak et al. 2007). TagRFP has shown to be an excellent FRET pair with TagGFP (Shcherbo et al. 2009) and this red variant is used as a FRET acceptor with NowGFP in paper **IV** of this thesis. Another improved variant derived from *E. quadricolor* is the mRuby which displays emission maximum at 605 nm with a Stokes shift of 47 nm from the excitation maximum. The high Stokes shift combined with single exponential decay, good quantum yield (0.35) and high molar extinction coefficient of 112,000 M^{-1} cm^{-1} makes mRuby a superior probe in the red spectral range (Kredel et al. 2009). The mRuby was further modified to mRuby2 with improved brightness, quantum yield, maturation rate and photo-stability than its predecessor (Amy et al. 2012). This superior version is shown to be an excellent FRET acceptor with Clover fluorescent protein, with improved FRET dynamic range. mRuby2 is the brightest monomeric red fluorescent protein till date and this protein is employed in paper **IV** of this thesis.

Moving to the fluorescent protein variants in the far-red region of the spectra, one of the first variant developed is mPlum (emission maximum – 649 nm) and mRasberry (emission maximum – 625 nm) (Wang et al. 2004). These variants were developed by Wang *et al.*, using a novel technique "iterative somatic hypermutation". The mPlum was a photostable protein and it offers the possibility to monitor the emission beyond 650 nm. Above this wavelength, mammalian tissue is more transparent during imaging as high absorbance of hemoglobin is present below 650 nm which increases signal-noise ratio (Shcherbakova et al. 2012). The disadvantages of these proteins which include long maturation time and low brightness was overcome with the development of red fluorescent protein Katushka with emission maxima of 635 nm. This dimeric protein was generated by random mutagenesis of protein eqFP578 isolated from *E. quadricolor* (Shcherbo et al. 2007). The monomeric version which contains Katushka mutations, known as mKate and its successor mKate2, is the brightest monomeric protein in this spectral region (Shcherbo et al. 2009; Shcherbo et al. 2007). The further far-red shifted fluorescent protein includes mNeptune (Lin et al. 2009) and TagRFP657 (Morozova et al. 2010) which are monomeric, dimeric eqFP650 (Shcherbo et al. 2010), eqFP670 (commercially known as NirFP) (Shcherbo et al. 2010) and the tetrameric fluorescent protein E2-Crimson (Strack et al. 2009).

Furthermore, near infrared fluorescent proteins are developed from Bacterial phytochrome photoreceptors (BphPs). The BphPs exhibit multidomain architecture, consisting of PAS, GAF, PHY and effector domains. These near infrared fluorescent proteins are developed by deletion of PHY and effector domains, followed by mutagenesis to improve fluorescence properties (Shcherbakova & Verkhusha 2013).

The main near infrared proteins are iRFP713, IFP1.4, iRFP702 and iRFP720 (Shcherbakova & Verkhusha 2013; Shu et al. 2009). These proteins are used in experiments which require longer excitation wavelength. For example, in an application which needs retinal imaging, wavelength used to excite GFP will to lead to photoreceptor bleaching which diminishes photoresponsiveness in the retina. On the other hand, when iRFP or IFP1.4 is used, the excitation light (above 680 nm) will not affect the photoresponsiveness in retina (Fyk-Kolodziej et al. 2014).

Table 3.1 Properties of selected fluorescent variants showing the excitation (Ex) and emission (Em) maximum, molar extinction coefficient (ε), quantum yield (QY), relative brightness, and the quaternary structure of the proteins.

Protein	Ex/Em max (nm)	ε $M^{-1}cm^{-1}$	QY	Brightness	Quaternary structure	Reference
Blue variants of fluorescent protein						
EBFP	380/440	31500	0.20	27†	Monomer	(Yang et al. 1996b; Yang et al. 1998)
SBFP2	380/446	34000	0.47	373	Monomer	(Kremers et al. 2007)
EBFP2	383/448	32000	0.56	54†	Monomer	(Ai et al. 2007)
mKalama1	385/456	36000	0.45	47†	Monomer	(Ai et al. 2007)
Azurite	384/450	22000	0.59	38†	Monomer	(Ai et al. 2007)
mBlueberry2	402/467	51000	0.48	74†	Monomer	(Ai et al. 2007)
Sirius	355/424	15000	0.24	11†	Monomer	(Tomosugi et al. 2009)
TagBFP	402/457	52000	0.63	100	Monomer	(Subach et al. 2008)
Cyan variants of fluorescent protein						
ECFP	433/476	29000	0.37	40¶	Monomer	(Rizzo et al. 2004)
Cerulean	434/475	43000	0.62	100	Monomer	(Rizzo et al. 2004)
mCerulean3	433/475	40000	0.80	100¶	Monomer	(Markwardt et al. 2011)
mTurquoise	434/474	34000	0.84	100¶	Monomer	(Goedhart et al. 2012)
mTurquoise2	434/474	30000	0.93	110¶	Monomer	(Goedhart et al. 2012)
SCFP3A		30000	0.56	120¶	Monomer	(Kremers et al. 2006)
MiCy	472/495	27250	0.90		Dimer	(Karasawa et al. 2004)
amFP486	458/489	44000	0.24	31¶	Tetramer	(Matz et al. 1999; Day & Davidson 2009)
CyPet	435/477	35000	0.51	47¶	Monomer	(Nguyen & Daugherty 2005)
Green variants of fluorescent protein						
GFP	395/510			1‡	Dimer	(Heim et al. 1995)
GFPmut1	488/510	250000	0.70	25‡		(Cormack et al. 1996)
EGFP	488/507	56000	0.60	100	Monomer	(Yang et al. 1996b)
T-Sapphire	399/511	44000	0.60	79‡	Monomer	(Zapata-Hommer & Griesbeck 2003)
Emerald	487/509	57500	0.68	116‡	Monomer	(Day & Davidson 2009)
TagGFP	482/505	58200	0.59	104‡	Monomer	(Xia et al. 2002)
WasCFP	494/505	51000	0.85		Monomer	(Sarkisyan et al. 2012)
NowGFP	494/502	56700	0.76	130‡	Monomer	(Sarkisyan et al unpublished)
AceGFP	480/505	50000	0.55	82‡	Monomer	(Gurskaya et al. 2003)
CopGFP	482/502	70000	0.60	126‡	tetramer	(Shagin et al. 2004)
TurboGFP	482/502	70000	0.53	112‡	Dimer	(Evdokimov et al. 2006)
ZsGreen	493/505	35000	0.63	102‡	Tetramer	(Matz et al. 1999)
sfGFP	492/511	83300	0.65	160‡	Monomer	(Pedelacq et al. 2006)
Clover	500/515	111000	0.76	247‡	Monomer	(Amy et al. 2012)

Yellow variants of fluorescent protein						
EYFP	516/529	62000	0.71	100	Monomer	(Llopis et al. 1998)
Citrine	516/529	77000	0.76	115*	Monomer	(Griesbeck et al. 2001)
Venus	515/528	92200	0.57	103*	Monomer	(Nagai et al. 2002)
YPet	517/530	104000	0.77	157*	Monomer	(Nguyen & Daugherty 2005)
PhiYFPv	524/537	101305	0.59	105*	Dimer	(Pletneva et al. 2013)
TurboYFP	525/538	105000	0.53	111*	Dimer	(Shagin et al. 2004)
TagYFP	508/524	50000	0.62	62*	Monomer	(Xia et al. 2002)
Orange variants of fluorescent protein						
mKO	548/559	51600	0.60	52§	Monomer	(Karasawa et al. 2004)
mOrange	548/562	71000	0.69	83§	Monomer	(Shaner et al. 2004)
mOrange2	549/565	58000	0.60	59§	Monomer	(Shaner et al. 2008)
Red variants of fluorescent protein						
TagRFP	555/584	98000	0.41	68§	Monomer	(Shaner et al. 2008)
DsRed	558/583	75000	0.71	100§	Tetramer	(Shaner et al. 2004)
tdTomato	554/581	138000	0.69	160§	Tandem Dimer	(Shaner et al. 2004)
mRuby	558/605	112000	0.35	65§	Monomer	(Kredel et al. 2009)
mRuby2	559/600	113000	0.38	73§	Monomer	(Amy et al. 2012)
mRFP1	584/607	50000	0.25	21§	Monomer	(Shaner et al. 2004)
mCherry	587/610	72000	0.22	27§	Monomer	(Shaner et al. 2004)
Far-red variants of fluorescent protein						
mRasberry	598/625	86000	0.15	47‖	Monomer	(Wang et al. 2004)
mKate2	588/633	63000	0.40	100	Monomer	(Shcherbo et al. 2009)
E2-Crimson	611/646	126000	0.23		Tetramer	(Strack et al. 2009)
mPlum	590/649	41000	0.10	9‖	Monomer	(Wang et al. 2004)
mNeptune	600/650	67000	0.27	54‖	Monomer	(Lin et al. 2009)
TagRFP657	611/657	34000	0.10	14‖	Monomer	(Morozova et al. 2010)
Near-infrared fluorescent proteins						
iRFP702	673/702	93000	0.08	124^	Dimer	(Shcherbakova & Verkhusha 2013)
IFP1.4	684/708	102000	0.07	116^	Dimer	(Shu et al. 2009)
iRFP713	690/713	98000	0.06	100^	Dimer	(Shu et al. 2009)
iRFP720	702/720	96000	0.06	93^	Dimer	(Shcherbakova & Verkhusha 2013)

† Relative to TagBFP brightness

¶ Relative to Cerulean brightness

‡ Relative to EGFP brightness

* Relative to EYPF brightness

§ Relative to DsRed brightness

‖ Relative to mKate2 brightness

^ Relative to iRFP713 brightness

3.2.6. Other fluorescent protein variants

Derived from the coral and jellyfish proteins, there are fluorescent proteins variants that can be deliberately changed with light (other than photobleaching) and these collectively called as 'Optical highlighter' fluorescent proteins. The optical highlighters includes, *photoactivatable*, *photoswitchable* and *photoconvertable* fluorescent proteins together with *fluorescent times*. The *photoactivable* fluorescent proteins are proteins which can be activated from lower fluorescence intensity to brighter fluorescence emission upon illumination with UV or violet light. For example, the *photoactivatable* fluorescent protein named PA-mRFP1 will display a 70-fold increase in fluorescence intensity on activation with UV light (Verkhusha & Sorkin 2005). Another class of optical highlighter known as *photoconvertable* fluorescent exhibits a different photochemistry by changing its color with blue of UV light illumination. For instance, the fluorescent protein Dendra fluorescence green color, but on blue light illumination it changes its color from green to red (Gurskaya et al. 2006). These proteins have more applications than photoactivatable fluorescent proteins, as they can be tracked and imaged at its native fluorescent state making it easier to select the region of interest. A more spectacular photochemistry is displayed by fluorescent protein Dronpa, which natively emits green fluorescence and when excited with blue green light, the green fluorescence fades away similar to photobleaching and gets bleached completely. But when this bleached protein is excited with violet light, it retains back its green fluorescence to almost 100%. This process of bleaching followed by violet light excitation can be repeated for many cycles without losing this photochemical property. This category of protein variants which exhibits the phenomenon of photochromism (ability to switch between fluorescent and dark states) is referred to as *photoswitchable* fluorescent proteins. A different class of fluorescent proteins known as *fluorescent timers* changes its color with time. In an example, a monomeric mCherry derivative *fluorescent timer* changes its fluorescence from the blue to red over time (Subach et al. 2009). The change in color is due to the chromophore maturation rate. A medium fast *fluorescent timer* variant of mCherry, at 37 °C, the maxima of the blue fluorescence are observed at 1.2 h and the half-maxima of the red fluorescence is reached at 3.9 h, respectively. These timers can be used for tracking of the intracellular dynamics of proteins and promoter activity (Subach et al. 2009; Terskikh et al. 2000).

Though the category of 'Optical highlighter' has many more fluorescent protein variants and applications, they are not discussed in detail in this thesis as optical highlighters are not in the focus of this thesis. Nevertheless, when mentioning about fluorescent protein variants, one cannot ignore these variants as they are of high value fluorescent protein tool in studying cell biology.

3.3. Application of fluorescent proteins

The fluorescent protein offers many advantages over chemical fluorophores and other methods to study cellular dynamics and function. They are non-invasive biological probes which can be even targeted to organelles without perturbing the cellular environment. They offer possibility of single, dual, and multicolor fluorescence analysis to visualize and understand the biological processes in live cells that were previously invisible. These advantages lead to immense applications of fluorescent protein in the field of biological science.

With the increasing palette of fluorescent proteins and advanced imaging techniques, the applications of fluorescent proteins spread all through the biological research from its use inside living cells for single-molecule detection using super-resolution microscopy to imaging deep tissues and live whole organisms. However, this section describes briefly the basic intracellular applications of fluorescent proteins which include protein labelling, tracking and fluorescent reporters. Although, each of this application deserves a separate comprehensive review, an overview of these applications is provided in this section

3.3.1. Protein Labeling and tracking

Labeling of proteins with fluorescent protein has emerged as one of the most widely used applications of fluorescent proteins. The labeling of the protein of interest with fluorescent protein helps to visualize protein expression, localization, interactions, degradation and translocation between cell compartments. In most cases, the monomeric improved versions of fluorescent protein are used for protein labeling, and studies have shown that the labeling of proteins of interest with monomeric fluorescent protein will not affect protein localization and function (Pedelacq et al. 2006; Cava et al. 2008; Meile et al. 2006). However, there can be variation in the expression level of the protein of interest and fluorescent protein fusion, and the expression level is crucial especially in multicolor imaging of two or more protein of interest (Chudakov et al. 2010). The main factors which affect the expression level of the fusion constructs includes; mRNA stability, efficiency of transcription/translation, maturation rate and the stability of the fusion construct (Chudakov et al. 2010).

The protein labeling has enabled in studying the regulation of gene expression and promoter activity in live cells at single cell stage (Wu et al. 2011; Kandhavelu et al. 2012). The labeling of protein with fluorescent protein also enabled the study of protein dynamics in living cells with good spatial and temporal resolution. This is done by the photobleaching technique, in which a region of interest (ROI) inside the cell is photobleached with intense light irradiation, followed by monitoring the diffusion of the labeled protein into the photo bleached region. The rate of fluorescence recovery into

the ROI indicates the migration of the protein into the bleached ROI. This technique known as fluorescence recovery after photobleaching (FRAP), can be also used to monitor the cellular membrane mobility (Adkins et al. 2007; for reviews see Sprague & McNally 2005; Reits & Neefjes 2001). Another closely related technique used to study the mobility of proteins is known as Fluorescence Loss in Photobleaching (FLIP). In this technique, a laser beam is used to bleach the ROI repeatedly and the fluorescent intensity is measures outside the ROI. FLIP measures decrease in fluorescence intensity outside the ROI as a result of labelled protein migration to the bleached ROI. By this method, protein mobility, cell membrane mobility as well as protein shuttling between the cellular compartments can be studied (Wüstner et al. 2012; Ishikawa-Ankerhold et al. 2012; Köster et al. 2005).

The fluorescence microscopy is used to study the protein the protein dynamics. The main limitation of fluorescence microscopy in studying the cellular dynamics is the spatial resolution of the microscope. This was limited to ~200 nm for many years till the invention of super-resolution microscopy techniques (Fernández-Suárez & Ting 2008). The super-resolution microscopy techniques can be divided into two categories. The main technique used in the first category for cell imaging is STED (stimulated emission depletion) which involves illumination of samples with two laser beams: an excitation laser pulse which is immediately followed by a red-shifted pulse with doughnut-shaped beam called the STED beam, generating a fluorescent spot. Super-resolution is achieved by increasing the intensity of STED beam which narrows down the fluorescence spot progressively, and this can be used in cell imaging applications when combined with fluorescent proteins (Fernández-Suárez & Ting 2008; Hein et al. 2008; Hell & Wichmann 1994). For example, STED technique combined with Citrine fluorescent protein-labelled organelle, enabled imaging of the endoplasmic reticulum with sub-diffraction resolution in the interior of a cell (Hein et al. 2008). The second category of super-resolution imaging involves PALM (photoactivated localization microscopy) (Betzig et al. 2006), and STORM (stochastic optical reconstruction microscopy) (Huang et al. 2008) techniques. In this, super-resolution is achieved by sequentially switching of fluorescent molecule to ON and OFF using light of different wavelengths. This repeated switching ON and OFF defines the precise location of the fluorescent molecule at each cycle. From many cycles of this single-molecule detection, the super-resolution image will be reconstructed (Fernández-Suárez & Ting 2008; Stepanenko et al. 2011). In an example, HIV-1 Gag membrane proteins was imaged and tracked in living cells with a resolution of less than 25 nm using photoactivatable fluorescent protein and PALM technique (Manley et al. 2008).

Besides protein localization studies, other main application of protein labeling with fluorescent proteins is to study protein-protein interaction. Studying protein-protein interaction is crucial in understanding its function in living cells, and fluorescent

proteins can be employed in three different techniques to study the interaction of protein of interest. The three techniques are FCS (Fluorescence correlation spectroscopy), BiFC (Bimolecular fluorescence complementation) and FRET (Fluorescence resonance energy transfer). Figure 3.3 depicts these three techniques.

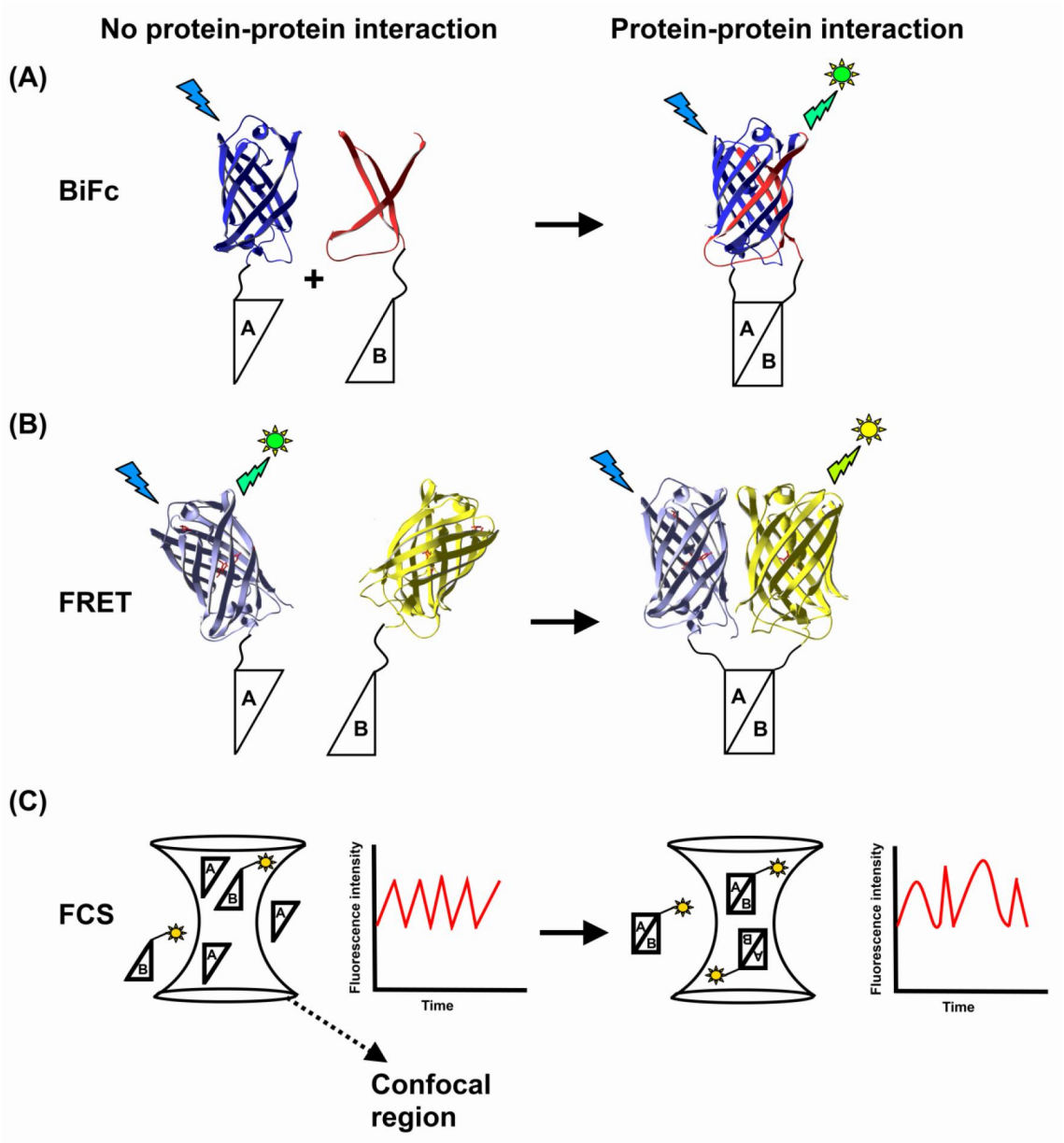

Figure 3.3. Fluorescence based techniques to study protein-protein interactions in live cells. The protein-protein interaction will result in a change of fluorescence signal which is detected to analyze the interaction. The techniques depicted here are (A) BiFc (Bimolecular fluorescence complementation), (B) FRET (Fluorescence resonance energy transfer) and (C) FCS (Fluorescence correlation spectroscopy). The change in the fluorescence property when the proteins are interacting is shown in the right side. The protein structures were drawn using PDB files (1HUY and 2Q57) and Swiss-PdbViewer.

FCS is a powerful technique based on fluorescence intensity fluctuations at single molecule level within a limited volume. The fluorescence intensity fluctuation depends on the average number of fluorescent molecule in the excitation volume and the diffusion constant of the molecules. This can be used to study rapid and reversible

interaction between proteins fused with fluorescent protein without perturbing the cellular environment (Chudakov et al. 2010; Yan & Marriott 2003). This technique has been used to study the enzyme kinetics (Kettling et al. 1998), compare mobility and molecular interactions during intracellular signaling (Kim et al. 2004), and protein dynamics (Kim & Schwille 2003). Contrary to the other techniques to study protein-protein interaction, which required the fluorescent proteins to be in close proximity and in favorable orientation, FCS is independent of both of these factors. Moreover, FCS requires only minimal protein expression which reduces the interference in normal cellular environment (Chudakov et al. 2010).

BiFC is based on the finding that two non-fluorescent protein fragments can associate to form a fluorescent molecule when they are fused to proteins that can interact with each other (Kerppola 2006). This ability of non-fluorescent fragments to form non-covalent association to turn into a complete fluorescent protein is exploited in studying the protein-protein interaction by fusing non-fluorescent fragments to two different proteins which is speculated to interact. If the protein interacts, then the non-fluorescent fragments associate to form a fluorescent molecule, and the formation of fluorescence indicates the interaction between the proteins of interest. Split versions of many fluorescent protein variants are developed for BiFC assays and this is widely used to determine the protein-protein interaction to provide insights to the cellular functions (Chu et al. 2009; Zilian & Maiss 2011; Hoff & Kück 2005). Although BiFC enables direct visualization of protein-protein interactions and requires only an inverted fluorescence microscope for the assay, it has some limitations. The probability of self-association of the split fragments without the protein-protein interaction can result in high background signal, and the long time required for fluorophore maturation are its main disadvantages (Kerppola 2006).

The most widely used technique to determine protein-protein interaction is FRET and this is described in detail in section 4 of this thesis. However, from the application of these techniques it is clear that labeling using fluorescent protein is the most superior method to determine cellular interaction and functions in real time, without perturbing the cellular environment. Apart from studying protein dynamics and intracellular tracking, labelled fluorescent proteins are also used as reporters to monitor cellular activities and intracellular physiological changes.

3.3.2. Fluorescent reporters

Fluorescent protein based reporters and biosensors allow researchers to quantify the enzymatic activity, monitor change in concentration of small molecules, study conformational state of protein of interest, and analyze the physiological factors which include redox, pH and temperature inside cellular organelles or cells or tissues or even

at whole organism level. In the whole organism level, fluorescent protein based calcium reporters are used in imaging neural activity in transgenic worms, flies and mice (Tian et al. 2009). Fluorescent proteins also provide the basis for multicolor labelling in Brainbow neuroimaging technique in which individual neurons inside the brain can be distinguished by combinatorial expression of different fluorescent protein having different spectral profiles (Livet et al. 2007; Weissman & Pan 2015). The same concept is applied in 'Zebrabow' which used multicolor fluorescent protein labeling to study the changes in zebrafish cells (Albert Pan et al. 2013). Moving the focus towards intracellular sensors using fluorescent proteins, these can be divided in the three broad classes. (a) Sensors based on Single fluorescent proteins, (b) Sensors with single fluorescent protein and a detector domain and (c) Sensors with two fluorescent proteins or FRET based sensors (Figure 3.4).

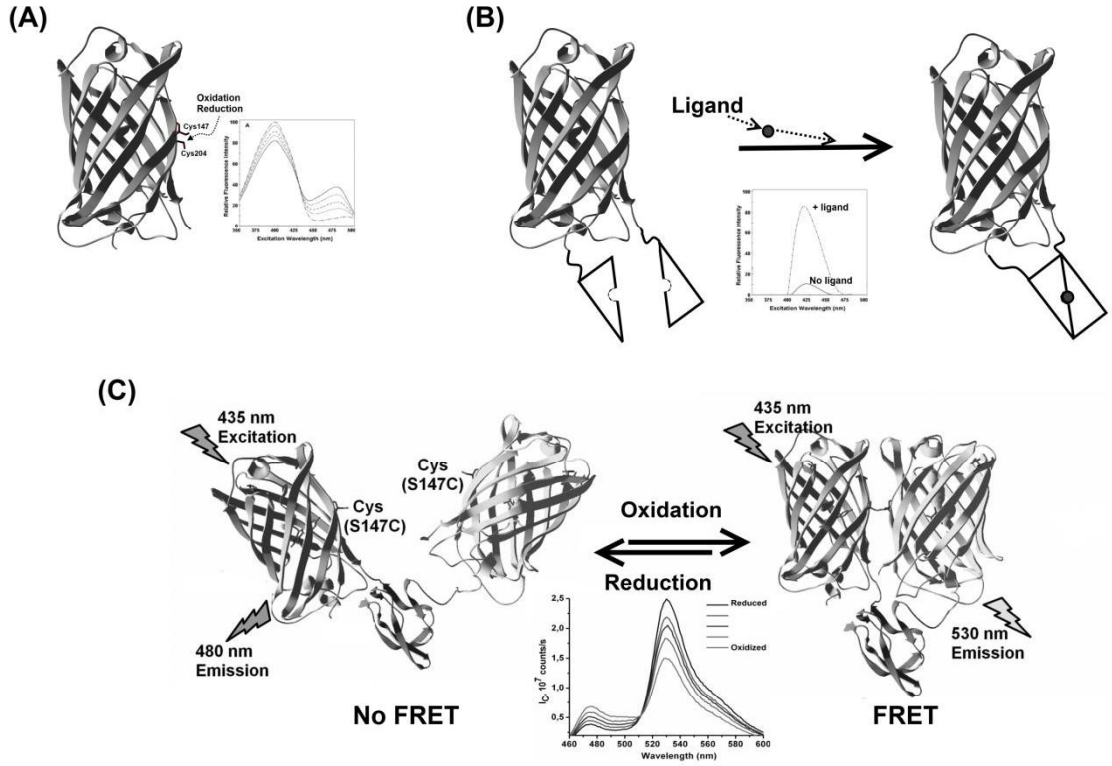

Figure 3.4 Scheme showing different types of fluorescent protein based reporters as examples. (A) Fluorescent protein based sensors based on single fluorescent protein, (B) Sensors with fluorescent protein and a sensing domain and (C) Sensors employing two fluorescent proteins. The protein structures were drawn using PDB files - 1HUY, 2Q57 and Swiss-PdbViewer.

The tightly packed β-barrel prevents GFP chromophore from interacting from the outside environment. However, mutagenesis can expose the chromophore to outside environment which typically changes protonation state or can create structural changes, when exposed to specific physicochemical conditions. The change in optical signal as a result of this provides the basis for the development of sensors with single fluorescent proteins. In these sensors, a change in physiological condition or a ligand binding

modulates the spectral property of the chromophore enabling the single fluorescent protein to perform as a sensor. The modulation of spectral property can be, the change in fluorescence brightness of the single emission peak, or ratiometric brightness change at two different wavelengths. These sensors are most useful when the sensing results in a change of spectral property which can ratioed at two wavelengths. The ratiometric measurements are not affected by change in protein concentration, optical pathlength, cell movement or excitation intensity (VanEngelenburg & Palmer 2008; Chudakov et al. 2010). Single fluorescent protein based sensors are developed for the detection of intracellular pH (Hanson et al. 2002; Kneen et al. 1998), redox (Hanson et al. 2004), Ca^{2+} (Griesbeck et al. 2001) and temperature (Wong et al. 2007). Among these, pH, Ca^{2+} and temperature sensors works on the modulation in spectral property as a result of protonation–deprotonation reaction in the chromophore (Griesbeck et al. 2001; Hanson et al. 2002; Wong et al. 2007). Conversely, the redox sensor (roGFP) generates optical signal modulation based on the change in protein structure, as a result of oxidation/reduction of the genetically incorporated cysteine residues inside the protein (Hanson et al. 2004).

The possibility for sensor design by mutagenesis of just the single fluorescent protein structure is restricted due to the limitations in obtaining different ligand binding sites in the fluorescent protein structure without perturbing the fluorescence property. This can be overcome by genetically fusing an extrinsic molecular recognition module (sensing domain) to the fluorescent protein (Figure 3.4*B*). The conformational changes occur in the sensing domain as a result of variations in specific analyte concentration, or due to ligand binding, or change in protein activity, will cause a change in the structure of the fluorescent protein altering its spectral property. The variations in spectral property were detected, and this signal modulation provides the basis of sensors with single fluorescent protein fused to a detector domain.

However, due to the stable β- barrel structure and the location of amino and carboxyl termini far from the chromophore, the spectral changes occurs as a result of the sensing activity is low when the detector domain is fused to N- and C- terminal. This can be overcome by using circularly permuted fluorescent proteins (Baird et al. 1999; Topell et al. 1999). A circularly permuted fluorescent protein is made by fusing N- and C-terminal of the traditional fluorescent protein with a flexible linker and a new N- and C-terminal is generated in a different site on the protein. This allows the fusion of detector domain close to the chromophore of the fluorescent protein, and this creates more impact on the spectral property generating large dynamic range for the sensor (Nagai et al. 2004). A wide range of sensors are developed using this technique for cellular monitoring, and this includes intracellular sensors for Ca^{2+} (Akerboom et al. 2013), H_2O_2 (Belousov et al. 2006), pH (Porcelli et al. 2005), O_2^- (Schwarzländer et al. 2011), $NADH/NAD^+$ (Hung et al. 2011), phosphorylation (Kawai et al. 2004) and membrane

potential (Knöpfel et al. 2003) (For reviews see VanEngelenburg & Palmer 2008; Chudakov et al. 2010; De Michele et al. 2014).

The narrow dynamic range, weak quantum yield of the secondary peak, limited sensitivity to measure subtle changes in cellular physiological conditions, and the limited versatility in sensor design for reporter specificities, is often considered as a disadvantage for single fluorescent protein based sensors (Yano et al. 2010). These can be overcome using FRET based sensors employing two fluorescent proteins as demonstrated by the FRET based redox sensor in paper **IV** of this thesis. The FRET phenomenon and its applications are described in the following section of this thesis.

4. FLUORESCENCE RESONANCE ENERGY TRANSFER (FRET)

Fluorescence Resonance Energy Transfer, also known as Förster Resonance Energy Transfer FRET can be defined as distance dependent nonradiative dipole-dipole coupling process in which the excited state energy from a donor fluorophore is transferred to an acceptor fluorophore. This phenomenon got popular after the discovery of fluorescent proteins as reporters. The availability of wide range of fluorophores and fluorescent proteins variants, together with the development in microscopy and imaging techniques in late 1990's, increased the popularity and applications of FRET in biological science. FRET is used to understand, visualize, track and measure physiological processes in many life-forms on earth (Sun et al. 2011b). It is widely employed in cell biology applications to study protein-protein interactions and to analyze the physiological and chemical information inside live cells and organelles.

FRET was first described by the German scientist Theodor Förster in 1948 and the phenomenon is named after him (Förster 1946) (For English translation see (Förster 2012)). Although Theodor Förster (in 1946) was first person to report the correct theoretical explanation of nonradiative energy transfer, the history of dipole-dipole model of energy transfer dates back to 1920's. In 1920's, Perrins (Father (J.) and son (F.)) explained the transfer of energy between two identical molecules in solution involving intermolecular dipole-dipole interaction. They observed that the energy transfer is distance dependent which occurs between 15∼25 nm. But T. Förster established the correct distance (1∼10 nm) for FRET to occur and this provided the basis for a quantitative means to study molecular interactions happening in 1-10 nm, much less than the theoretical resolution limits of light (∼200 nm), in light microscopy (For more historical background see Sun et al. 2011b; Clegg 2009).

Apart from the non-radiative FRET mechanism, energy transfer can also occur through radiative and non-radiative Dexter mechanism. Dexter energy transfer (Dexter 1953) also referred to as collisional or exchange energy transfer is a non-radiative process involving electron exchange and occurs at smaller distance (usually <0.5 nm) than FRET, while radiative energy transfer is phenomenon of energy transfer which involves emission and reabsorption of photons (Lakowicz 1999). However, these two processes are not described here in detail as this thesis focus only on FRET. The basic principle of FRET, methods to detect FRET and its applications in cell biology are described under this section.

4.1. FRET basics

FRET is the transfer of energy from an excited-state donor to a ground-state acceptor via long-range dipole–dipole interaction. For FRET to occur the fluorophores should satisfy three primary conditions

1. The donor and acceptor molecules should be in close proximity (optimally between ~1-10 nm) (Figure 4.1B).
2. Donor and acceptor fluorophore transition dipole orientations should be favorable for the interaction (the best is parallel) (Figure 4.1A).
3. The fluorescence emission spectrum of the donor fluorophore should overlap the absorption spectrum of the acceptor. (Figure 4.1C). (For reviews see (Clegg 2009; Hoi et al. 2013; Jares-Erijman & Jovin 2003)

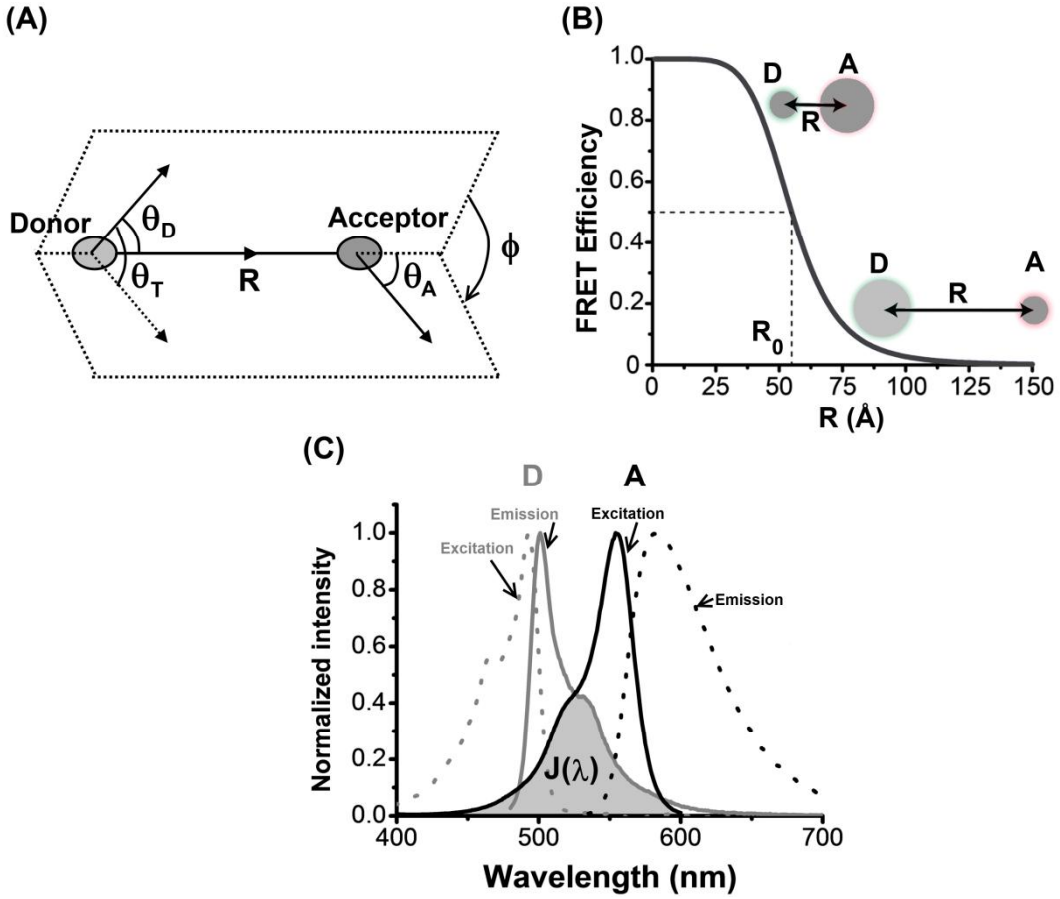

Figure 4.1 Conditions for FRET to occur (A) Donor and acceptor fluorophore transition dipole orientation. The relative angle between two transition dipoles results in the depolarization of fluorescence upon energy transfer (Modified from figure adapted with permission from copyright © of the National Academy of Sciences from (Iqbal et al. 2008) (B) FRET efficiency as function of distance 'R' between donor and acceptor fluorophore. 'D' and 'A' represents donor and acceptor, respectively (Modified from figure adapted with permission of Macmillan Publishers Ltd: [Nature Methods], © 2008, from (Roy et al. 2008)) (C) Spectral overlap between the donor emission and absorption spectrum of acceptor. J(λ) is the spectral overlap integral (The donor displayed is the fluorescence spectrum of NowGFP and the acceptor is the spectrum of TagRFP fluorescent protein).

4.2. Principle of FRET

The principle of FRET cannot be explained without describing fluorescence or luminescence, as the methods which utilizes FRET generally involves either fluorescence or luminescence process. Luminescence is the process of emission of light (photons) from a substance as a result of relaxation from its excited state to ground state. If this occurs for an electron in the excited singlet state with a spin opposite to a paired second electron in the ground state, then the return of excited state electron to ground state is spin allowed, and will occur rapidly with the emission of photons. This process of emission which occurs in the range of nanoseconds is denoted as fluorescence. Normally, the fluorescent molecule will get excited to either S1 or S2 electronic energy levels. The fluorophores can exist in a number of vibrational levels at these electronic energy levels. The molecules gets excited to the higher vibrational levels and relaxes back rapidly to the lower vibrational levels of S1 by a process known as internal conversion. The loss of energy due to internal conversion is responsible for emission to be at lower energy (red-shifted), and this is the reason behind energy difference between absorption and emission spectrum. This is referred to as Stokes' shift. But, in the presence of appropriate FRET acceptor located near the excited state donor, the energy is non-radiatively transferred to the ground state acceptor result in quenching of donor fluorescence and emission of photons from the acceptor. This is shown in Figure 4.2. (For reviews see (Ishikawa-Ankerhold et al. 2012; Dickenson & Picking 2012; Berezin & Achilefu 2010; Suhling 2014)

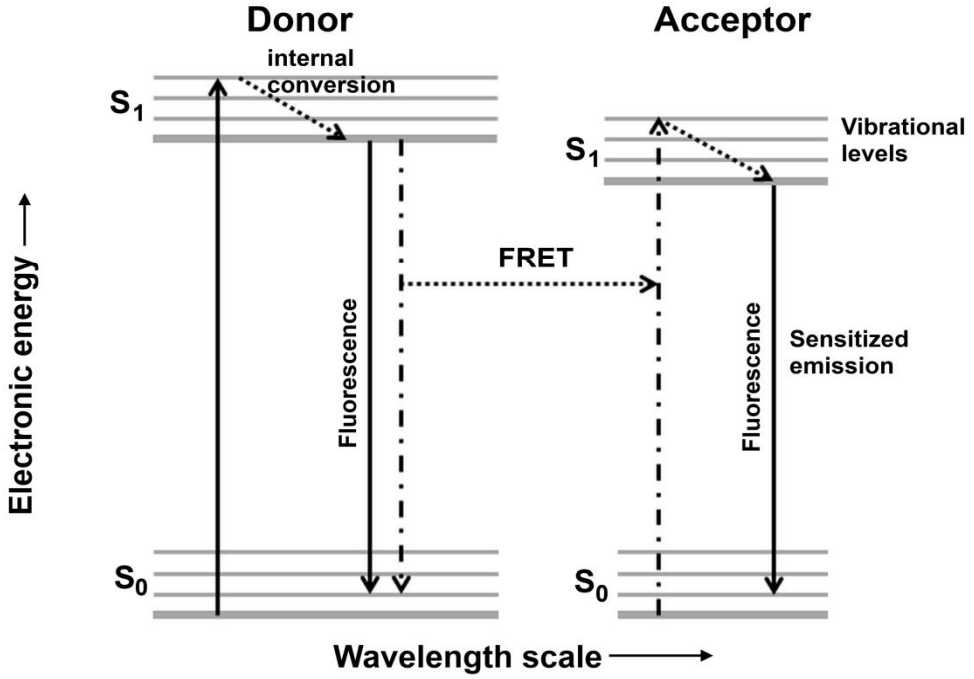

Figure 4.2 Jablonski diagram showing FRET between donor and acceptor. S_0 represents singlet ground state and S_1 represents excited singlet state. The energy transitions not directly affecting FRET such as intersystem crossing and rotational energy levels and were excluded from the figure for clarity.

The distance dependent property of FRET can be exploited in biological applications. The rate of energy transfer, FRET efficiency, Förster distance and spectral overlap integral is calculated to extract valuable information at nano-scale range from the molecules or processes in study. The rate of energy transfer (k_T) from donor to acceptor is distance dependent and it is described by:

$$k_T = \frac{1}{\tau_D}\left(\frac{R_0}{r}\right)^6 \tag{4.1}$$

where τ_D is the lifetime of donor, R_0 is the Förster distance and r is the distance between the donor and acceptor (Lakowicz 2006b). The efficiency of transfer or the FRET efficiency (E), depends on the distance separating the fluorophores (r) (Figure 4.1B) and is given by (Evers et al. 2007):

$$E = \frac{(R_0)^6}{[(R_0)^6 + (r)^6]} \tag{4.2}$$

Förster radius, R_0, is the distance at which the energy transfer efficiency is 50% between the donor and the acceptor pair. R_0 can be calculated by using the expression which is derived from Förster theory as reviewed in (Patterson et al. 2000).

$$R_0^6 = \frac{9}{4(2\Pi)_a^5} \frac{2303}{N} \kappa^2 Q_D n^{-4} J(\lambda) \tag{4.3}$$

where 2303 is In10 × 1000 cm^3L^{-1}, N is the Avogadro's number, κ^2 is the orientation factor, Q_D is the quantum yield of the donor and n is the refractive index of the medium separating the chromophores. $J(\lambda)$ represents the degree of spectral overlap between the emission spectra of the donor and the absorption spectrum of the acceptor (Figure 4.1C) and it is given by :

$$J(\lambda) = \int F_D(\lambda)\varepsilon_A(\lambda)\lambda^4 d\lambda \tag{4.4}$$

where $F_D(\lambda)$ is the emission of the donor, $\varepsilon_A(\lambda)$ is the absorption spectrum of the acceptor (with intensities plotted as molar extinction coefficients), both as a function of wavelength (λ) (Hink et al. 2003).

The orientation factor, κ^2, used in calculation R_0 depends on the angular relationship between the donor and acceptor transition dipole moments (Figure 4.1A). It can be expressed by the following equation as described in (Dale et al. 1979).

$$\kappa^2 = [\mathrm{Cos}\ \theta_T - 3\mathrm{Cos}\ \theta_D \times \mathrm{Cos}\ \theta_A]^2 \tag{4.5}$$

where θ_T is the angle between donor and acceptor dipole moments which is given by

$$\text{Cos } \theta_T = (\text{Sin } \theta_A * \text{Sin } \theta_D * \text{Cos}\varphi) + (\text{Cos } \theta_D * \text{Cos } \theta_A) \quad (4.6)$$

where θ_D and θ_A are the angles between the separation vectors, R, and D and A respectively (D is donor, A is acceptor and R is the D-A separation) φ is the azimuth between the planes (D,R) and (A,R) (Dale et al. 1979). This is shown in (Figure 4.1A). The value of κ^2 is in the range 0-4 depending on the relative orientation of the donor and acceptor. For a perfectly aligned collinear transition dipole orientation, the κ^2 is 4 and for an in-line orientation the κ^2 value is 1 (Dale et al. 1979; van der Meer et al. 2013). In biological systems, for FRET measurements with fluorescent proteins, the orientation factor κ^2, is taken as 2/3 and this corresponds to random orientation of the transition dipoles of the donor and acceptor (Tsien 1998; Vogel et al. 2014). Although, the fluorescent protein chromophore is tightly immobilized in the β barrel, the whole fluorescent protein will have a degree of rotational freedom relative to the tagged protein. Moreover, in most cases, an additional flexible amino acid linker will be added between the fluorescent proteins or tags and this provides rotational freedom. In these cases, the orientation factor is taken as 2/3 considering random orientation (Tramier et al. 2005).

Accurate determination of FRET is crucial for calculating these FRET parameters which includes FRET efficiency and energy transfer rate. The methods to determine the rate of FRET is explained in the next section.

4.3. Measurement of FRET

Each fluorescent protein based FRET pair has different photochemical properties and hence the method by which the FRET studied is crucial in obtaining accurate information. It is always recommended to compare different measurement methods and to standardize the FRET method for a specific FRET pair and experiment. The methods to determine FRET can be broadly divided into steady-state fluorescence measurements, and time resolved fluorescence measurements. The FRET determination method depends on what property of the donor or acceptor is to be monitored and also on the instrumentation available to measure FRET. Irrespective of the method used, the detection is based on either steady-state or time-resolved emission intensity based methods. For reviews see (Clegg 2009; Tramier et al. 2005; Sekar & Periasamy 2003b; Piston & Kremers 2007).

4.3.1. Steady state measurements

Intensity based measurements also known as steady-state measurements is the most popular and widely used method to determine FRET. The main reason behind this is that this method requires only conventional fluorescence microscope or fluorescence steady-state spectrofluorometer. In steady-state measurements, the sample is illuminated with a beam of light of suitable wavelength, and the emission spectrum or intensity is recorded. As a result of the nanosecond timescale of fluorescence, once the sample is excited by light, the steady-state equilibrium of excited and non-excited fluorophores is reached almost immediately and so most measurements are steady state (Lakowicz 2006a). The increased emission of acceptor (Müller et al. 2013), or the quenching of donor emission due to FRET (Marras et al. 2002), or the change in donor intensity as a result of photobleaching of acceptor (Wouters et al. 1998) is usually analyzed and this is used to calculate the FRET efficiency.

Sensitized emission or two-color ratio imaging is the measurement of change in ratio between the donor-acceptor emissions as a result of FRET and this provide the basis for many fluorescent protein based FRET sensors (Yano et al. 2010; Bregestovski et al. 2009). This is the simplest method to analyze FRET and this involves either two-channel imaging with appropriate controls or spectral imaging by measuring the emission spectrum of the donor and acceptor (Figure 4.3). The two-channel imaging involves excitation of the donor at donor specific wavelength and monitor the emission using emission filters appropriate for capturing donor fluorescence and acceptor fluorescence, separately. This is a perfect method to determine FRET, provided there were no cross-talk between excitation and emission of the donor and acceptor. However, in most cases, fluorescent protein FRET pair's exhibit cross-talk resulting in either excitation of acceptor at donor excitation wavelength, or spectral bleed-through of

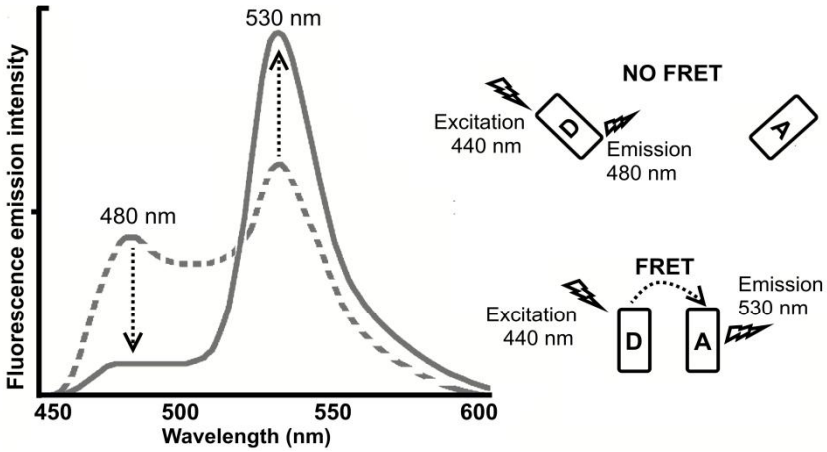

Figure 4.3 Steady state fluorescence emission spectrum (at donor excitation) showing decrease in the donor emission and increase in in acceptor emission as a result of FRET (Left). The dashed line represents emission spectrum at no FRET stage and the continuous line represents emission spectrum of the FRET pair on FRET. The arrows represent donor quenching and sensitised acceptor emission as a result of FRET. Schematic representation of donor (D) and acceptor (A) at no FRET and FRET condition (Right).

acceptor emission in donor channel and vice versa. Due to this, the method involves extensive control experiments, calibration and image processing to quantify FRET. Although, this makes the process complicated, several correction methods and processing algorithms were developed to quantify FRET from two-channel imaging (Piston & Kremers 2007; van Rheenen et al. 2004; Berney & Danuser 2003). However, in spite of the correction methods and algorithms, to retrieve accurate FRET information, the parameters have to be modified for each FRET pairs for a given experiment.

Sensitized emission is also determined by spectral measurements from the complete emission spectrum of the donor and acceptor on excitation of the donor (Figure 4.3). This approach is traditionally used for spectroscopic experiments using cuvettes. This method is often used to measure the change in acceptor emission as a result of energy transfer. The FRET efficiency is determined by comparing the emission intensity of acceptor when the donor is excited, to the acceptor intensity when the acceptor is directly excited (Graham et al. 2001; Evers et al. 2006). The FRET efficiency can also be determined by analyzing the fractional contribution (ratios of FRET complexes over total donor or total acceptor) of the FRET pairs (Wlodarczyk et al. 2008; Hoppe et al. 2002). In these methods, the presence of unpaired or self-associated donor or acceptor can pose complication in the FRET efficiency values. However, many intracellular experiments relay on merely identifying FRET or apparent FRET efficiency (which is proportional to the FRET efficiency and fraction of molecules) rather than quantification of FRET efficiencies or rate of energy transfer, and so these methods are useful in such studies.

With the increasing popularity of FRET based studies in biological systems, and the advancement in imaging techniques, wide range of instrumentation is currently

available to make spectral measurements from samples in microtitre plates or by microscopy referred to as spectral imaging. Spectrally resolved microscopy is used to obtain the whole emission spectrum of the sample from each pixel of the image (Thaler et al. 2005). In this technique, the overlapping fluorescence spectrum can be separated by not just from the peak fluorescence, but also by the shape of the spectral profile (Piston & Kremers 2007). This enables to estimate the spectral cross-talk and aids in increasing the accuracy in determining the rate of FRET. The main drawback of this method is the reduced signal-to-noise and the increased time needed to acquire image (Piston & Kremers 2007; Pelet et al. 2006). The cuvette based spectral imaging to determine FRET efficiency is employed in paper **I**, **III** and **IV**, and the two color ratio imaging is performed in paper **III** of this thesis**.**

The measurement of sensitized emission requires either equimolar concentration of donor and acceptor or information about the concentrations of the donor and acceptor. This is possible in *in vitro* measurements, and equimolar concentration of donor and acceptor can be obtained in *in vivo* measurements if the both the donor and acceptor is expressed as a fusion protein. However, this is not possible in most of the scenarios, especially when studying protein-protein interactions whereby the donor and acceptor are tagged separately to the proteins of interest. This problem is addressed by measuring the donor emission in the presence of acceptor and then removing the acceptor fluorescence by selective photobleaching of the acceptor. The absence of FRET due to acceptor photobleaching will increase the donor emission, and the change in donor emission before and after photobleaching is used to quantify FRET (Wouters et al. 1998; Van Munster et al. 2005; Kleemola et al. 2007). Photobleaching of acceptor is a widely established technique to quantify FRET and have even been used when the concentration ratios of donor and acceptor is known (donor and acceptor expressed as a fusion protein) (Gu et al. 2004).

Photobleaching will disrupt the acceptor fluorescence and therefore this method can be used only for one time measurement. Due to this limitation, the acceptor photobleaching technique cannot be used for measurements of dynamic processes and this is one major drawback for this method. Photo-switchable acceptors have been used to overcome this disadvantage and to provide possibility for repeated measurements (Giordano et al. 2002). This method requires an additional excitation wavelength for photo-activation of bleached acceptor and does not provide quantitative information on expression ratio of donor and acceptor, limiting its applications in quantitative FRET measurements.

As mentioned in this section, the intensity based FRET measurements suffers from various disadvantages. These methods are sensitive to variations in probe concentration and optical path length (Dewitt et al. 2009; McGinty et al. 2009). Intensity based methods involves complex calibration and correction procedures to compensate for

various factors which includes, auto-fluorescence, background noise, photobleaching rate, spectral bleed-through, excitation crosstalk and brightness difference between the donor and acceptor (Piston & Kremers 2007; Berney & Danuser 2003; Gordon et al. 1998). Additionally, the high intensity excitation (from laser of arc lamp) in wide-field and confocal microscopy induces cytotoxicity and result in faster photobleaching of fluorescent proteins. Most of these drawbacks can be overcome by using non-scanning approach, providing low intensity excitation light, and measuring fluorescence lifetime of the donor and acceptor rather than intensity based methods to study the intracellular processes. This can be done by using fluorescence lifetime measurements which includes Fluorescence Lifetime Imaging Microscopy (FLIM) and Time correlated single photon counting (TCSPC).

4.3.2. Fluorescence lifetime measurements

The fluorescence lifetime of a fluorophore can be defined as the time it exist in the excited state before returning to the ground state while emitting a photon. The relaxation of an excited state fluorophore can occur radiatively (emitting photons, Figure 4.2) or non-radiatively (as heat or by collisional quenching). The lifetime of the fluorophore (τ_D) is given by:

$$\tau_D = \frac{1}{(k_r + k_{nr})} \tag{4.7}$$

where k_r and k_{nr} are the rate of radiative and non-radiative decay, respectively. When the fluorophore is undergoing FRET, the rate of energy transfer (k_t) also has to be taken into account and in this case the lifetime of the donor fluorophore (τ_{DA}) will be:

$$\tau_{DA} = \frac{1}{(k_r + k_{nr} + k_t)} \tag{4.8}$$

From equations 7 and 8, it is obvious that the lifetime of donor will be shorter in the presence of a FRET pair and this change in lifetime in the presence and absence of FRET, provides the basis for fluorescence lifetime measurements in FRET. The FRET efficiency (E) is thus determined according to:

$$\mathrm{E} = 1 - \frac{\tau_{DA}}{\tau_D} \tag{4.9}$$

Once a single molecule is excited, its decay to the ground state will follow exponential law. If the same molecule is re-excited many times an exponential histogram can be obtained which represents the lifetime of the fluorophore as displayed in Figure 4.4

Depending on the properties of fluorophore, the typical decay lifetime is usually in the range of 100 ps to 100 ns. The typical decay time for fluorescent protein is below 6 ns ((Sarkisyan et al. 2012)**, Paper** IV). Apart from FRET, the fluorescence lifetime can also be affected by the change in refractive index of the medium, and collision with

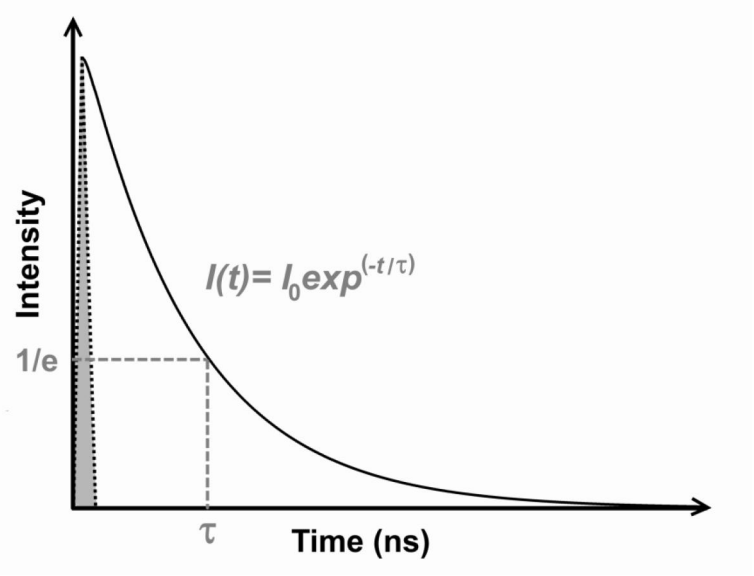

Figure 4.4 Fluorescence intensity decay (black curve) on excitation with a pulsed light (gray shaded area). The fluorescence lifetime (τ) is time at which the fluorescence intensity reaches 1/e of its initial value. This can be described by the equation which shows the time dependent intensity (I_t) for the exponential decay. I_0 represents the initial fluorescence at time t=0 and τ represents the lifetime.

other molecules (collisional quenching) (Suhling et al. 2005; Borst et al. 2005). The FRET lifetime can be measured either in Time-domain or in Frequency domain.

The time-domain method involves monitoring the fluorescence decay after excitation of sample with a pulse of light which is much shorter than the lifetime (τ) of the sample. Time-correlated single-photon counting (TCSPC) technique is commonly used to perform time-domain measurements (Lakowicz 2006c; O'Connor et al. 1979). In this technique, a short light pulse excites the sample. The time delay between the excitation pulse and the arrival of the first emitted photon is detected and stored. This process is repeated to yield a histogram of arrival times as shown in Figure 4.4. The decay histogram corresponds to the fluorophore's emission probability, which in turn is proportional to the population of the excited fluorophore after a short pulse excitation. The data obtained from the histogram is fitted using exponential fit and fluorescence lifetime value is computed as the decay constant of the fit.

To obtain accurate lifetime, careful selection of the technical parameters for the excitation pulse is crucial. The width of the excitation pulse should be made as short as possible, so that it is negligible when compared to the lifetime of the sample. To obtain single photon for a single pulsed excitation, the count rate of the measured photons should be less than 1% of the excitation pulse frequency. This reduces so-called pile-up distortion and the probability to see more than one photon after each excitation pulse will be reduced to a negligible level (Tkachenko & Lemmetyinen 2008). This will increase the time required to acquire enough photons to obtain a statistical relevant data histogram, and this is a limitation for this method. However, TCSPC is sensitive and it requires only low excitation level and this is an added advantage in live cell

measurements as it reduces photobleaching and cellular photo-toxicity, and this increased its popularity in the field. (Tramier et al. 2005; Pelet et al. 2006)

TCSPC can be combined with microscopy to yield Fluorescence lifetime imaging microscopy (FLIM), which is getting popular recently and considered as a superior method to determine FRET in cell biology. In FLIM, the TCSPC emission lifetime profile from each pixel of the sample is collected. This helps in analyzing the lifetime distribution of the sample. For example, the lifetime distribution within the living cell or cellular organelles can be analyzed. This helps in protein localization analysis, cellular dynamic studies, FRET based studies to analyze protein-protein interaction, and in FRET based intracellular sensors (Shcherbo et al. 2009; Jares-Erijman & Jovin 2003; Pepperkok et al. 1999; Duncan et al. 2004; Sun et al. 2011a).

The time-domain method also involves measuring ultrafast fluorescence measurements, in particular up-conversion technique to time-resolve reactions which takes place in sub-picosecond or even shorter time domain. This involves use of femtosecond lasers and optical methods to obtain time –resolution in femtosecond ranges with femtosecond pulse widths (Lakowicz 2006c; Tkachenko & Lemmetyinen 2008). Though this technique is used in *in vitro* experiments with fluorescent proteins ((Shi et al. 2007a; Fron et al. 2013), Paper **I**), the intracellular applications has not yet been reported, to the best of our knowledge.

Apart from the direct time-domain methods, an indirect method called frequency-domain method is also used to analyze fluorescence lifetime (Shcherbo et al. 2009; Leray et al. 2009; Veetil et al. 2012). This method is based on the mathematical fact that for any time domain function, an equivalent unique frequency domain function exists. The conversion of frequency to time domain can be done using inverse Fourier transform and vice versa using Fourier transform (Tkachenko & Lemmetyinen 2008). In the frequency domain method, the sample is excited with intensity-modulated light (sinusoidal excitation). In this case, the emissions will also respond at the same modulation frequency. The lifetime of the molecule will result in phase shift and change in amplitude. Fluorescence lifetime is obtained by analyzing this change in phase shift and amplitude attenuation of the emission relative to the excitation source (Lakowicz 2006c; Sun et al. 2011a).

The time-domain fluorescence lifetime measurement was used in this thesis to analyze fluorescence lifetime of the fluorescent proteins and chemical labels. The TCSPC technique is used in paper **I**, **III** and **IV**, FLIM in paper **II**, **III** and **IV** and up-conversion technique in paper **I**. The frequency-domain method was not employed in this study.

4.4. Applications of FRET with fluorescent proteins

The first applications of fluorescent proteins, which include reporters and sensors, were proposed right after its cloning and were based on single fluorescent proteins (See section 2.3). Most of these sensors relay on change in fluorescence intensity, which makes them less attractive as the fluctuation in the fluorescent protein concentration can be mistaken as actual signals. To overcome this disadvantage, sensors were developed which had ratiometric response (Hanson et al. 2002; 2004). However, only few single fluorescent proteins based ratiometric sensors have been developed so far. This is due to the limitation on the versatility of sensor design using single fluorescent proteins. In the sensor with only one fluorescent protein, a sensing event should modulate the chromophore for obtaining ratiometric response and this poses serious protein engineering challenges.

The limited versatility of the single fluorescent protein based sensors can be overcome by using two fluorescent proteins and FRET technique. This provides immense options to design sensing domain in various combinations and locations to generate ratiometric sensor response due to the change in FRET (Figure 4.5)

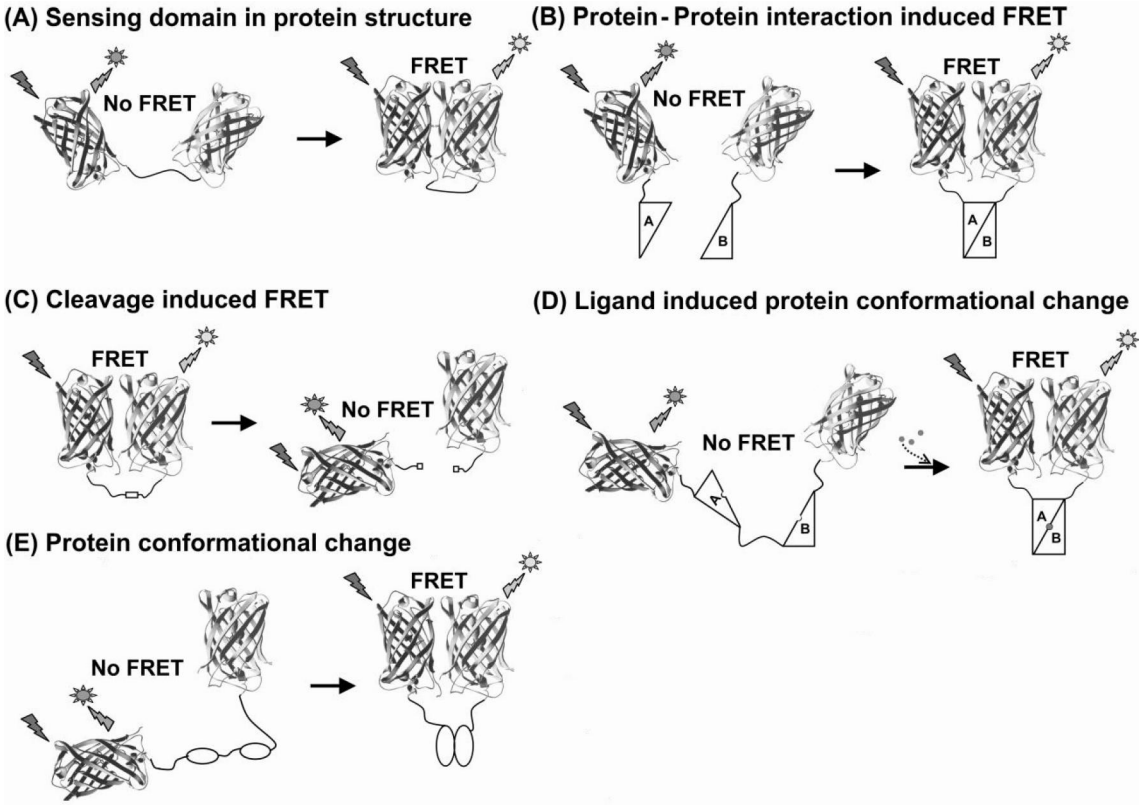

Figure 4.5 General design strategies of FRET based fluorescent protein based probes. (*A*) The sensing domain is present in the fluorescent protein and the protein will come together on response to sensing event as demonstrated in paper **III**. (*B*) Protein-protein interaction brings FRET pairs together. (*C*) Acceptor dequenching as a result of disruption of FRET as shown in paper **IV**. (*D*) Binding of a ligand/substrate changes protein structure and changes distance between FRET pairs resulting in FRET variations. (*E*) Protein conformational change brings FRET pairs in close proximity. The protein structures were drawn using PDB files (1HUY and 2Q57) and Swiss-PdbViewer.

By the ability to monitor changes in nanometer scale level, FRET has become the most popular non-invasive tool to study molecular events in live cells and organelles. The applications of FRET using fluorescent protein based FRET pairs can be divided into two broad categories: (a) FRET based sensors and (b) Protein-protein interaction analysis.

4.4.1. FRET based sensors

One of the first applications of fluorescent protein based FRET pairs was the protease sensor which consisted of BFP and GFP fused with a protease sensitive linker. On proteolysis, BFP and GFP will get separated disrupting FRET (Mitra et al. 1996). Following this, a series of FRET based protease sensors were developed aiming to study FRET, optimizing FRET pairs and monitoring apoptosis using Caspase protease activity (Caspase protease activity aberration results in numerous diseases) (Shcherbo et al. 2009; Vinkenborg et al. 2007; Detert Oude Weme et al. 2015; Ai et al. 2008; Ding et al. 2011). The development of FRET based protease sensor is followed by the development of FRET based sensors to detect Ca^{2+} signals in cytosol and organelles. This is developed by incorporating calmodulin and calmodulin-binding peptide M13 between the fluorescent protein pairs. Binding of Ca^{2+} induces calmodulin wrap around M13 bringing the fluorescent proteins in close proximity thereby increasing FRET. These fluorescent sensors were named ‘cameleons’ (Miyawaki et al. 1997).

The development of protease and Ca^{2+} provide indications on prospects of intracellular sensors using fluorescent protein based FRET pairs, and what followed is the development of a wide range of FRET based sensors for analyzing various metabolites, signaling cascades and physiological status inside live cells. Apart from Ca^{2+} FRET based sensors are developed for the detection other ions which include Zinc, chloride and phosphate ions (Genevieve Park et al. 2012; Kuner & Augustine 2000; Gu et al. 2006). FRET based sensors were also developed for the detection of various metabolites (which includes ribose, glucose, maltose and glutamate) (Lager et al. 2003; Fehr et al. 2003; Fehr et al. 2002; Okumoto et al. 2005), cyclic nucleotides (cGMP, cAMP and ATP) (Nikolaev et al. 2006; Bagorda et al. 2009; Imamura et al. 2009), membrane potential, (Knöpfel et al. 2003) redox (Yano et al. 2010), steroids (estrogen, retinoic acid and androgen) (De et al. 2005; Shimozono et al. 2013; Awais et al. 2006) and signaling cascades ((Remus et al. 2006; Cicchetti et al. 2004). The above are few examples showing the potential of FRET based sensors.

Approaches have also been made to improve the sensitivity and efficiency of the previous FRET based sensors. Replacing the sensing domain is one approach for improving sensitivity. For example, the calmodulin-binding peptide M13 in ‘cameleons’ has been replaced by another binding peptide - CaM-dependent kinase, and this

increased the dynamic range of the FRET sensor (Truong et al. 2001). The approach of replacing sensing domain is used in paper **III** of this thesis for the development of FRET based redox sensor. Optimizing the linker is another approach to improve the dynamic range of the FRET based sensor (Evers et al. 2006; Van Dongen et al. 2007; Kolossov et al. 2008). Modifying the fluorescent protein structure to alter the orientation of the fluorophores participating in energy transfer is also done to improve FRET response. The fluorescent protein structure modification is done either by site-directed amino acid changes (Evers et al. 2007; Vinkenborg et al. 2007), or by employing circularly permuted fluorescent proteins in FRET pair (Nagai et al. 2004).

Spectral modification and changing detection methods can also be used to increase the efficiency and accuracy of FRET measurements. Changing the FRET pairs from traditional CFP/YFP to GFP/RFP is advantageous as it reduces background noise and cellular photo toxicity. This has prompted in developing FRET pairs which has red shifted spectrum (Amy et al. 2012; Shcherbo et al. 2009). The earlier FRET based sensors used intensity based detection measurements which has many disadvantages as mentioned in section 3.3.1. The introduction of FLIM, improved the accuracy for FRET measurements and FRET based sensors (Oliveira & Yasuda 2013; Klarenbeek et al. 2011; Wallrabe & Periasamy 2005). The advantages of moving to the red region of the spectrum and FLIM were exploited in paper **IV** of this thesis.

4.4.2. Protein-Protein interaction

FRET has been extensively used to detect interactions between two protein partners in real time. This is done by fusing the donor and acceptor fluorescent proteins separately to each of the interacting proteins partners. The appearance of FRET indicates the protein-protein interaction. FRET dependent protein-protein interaction studies helped to reveal and visualize interactions related to transcription (Llopis et al. 2000), nucleocytoplasmic transport (Damelin & Silver 2000), G-protein signaling (Janetopoulos et al. 2001) and cell adhesion (Del Pozo et al. 2002), to name a few. FRET with fluorescent proteins offers the possibility to study receptor-ligand interaction (Krasel et al. 2004), protein dimerization/oligomerization as well as transport of proteins within organelles (Majoul et al. 2001) inside live cells. The immense protein-protein interaction application using fluorescent protein based FRET pairs is not covered in detail, as this thesis does not involve protein-protein interaction studies (For reviews see Sekar & Periasamy 2003a; Zhang et al. 2002).

One major disadvantage of using fluorescent proteins in protein interaction studies is its relatively large size which interferes with localization or the structure of the protein providing false results. This can be overcome by using smaller chemical fluorescent labels and performing protein studies in *in vitro* conditions.

4.5. FRET with chemical label pairs

In biosensors, live-cell imaging and FRET studies, apart from fluorescent proteins, chemical molecular probes and intrinsic fluorophores (which includes amino acid Tryptophan, NADH and flavins) are used as fluorescent probes. While fluorescent proteins can be cloned into the cell and fused or targeted to the molecule or organelle, non-invasively, the chemical fluorophores are conjugated to the biomolecule either *in vitro* or by passing through the membrane (membrane permeable dye). The chemical fluorophores are used widely in biology to modify biomolecules (proteins, peptides, ligands and synthetic oligonucleotides) and also serves as probes for studying protein structure, dynamics and function (Proudnikov & Mirzabekov 1996; Hägglöf et al. 2004).

The smaller sizes of the chemical label will not interfere with the structure or dynamics of the protein as opposed to the large sized fluorescent proteins and this is an advantage in using chemical labels for FRET studies involving protein dynamics. FRET using chemical labels are used to study conformational changes in cellular structures and protein dynamics (Shih et al. 2000; Schuler 2013). Its application further extends in studies involving membrane biophysics (Loura & Prieto 2011), tracking proteins and single molecules (Howarth et al. 2005), and in studying protein-protein (Jäger et al. 2005) and protein-DNA (Rizvi et al. 2010) interactions *in vivo*.

Apart from these *in vivo* applications, chemical labels as well as fluorescent proteins are used in FRET based *in vitro* assays. The availability of amine-reactive and thiol-reactive derivatives of fluorescent probes enabled site-specific bioconjugation of labels to the proteins and oligonucleotides. This enabled FRET based studies involving single molecule, protein folding, protein-protein interaction, and ligand interaction studies *in vitro* (Jäger et al. 2005; Jäger et al. 2006; Sridharan et al. 2014). Furthermore, site-specific labeling followed by FRET measurements enabled the study on intramolecular distances inside the proteins (Karolin et al. 1998). In one example, site specific labeling of protein and FRET analysis revealed a structural change of Plasminogen activator inhibitor-1 from the X-ray resolved structure indicating that the X-ray structure of proteins might differ from the actual structure in solution (Hägglöf et al. 2004). The intrinsic fluorophores present inside the protein structure also are also exploited for FRET analysis. FRET between amino acid tryptophan and chemical label BODIPY, is reported to be a versatile FRET pair for studying intraprotein distances (Olofsson et al. 2006). The chemical labels are used in paper **I** to study intramolecular FRET in fluorescent proteins.

Along with the protein structure and dynamics studies in solution, bioconjuation of fluorescent probe labelled molecules on to solid surfaces also provides a platform for development of FRET based biosensors and immunoassays, which can be employed in

real-life diagnostic and medical applications (Chang et al. 2010; Jung et al. 2010; Morgner et al. 2011; Jin & Hildebrandt 2012). Although chemicals labels were widely used for bioconjugation to solid surfaces and *in vitro* applications, the use of fluorescent protein in these applications were limited. One probable reason for this is the reduced stability of fluorescent proteins in outside environment. However, with development of improved variants of fluorescent proteins which are stable and have reduced environmental sensitivity, there is wide range of possibility to exploit its inherent ability to act as sensing component in *in vitro* biosensors. Attempts have been made in this direction by bioconjugating fluorescent proteins for bioassays to solid surfaces which includes microarray and glass slides and this has been demonstrated its potential in *in vitro* bio-sensing applications (Kwon et al. 2006; Wong et al. 2009; Lin et al. 2006). Site-specific deposition of fluorescent proteins to different solid surfaces as demonstrated in paper **II** and **III** can aid in developing novel biosensors with higher detection limit and sensitivity.

5. HYPOTHESIS AND OBJECTIVES

The general aim of this thesis was to develop novel applications of fluorescent proteins by employing protein engineering, cell biology, bioconjugation and fluorescence spectroscopy techniques.

The cell biology research is shifting towards organelle and macromolecule level studies to unravel the molecular mechanisms underlying the functions of biological molecules. To complement this, it is essential to develop improved FRET pairs and novel FRET based sensors which can enable studies with high precision at nano-scale level. Furthermore, the common applications of fluorescent proteins are focused on non-invasive live cell studies. However, there *in vitro* applications are yet to be exploited. With the availability improved variants of fluorescent protein with high stability and sensing abilities, I hypothesize that the fluorescent proteins can be used in the development of *in vitro* biosensors.

Based on these aspects and hypothesis, this thesis is focused on four specific objectives.

1. Study the intermolecular FRET in fluorescent proteins by site-specific engineering of fluorescent protein and bioconjugation of chemical fluorophores.
2. Generate self-assembled monolayers of fluorescent proteins on etched optical fiber and analyze its stability and properties aiming towards the development of fluorescent protein based *in vitro* biosensors.
3. Develop FRET based redox sensor to study changes in the redox status in living bacterial cells
4. Create novel FRET pairs to overcome the disadvantage of low FRET lifetime dynamic range in FRET based sensors used in FLIM.

This page intentionally left blank

6. SUMMARY OF MATERIALS AND METHODS

Detailed information on the materials and methods used in this study are described in papers **I – IV**

6.1. Molecular biology

The Molecular biology techniques were performed using standard procedures as described (Maniatis et al. 1989). Site-directed mutagenesis was performed by introducing the required changes in the primer sequence followed by joining the DNA fragments by overlap extension PCR technique (Ho et al. 1989) using overlapping primers. Overlap extension PCR was also used to join DNA sequences to generate fusion protein constructs. The short amino acid sequences (Serine-Glycine rich linkers and protease cleavage site in paper **IV**) were made by adding required amino acid sequence to the primers involved in PCR reactions. All the primers used in this study were ordered from ThermoFisher Scientific (USA) and the sequences with the names and details are provided in the corresponding original publications **I – IV**.

6.1.1. Plasmids and strains

The plasmid used for subcloning and protein production in paper **I, II** and **III** is a modified pAK400 vector (Krebber et al. 1997) named p1.3sTc (The plasmid described in (Santala & Lamminmäki 2004), but the biotinylation domain of *E.coli* is replaced by 1.3S transcarboxylase domain of *P. shermanii*). The fluorescent protein constructs were inserted to the *Nde*I/*Hind*III site of the plasmid so that the gene is under the control of Lac promotor. In paper **IV**, the FRET constructs were subcloned to pQE-30 (Qiagen) vector using *EcoR*I/*Hind*III site.

Escherichia coli XL1-Blue (Stratagene, USA) bacterial strain was used for cloning and protein production in papers **I**, **II** and **IV.** *E. coli* BL21 cells (Novagen, USA) were used for cloning and protein production in paper **III**. The *in vivo* redox analysis in paper **III** used *E. coli* Origami B (Genotype: F^- *ompT hsdS*$_B$(r_B^- m_B^-) *gal dcm lacY1 ahpC gor522*:: Tn*10 trxB* (Kan^R, Tet^R)) and BL21 (DE3) (Genotype: F^- *ompT hsdS*$_B$ (r_B^- m_B^-) *gal dcm* (DE3)) strains (Novagen).

The plasmid constructs were introduced to bacterial strains by electroporation. This is followed by antibiotic selection and fluorescence screening for the appropriate

transformed cells. All plasmids with the planned constructs were verified by sequencing in Macrogen Europe (Netherlands).

6.1.2. Protein production and purification

For expression and protein production, the cells were cultivated in low-salt LB medium (10 g/L tryptone, 5 g/L yeast extract, 5 g/L NaCl, pH 7.0) with appropriate antibiotics at at 37°C and 300 rpm in fermentor (1 L) (Biostat-B plus, Sartorius BBI systems, GmbH). The antibiotics used in the experiments were 25 μg/mL of chloramphenicol (for cells with p1.3sTc vector) and 50 μg/mL of ampicillin (for cells with pQE-30 vector). Isopropyl β-D-thiogalactoside (IPTG) (Fermentas, Lithuania) was used to induce protein expression when the OD_{600} reached 0.5. After addition of IPTG, the temperature reduced was to 22 °C for 4 hours, and incubated overnight at 16 °C to allow the efficient folding of proteins.

Protein purification was performed by nickel-affinity chromatography by using His-bind resin (Novagen, USA) according to the manufacturer's instructions. The purified proteins was buffer exchanged to appropriate buffers using NAP columns (Sephadex G-25, Novagen) and were stored in dark at 4 °C.

6.2. Bioconjugation and labeling

Bioconjugation of fluorescent proteins to solid surfaces or with chemical labels are performed in Paper **I, II**, and **III**.

In paper **I**, thiol reactive derivatives of 7-diethylamino-3-(((2-maleimidyl) ethyl) amino) carbonyl) coumarin (C20H21N3O5) (MDCC) and Alexa Fluor®568 maleimide ($C_{42}H_{41}N_4NaO_12S_2$) (Molecular Probes Inc., USA), were attached site specifically to the fluorescent protein suspended in PBS (pH 7.4).

Bioconjugation of the fluorescent proteins to develop self-assembled monolayers (SAM) on surface of optical fibers and glass slides were performed in a three step reaction. In the first step, the solid surface was activated by (3-Aminopropyl) trimethoxysilane (APTMS) to generate surfaces exposed amino group. The second step involves generation of sulfhydryl-reactive maleimide group on the surface by using amine-to-sulfhydryl crosslinker (Sulfo-SMCC). The last step involves site-specific conjugation of the fluorescent protein to the maleimide-activated surface using engineered surface exposed Cysteine residue on the fluorescent protein. Detailed explanation of these steps is provided in paper **II**.

Conjugation of the redox construct to the streptavidin surfaces was accomplished by a two-step process. The first step involved site-specific biotinylation of the biotinyl

domain of the fusion protein. This is done by attaching the biotin moiety enzymatically to the biotinyl domain of the protein by biotin ligase BirA (Avidity, USA) using the supplementary reagents and instructions provided by the manufacturer. The second step involved conjugation of the biotinylated protein to the microtiter plates (Kaivogen, Finland) and cover slips (Xenopore, USA), both coated with streptavidin as described in paper **III**.

6.3. Spectroscopy analysis

All the original publications in this thesis involved steady-state and time resolved measurements. The analysis method and instrumentation used in the studies is listed in table 6.1

Table 6.1 The fluorescence analysis methods and instrumentation used in this studies

Analysis	**Instrumentation**	**Paper**
Absorbance	Spectrophotometer	I-IV
	Manual setup	III
Steady state emission	Fluorolog	I-IV
	Microtitre plate reader	III
	Manual setup	II
	Epi-fluorescence microscope	IV
Time resolved measurements	TCSPC	I,IV
	FLIM	II-IV
	Fluorescence up-conversion	I

6.3.1. Steady state measurement

The absorbance measurements of fluorescent proteins were performed using UV-VIS Recording Spectrophotometer UV-2501PC (Shimadzu, Japan) and NanoDrop2000 (Thermo Fisher Scientific Inc., USA). The absorbance measurement of SAM of protein on etched optical fiber (EOF) was performed using a manual setup as shown in Figure 2a of paper **II**. The light source used was tungsten halogen lamp AvaLight-HAL (Avantes) having an output optical power of 700 μW and the light beam was delivered to the EOF with the help of a 200 μm optical fiber. The transmitted light was detected at the other end of the fiber using a 200 μm optical fiber attached to spectrometer (AvaSpec-2048, Avantes) having a spectral resolution of 2.1 nm. The absorbance *A* is determined according to the Beer-Lambert law:

$$A = -\log_{10}\left(\frac{I}{I_0}\right) \tag{7.1}$$

where I_0 is the transmitted light intensity of EOF without protein SAM, and I is the transmitted light signal with the protein SAM on EOF.

The steady-state fluorescence excitation and emission measurements were performed by Fluorometer Fluorolog-3-111 (ISA-Jobin Yvon, France). The emission spectra were corrected using the correction function supplied by the manufacturer after subtracting dark counts of the photomultiplier. Fluorescence emission measurements in microtiter plate (paper **II**) were recorded by plate reader (Chameleon, Hidex, Finland) at an excitation of 435 nm and monitoring the emission through 483/35 nm and 535/30 nm filters. The emission measurements for proteins in EOF were measured using a manual setup shown in Figure 2b of paper **II**. Laser diode LDH-P-C-485 (PicoQuant) emitting at 483 nm was used for excitation with an excitation repetition rate of 40 MHz. The emitted light was passed through a dichroic mirror, DM (NT47-267, Edmund Optics) and was focused onto the facet of 200 μm optical fiber connected to the spectrometer to monitor the emission.

6.3.2. Time-resolved measurements

Time-resolved measurements were performed primarily by using time-correlated single photon counting (TCSPC) technique. The TCSPC instrument setup composed of pulsed laser diode (LDH-P-C-405B, and LDH-P-C-485, PicoQuant Germany), cooled multichannel Photon Multiplying Tube (R3809U-50,Hamamatsu, Japan), and TCSPC module (PicoHarp 300, PicoQuant Germany), which combine constant fraction discriminators, time-to-amplitude converter (TAC), and multichannel analyzer (MCA) (PicoQuant, Germany). Based on the excitation spectrum, the excitation wavelengths used in different studies were 405 nm (Instrument response function (FWHM) = ~64 ps) and 483 nm (FWHM= ~100 ps). Emission cutoff filters were used prevent the excitation source to reach the photomultiplier tube. Fluorescence decays were collected until 10,000 counts accumulated at maximum.

Fluorescence Lifetime Imaging Microscope (FLIM) MicroTime 200 (PicoQuant) was used for imaging *E.coli* cells. The cells were placed on a microscope coverslip coated with 2 % agarose gel in either LB medium or buffer. A second coverslip was placed after the addition of cells for fixing the cells and obtaining uniform surface. The TCSPC lasers were used for excitation, and emission was selectively monitored by using narrow bandpass detection filters appropriate for the particular emission wavelengths. For bacterial cells, 100 × (1.49NA, oil) objective was used and intensity and lifetime images were acquired with scan steps of 0.1 μm and the total scan area of 20 × 20 μm^2. For SAM measurements in glass slide and optical fiber, 40× (NA 0.65, air) objective enabled imaging with the minimum spatial resolution of 0.5 μm and total scan area of 80 × 80 μm^2.

6.4. Data analysis

For FRET analysis, from steady state measurement data, the Förster radius, and spectral overlap integral was calculated according to eq. 4.3 and 4.4 (Chapter 4), respectively. The FRET efficiency from the steady state measurements were calculated by $(ratio)_A$ method. This method takes account of the ratio of change in acceptor fluorescence at donor excitation to the acceptor fluorescence on direct acceptor excitation. (Kolossov et al. 2008; Clegg 1992). The fluorescence spectrum was used to calculated the $(ratio)_A$ according eq. 7.2 (Kolossov et al. 2008) .

$$(ratio)_A = \frac{[F_{DA}(\lambda^D_{exc}) - F_D(\lambda^D_{exc})]}{F_A(\lambda^A_{exc})} \tag{7.2}$$

where $F_{DA}(\lambda^D_{exc})$ is the emission intensity of the donor and acceptor molecules during donor excitation, $F_D(\lambda^D_{exc})$ is the emission intensity of donor alone at donor excitation and $F_A(\lambda^A_{exc})$ is the emission intensity of acceptor on direct acceptor excitation. From $(ratio)_A$ value, the FRET efficiency (E) is obtained by eq. 7.3 (Kolossov et al. 2008).

$$E = \frac{\varepsilon_A(\lambda^A_{exc})}{\varepsilon_D(\lambda^D_{exc})}\left[(ratio)_A - \frac{\varepsilon_A(\lambda^D_{exc})}{\varepsilon_A(\lambda^A_{exc})}\right] \tag{7.3}$$

where $\varepsilon_D(\lambda^D_{exc})$ is the extinction coefficient of donor at donor excitation wavelength and $\varepsilon_A(\lambda^A_{exc})$ and $\varepsilon_A(\lambda^D_{exc})$ are the extinction coefficients of acceptor at acceptor and donor excitation wavelengths respectively.

In time-resolved measurements, emission decay curves were fitted to obtain the life times. This was done using deconvolution with the instrument response function and applying exponential and bi-exponential decay models. The fitting was performed using in-house software (DecFit). For intracellular measurements in FLIM, image analysis and curve fitting was performed using the SymPhoTimev. 4.7 software (PicoQuant). The results obtained from curve fitting were used to calculate the FRET efficiency. In labeling studies the emission decays of the fluorophores were found to be non-exponential. In this case, FRET efficiency was calculated based on the ratio on the emission intensities of labeled and unlabeled proteins. In paper **IV**, FRET efficiency was calculated according to eq. 4.9 (Chapter 4). The distance of separation between the donor and acceptor chromophores was calculated according to eq. 4.2. The fluorescence intensity from microscopy images were quantified using ImageJ software (Schneider et al. 2012) as described elsewhere (Gavet & Pines 2010).

This page intentionally left blank

7. SUMMARY OF RESULTS AND DISCUSSION

This chapter describes the summary of results and discussion from the original publication of this thesis (**I-IV**). The first part describes the protein modifications performed in this thesis, followed by the fluorescence analysis results and discussion of the individual papers.

7.1. Protein modifications

The yellow fluorescent protein variant - Citrine (Griesbeck et al. 2001) was used for site-specific labeling and bioconjugation to EOF's and glass slides. The labeling and bioconjugation was performed by exploiting cysteine-maleimide chemistry. To ensure site-specificity, the native cysteine's present in the protein was examined from the protein structure. Modeling of Citrine structure (PDB ID: 1HUY) showed cysteine (Cys48) as an attractive binding site for chemical modification using Cys-reactivity as it is exposed to the outer surface of the protein. Site-directed mutagenesis was performed to replace Cys48 with Val (C48V). The other Cysteine residue (Cys-70) present in the Citrine is buried inside the structure of protein, making it inaccessible to the outside environment and hence it cannot be labelled. Moreover, Cys-70 has proved to be crucial in obtaining soluble fluorescent protein (Hanson et al. 2004) and hence it was not replaced. The replacement C48V ensured that there is no surface exposed cysteine present in Citrine. The fluorescence measurements revealed absence of binding to thiol-exposed surface for the control protein (Citrine with no surface exposed cysteine). This confirms the absence of thiol-reactive surface on the C48V mutant of Citrine.

For site-specific labeling and conjugation using cysteine-maleimide chemistry, new Cysteine site was created in the fluorescent protein by site-directed mutagenesis (Figure 7.1*A*). The sites created were Cys-147 (S147C) in one construct and in the second construct, Cysteine (Cys-240) was introduced at the C-terminal of the protein preceding a short linker containing (Ser-Gly). Steady-state measurements indicated that the modifications have little or no effect on the fluorescence properties of the protein (Table 7.1). Intramolecular FRET was studied (in paper **I**) by conjugating thiol-reactive derivatives of fluorophores MDCC and Alexa Fluor®568 (AF-568) to the Cysteine sites created in the protein. On conjugation with Citrine, the spectral property of MDCC makes it an energy donor (MDCC→Citrine), and AF-568 as an energy acceptor with citrine (Citrine→ Alexa Fluor 568). The (Cys-240) construct was used in the bioconjugation of the protein to the solid surfaces (in paper **II**). The conjugation of the

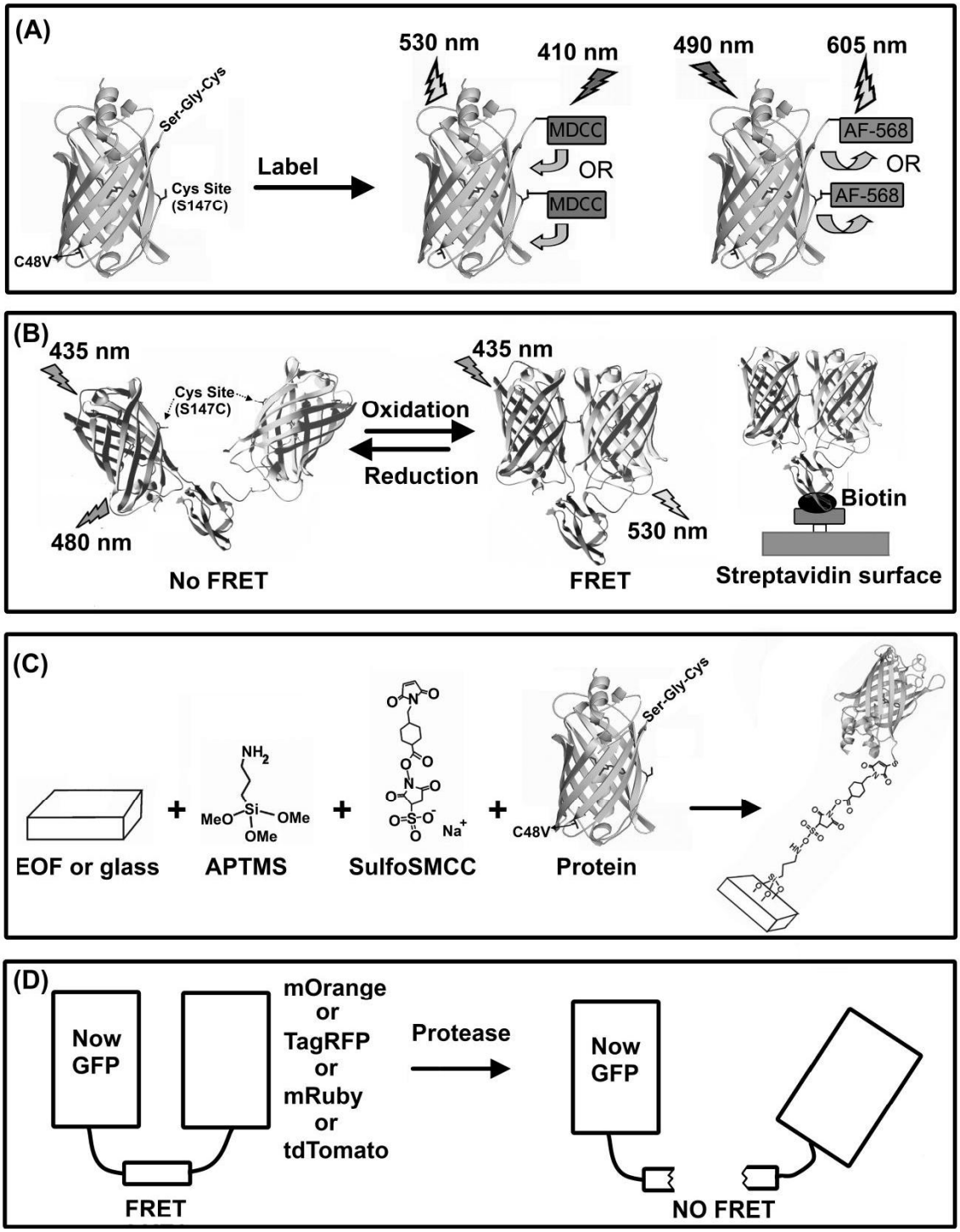

Figure 7.1 Scheme displaying different protein modifications performed in this thesis. (*A*) Structure of Citrine with modified sites and scheme showing intramolecular FRET from conjugated labels to different sites in protein (MDCC-Citrine) and from protein to label (Citrine – AF-668). (*B*) Design of the FRET based redox sensor with Cerulean-Citrine FRET pairs linked by 1.3Tc, the polypeptide containing amino acid sequence allowing site-directed biotinylation to streptavidin surface (right side). In oxidized state, disulphide bonds are formed between the modified cysteine residues resulting in increased FRET and in reduced state the disulphide bonds are cleaved resulting in a low FRET state. (*C*) Development of fluorescent protein SAM on the surface of EOF or glass. The conjugation is initiated by surface activation using APTMS to generate amino-exposed surface followed by maleimide-activation with sulfo-SMCC and site-specific attachment of modified Citrine to the activated surface. (*D*) Design of novel FRET pairs with NowGFP as donor. The GFP-RFP pairs are fused by linker containing thrombin protease site. Protease cleavage separated the fusion protein diminishing FRET.

Table 7.1 Spectral properties of the fluorescent proteins and the corresponding FRET pairs used in this study

Fluorescent protein	**λ_{Abs} (nm)**	**λ_{Emiss} (nm)**	**ε ($M^{-1} cm^{-1}$)**	**QY**	**Partner in FRET**	**J (λ)$M^{-1}cm^{-1}nm^4$**	**R_0 (Å)**
Citrine	514	528	75000	0.73	-	-	
Citrine C147	515	528	63000	0.75	MDCC	1.2×10^{15}	43
					AF- 568	3.57×10^{15}	61
Citrine C240	514	528	80000	0.71	MDCC	1.6×10^{15}	45
					AF- 568	3.64×10^{15}	61
Cerulean	433	475	43000	0.62	Citrine	1.41×10^{15}	50
NowGFP	494	502	56700	0.76		-	
mOrange	548	562	71000*	0.69*	NowGFP	2.48×10^{15}	58
mRuby2	559	600	113000†	0,38†		3.74×10^{15}	62
TagRFP	555	584	100000‡	0.48‡		2.91×10^{15}	59
tdTomato	554	581	138000*	0.69*		5.43×10^{15}	66

* Values from ref. (Shaner et al. 2004)

† Values from ref. (Amy et al. 2012)

‡Values from ref. (Merzlyak et al. 2007)

thiol-exposed -Cysteine in fluorescent protein to the amino-exposed surface of glass slides and EOF was mediated by an amine-to-sulfhydryl crosslinker - Sulfo-SMCC (Figure 7.1*C*).

The labeling in intramolecular FRET studies proved that the surface exposed Cysteine in Citrine - S147C has thiol-group exposed to the outside environment of the protein. This was exploited in the development of FRET based redox sensor in paper **III**. The cyan variant of GFP - Cerulean (Rizzo et al. 2004) was used as donor generating Cerulean-Citrine FRET pairs for the development of FRET based redox sensor. This FRET pair has proved to be an excellent choice for designing FRET based sensors (Mank et al. 2006; Lundby et al. 2008; Lindenburg et al. 2013). Cerulean was genetically modified to generate Cerulean-S147C. This protein also has the modification - C48V similar to its FRET acceptor- Citrine. Both the fluorescent proteins were fused to generate fusion protein fusion protein Cerulean-Tc1.3S-Citrine. The TC1.3S (biotin carboxyl carrier domain of transcarboxylase) (Reddy et al. 2000) was incorporated between the FRET pair aiming for bioconjugation to streptavidin coated surfaces.

In this FRET pair, at an oxidized state disulphide bonds are formed between Cys-147 residues present in both Cerulean and Citrine variants, bringing the fluorescent protein domains in close proximity to exhibit higher FRET efficiency. The reduced state results

in the dissociation of the disulphide bond, so that the proteins move apart, resulting in reduced FRET efficiency and large dynamic range for the sensor response (Figure 7.1*B*). This forms the principle behind the working of FRET based redox sensor and this was proved by the fluorescence measurements as described later in this section.

For the development of novel-red shifted FRET pairs in paper **IV**, we used NowGFP which is modified version of WasCFP (Sarkisyan *et al.*, unpublished). WasCFP is reported to have the highest fluorescence lifetime among GFP variants yet developed (Sarkisyan et al. 2012). Its modified version - NowGFP retains the fluorescence lifetime of its predecessor while improving the brightness (30% brighter than EGFP), photostability and quantum yield (0.79) making it a potential donor for FRET based sensors and assays. FRET between NowGFP (donor) and red fluorescent protein variants (acceptor) was studied by generating FRET pairs fused with a flexible linker comprising thrombin protease cleavage site (Figure 7.1*D*).

Based on fluorescent properties and spectral overlap with NowGFP, four red variants of fluorescent proteins were selected to generate the following FRET pairs, NowGFP-mOrange, NowGFP-mRuby2, NowGFP-TagRFP and NowGFP-tdTomato. The monomeric red fluorescent protein variants mOrange, mRuby2 and TagRFP have been previously reported as excellent acceptors for FRET (Amy et al. 2012; Shcherbo et al. 2009; Bayle et al. 2008). tdTomato is a tandem dimer (two fluorescent proteins coded in a single open reading frame), which is one of the brightest red fluorescent protein variant and has been demonstrated to be an excellent FRET acceptor with GFP variants (Shaner et al. 2004; Ai et al. 2008). Other red fluorescent proteins such as mRFP and mCherry were not considered for this study as their emissions are weak to be detected above the donor emission tail causing challenges in ratiometric imaging as described previously (Amy et al. 2012).

FRET between the pairs were analyzed by treatment with thrombin protease. On protease action the fusion protein will be cleaved separating the FRET pairs. The change in FRET was analyzed and this was used to compare the FRET pairs. Our study indicated high FRET efficiency and dynamic range for NowGFP-tdTomato followed by NowGFP-mRuby2 on comparison with the other studied FRET pairs.

The protein modifications, labeling, bioconjugation and FRET was analyzed using fluorescence spectroscopy techniques which included steady state and time resolved measurements. The results and discussion from the fluorescence measurements is summarized in the following section.

7.2. Bidirectional FRET in fluorescent protein

Intramolecular FRET in fluorescent proteins was studied by conjugating chemical labels site-specifically to different sites in the fluorescent protein. Citrine-S147C (C147Cit) and Citrine with Cys-240 (C240Cit) were used for labeling, whereby the label is conjugated to the sole cysteine residue present in the protein. Steady state measurements were performed for primary validation of FRET between MDCC-Citrine and Citrine-AF568 FRET pairs. The spectral overlap integral values of MDCC−Citrine and Citrine−Alexa Fluor (Table 7.1) indicate that the FRET pairs have a good spectral overlap and Förster radius, which is advantageous for the energy transfer. This is reflected in the FRET analysis with steady state measurements of the labeled samples having similar donor absorbance. The samples were excited at donor excitation wavelength where only the donor will be excited and the emission spectrum showed remarkable quenching in the donor emission with an increase in the acceptor emission which indicates FRET between the donor and acceptor (Figure 7.2).

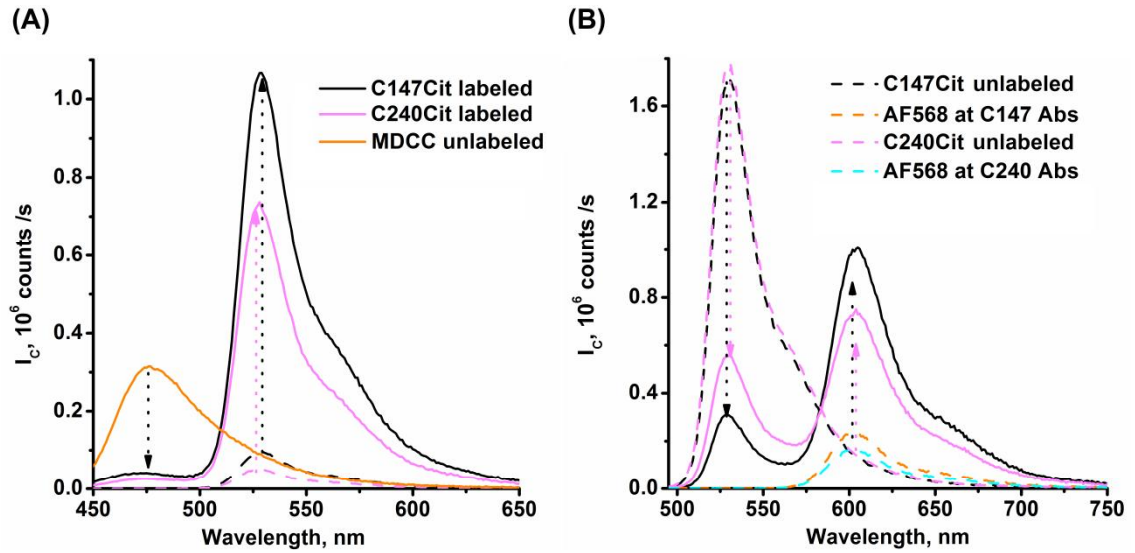

Figure 7.2 Fluorescence emission spectra of Citrine variants showing variation in FRET in the presence and absence of chemical label: MDCC (A) and Alexa Fluor 568 (B). In MDCC-labeled samples, at excitation of 435 nm, quenching of MDCC emission and an increase in emission of citrine variants can be observed. The dotted arrows indicate the increase and decrease in emission of labeled and unlabeled samples. The dashed lines indicate the respective unlabeled samples. For AF568 labeled samples, the excitation wavelength used is 490 nm. Also in this case, the quenching of the donor (arrow) with the rise in acceptor emission as a result of energy transfer can be observed. The lines indicate the labeled samples (C147Cit- black and C240Cit-pink) (modified from paper **I**).

On comparing the ratio of emission intensities at donor excitation to the ratio of intensities on selective acceptor excitation, MDCC labeled sample displayed higher FRET for C240Cit on comparison with C147Cit. In proteins labelled with AF568, C147Cit exhibited higher FRET on comparison to C240Cit. Even though, energy transfer can be confirmed from the steady-state measurements, this method provides less molecular information. Time-resolved measurements were performed to analyze FRET efficiency and fluorescence lifetimes from the labelled samples.

The single exponential fit of Citrine and its variants in TCSPC measurements showed fluorescence lifetime of ~3.3−3.7 ns which is in agreement with the previously reported lifetimes of Citrine (Heikal et al. 2000). For lifetime measurements, the MDCC labelled samples were excited at 400 nm and emission of donor was monitored at 470 nm which is the emission maximum of MDCC (Figure 7.3). The fluorescence lifetime fits showed multiexponential nature with three lifetimes. In MDCC labelled samples, 90% of the emission in C240Cit decays with time constant ~69 ps and the rest with longer lifetimes (3.57 and 0.67 ns) whereas, In C147 Cit, 80% of the emission decays with time constant ~82 ps and the rest with longer lifetimes (4.0 and 0.85 ns). This indicates that for MDCC labelled C240Cit exhibited higher FRET on comparison with MDCC labelled C147Cit, and this is in agreement with the results from steady state measurements. The prediction of possible distances between the fluorophores is calculated from the FRET data and by considering random orientation of the fluorophore. The predicted distance between fluorophores in C240Cit and C147Cit was found to be 3.1 nm and 3.4 nm, respectively. This is in agreement with the FRET efficiency obtained.

However, from the protein structure, MDCC labelled at C147Cit is closer to the chromophore, than MDCC labelled at C240Cit, and it is supposed to have higher FRET. The rigidity of the Cysteine in C147Cit, the bulky nature of MDCC, and the absence of a flexible coupling arm for MDCC might have limited the flexibility of the MDCC fluorophore affecting the fluorophore orientation which results in reduced FRET. In C240Cit, the Ser-Gly linker provides flexibility to the attached label resulting in

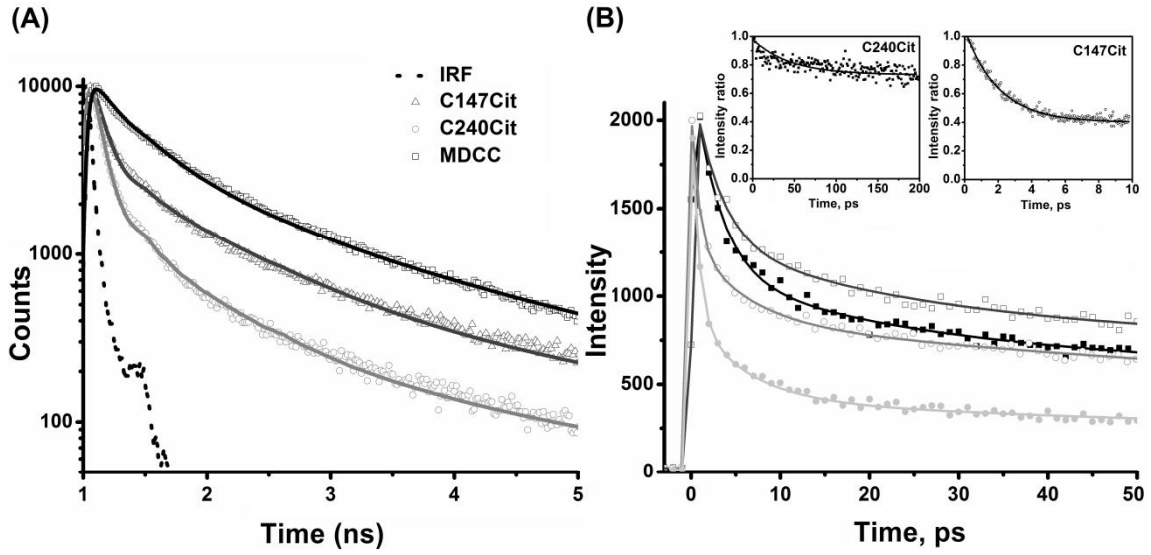

Figure 7.3 Fluorescence lifetime measurements (*A*) TCSPC data showing fluorescence decay and fits (solid lines) of MDCC labeled samples monitored at donor emission wavelength. The decrease in MDCC (Donor) lifetime on labeling can be observed from the figure (*B*) Fluorescence up-conversion data showing decay curve of AF568 labeled samples. The open symbol represents unlabeled and the closed symbol represents labeled samples. The square symbol represents decay curve of C240Cit and the circle represents decay curve of C147Cit. The inset figure shows time dependence of the intensity ratio and mono-exponential fit of the dependence in AF568 labeled and unlabeled FP (modified from paper **I**).

favorable orientation increasing the FRET. This emphasis importance of linker in designing FRET based sensors as reported previously (Evers et al. 2006; Van Dongen et al. 2007; Kolossov et al. 2008). It has also been demonstrated that the bulky nature of the molecules interacting in FRET, reduces FRET efficiency (Domingo et al. 2007). In both the labelled samples, at 530 nm (emission of Citrine), a fast rise in emission was observed which is indicative of FRET.

In TCSPC measurements of AF568 labelled samples, the emission at 530 nm (donor emission) showed biexponential nature with a fast decay component of ∼20 ps and a longer decay component of 3.39 ns. As expected, a fast rise in emission of acceptor (at 603 nm) was observed due to energy transfer. The fast decay component of ∼20 ps was too short to be resolve in TCSPC. In this case, ultra-fast fluorescence up-conversion spectroscopy having a time resolution of 200 fs was used to study the energy transfer. The up-conversion spectroscopy of AF568 labeled samples showed a fast decay at beginning due to FRET and a constant level at a longer delay originating from proteins not participating in FRET. The time evolution of the ratio of the emission intensities of labeled and unlabeled proteins was used to determine the energy transfer efficiency (Figure 7.3). The energy transfer occur in ~64% of C147Cit and its time constant is 2 ps, whereas in C240Cit the FRET time constant is 40 ps and only 25% of protein were involved in the energy transfer. These findings were in reasonable agreement with steady state and TCSPC measurements confirming FRET from Citrine to AF568. The predicted approximate distances between the fluorophores were 5.4 nm and 7.4 nm for C147Cit and C240Cit labeled samples, respectively. The difference in energy transfer time constants between C147Cit and C240Cit was also consistent with the difference in distances between the fluorophores of the protein and the conjugated label. The distance calculated in this study in reasonable agreements with the previously reported distances between the chromophores in YFP dimers, distance between fluorescent proteins in close proximity and in presence of linker, and also consistent with the distance between YFP coupled to DNA-fluorescent label conjugate (Evers et al. 2007; Evers et al. 2006; Shi et al. 2007b; Kukolka et al. 2007).

The up-conversion spectroscopy measurements of Citrine also revealed that the emission decay profile of Citrine is nonexponential, which is contrary to the previous studies on decay profile of Citrine (Mank et al. 2006; Heikal et al. 2000). The up-conversion spectroscopy measurements showed a fast decay component of few picoseconds and a longer decay component. However, it should be also noted that the previous studies were limited to nanosecond or picosecond resolution, and our TCSPC studies having time resolution of 60−80 ps was also not able to resolve the biexponential nature of Citrine fluorophore. It was resolved only in up-conversion measurements having a time resolution of 200 fs. Similar ultra-fast decay component was previously reported GFP variant (S65T/H148D) and this was attributed to small

proton displacement facilitated by a short hydrogen bond formed between the phenol oxygen of the chromophore and the carboxyl oxygen of nearby amino acid (Shi et al. 2007a). It could also be due to complex dynamics of the protein during relaxation of the "hot" excited state.

The potential application of Cysteine sites in the protein was exploited in this study as thiol-reactive fluorophores can be covalently bonded to it. The understanding of the location in fluorescent proteins to which another fluorophore can be conjugated or interacted for improved FRET will aid in the design of superior FRET based sensors. The original idea for the intramolecular FRET came from the study on FRET between tryptophan amino acid inside the protein and site-specifically labelled BODIPY for probing changes in intraprotein distances (Olofsson et al. 2006). Intramolecular FRET applications are common in nucleic acid chemistries (Nitsche et al. 1999). However, the biotechnological applications of intramolecular FRET in fluorescent proteins have not been exploited. By this study, we have laid a proof-of-concept for the idea of using this novel technique in proteins in the future.

7.3. Self-assembled monolayers of fluorescent proteins on etched optical fibers

7.3.1. Steady-state and time-resolved spectroscopy on Citrine SAM films

The YFP SAMs (with C240Cit variant of YFP) were deposited on the surface of EOF and glass plates as described in Section 7.2. The steady-state absorption measurements revealed no detectable absorption on the samples in glass plate, while relatively low absorbance on EOF was observed (Figure 7.4*A*). The absorbance peak is around 514 nm which is the absorption maximum of Citrine in solution (Griesbeck et al. 2001). The emission measurements revealed significant emission intensity at around 530 nm for both the glass plate and EOF, confirming the presence of Citrine (Figure 7.4*B*). On comparison with the normal Citrine emission in solution and Citrine SAM in glass plate, a slight red shift and a shoulder at around 560 nm is observed for Citrine SAM in fiber. This is due to the transmission properties of the dichromic mirror and not due to the difference in actual emission spectra of the two SAMs. The weak absorption in EOF and the lack of detectable absorption spectra in glass plates can be attributed to the relatively high mean molecular area of the deposited proteins (as proteins have a diameter of 2.4 - 3 nm (Ormö et al. 1996; Yang et al. 1996a) making the absorption of the layer too weak to be detected by a standard spectrophotometer. Despite the weak absorbance, the high emission intensity observed can be due to the high quantum yield of the YFP variant (71%).

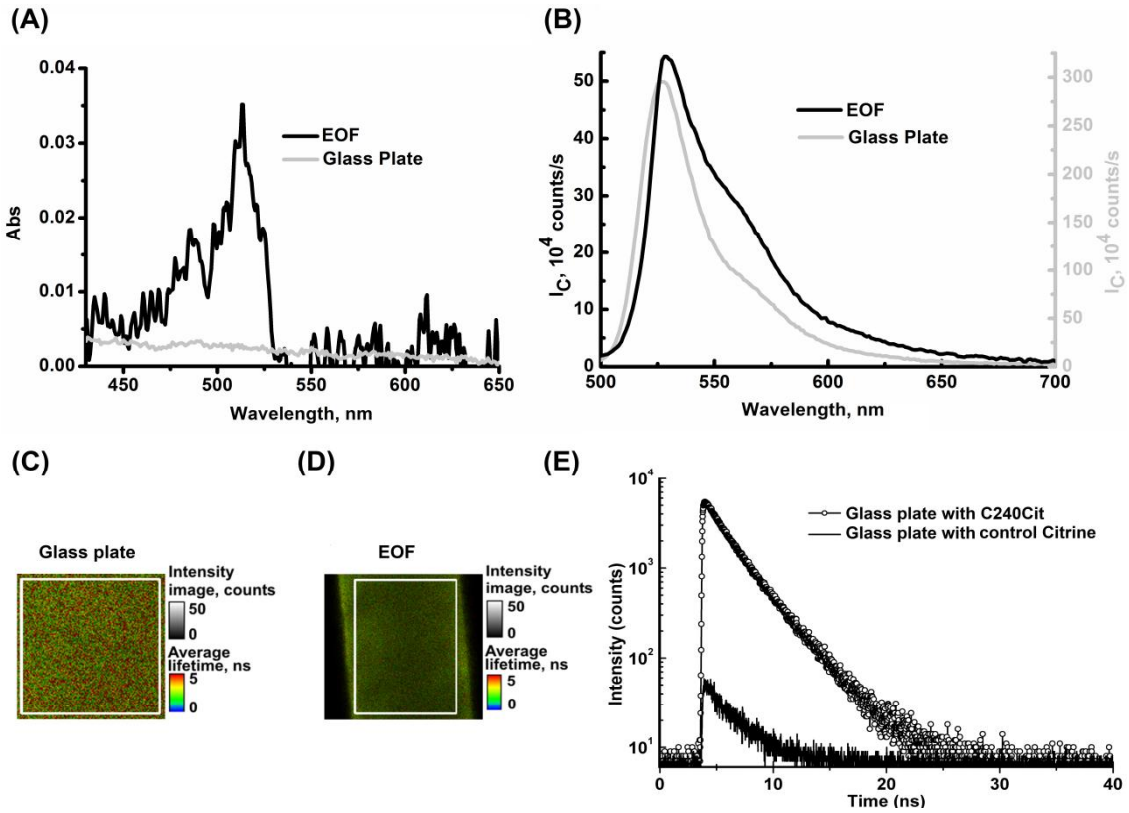

Figure 7.4 Steady-state and time-resolved measurements of YFP SAM on surfaces. Absorption (*A*), emission (*B*) spectra, and FLIM images (*C, D*) of YFP SAM on surface of EOF and glass plates. The white rectangle on FLIM images shows areas used to measure fluorescence lifetime. (*E*) Fluorescence decay curve from FLIM comparing the intensity of YFP SAM with the control YFP (Citrine with no surface exposed Cysteine) (modified from paper **II**)

The FLIM revealed that proteins form morphologically homogenous structures on glass plates and on EOF (Figure 7.4). The FLIM of Citrine variant without surface exposed Cysteine showed no fluorescence which confirms that the binding occurred through Cysteine residue. This confirms that the coupling is site-specific and covalent in nature. The fluorescence lifetime decay of YFP SAMs was found to be bi-exponential with average lifetime of 2.36±0.20 and 2.40±0.13 ns on glass surfaces and EOFs, respectively. The average lifetime values YFP SAM on both surfaces are only 28 % shorter, when compared with the lifetime of the similar YFP variant (3.3 ns) in solution. The change in fluorescence lifetime of fluorescent protein due to the change of microenvironment and refractive index has been previously reported (Borst et al. 2005; Sun et al. 2011a). This indicated that the dry conditions and protein aggregation has only minor effect on the fluorescence property on the protein. Furthermore, in this study, the stability of YFP SAM to various physiological and chemical factors has also been analyzed.

7.3.1. Effects of various pH, ions, denaturing agents and proteases on YFP SAM films

To analyse the possibility of using YFP SAMs in *in vitro* optical sensors and immunoassays, the stability of protein SAMs on EOF was studied. This was done by

treating the YFP SAM on EOF with various ions, detergents and proteases and compares the stability with proteins in solution. The effect of pH on the fluorescence intensity of YFP SAM on EOF was monitored at 530 nm. At pH 6, the fluorescence intensity decreases by 50 % relative to the maximum intensity observed at pH 8.5. This change is found to be reversible in the pH range 6.5 to 9 which is within the normal physiological range, but does not recover below pH 5 (Figure 7.5). This response was similar to the previously reported response of the YFP variant in solution indicating that the bioconjugation has not changed the pH response on the protein (Griesbeck et al. 2001). The irreversible reduction in the fluorescence intensity at the pH value below 5 can be attributed not only to the protonation of the chromophore, but also to conformational structural changes which occur close to the chromophore at low pH (Campbell & Choy 2001; Alkaabi et al. 2005).

The response of YFP SAM on calcium and magnesium was studied as these are the most important divalent cations present in the cell and in many of the body fluids. Moreover, Citrine possesses the similar mutation present in the Ca^{2+} fluorescent protein indicator-Camgaroo, enhancing our interest in studying its effect in the YFP SAM (Griesbeck et al. 2001). As expected, the fluorescence intensity varied with change in Ca^{2+} concentrations indicating its possible application to use in *in vitro* sensors, while Mg^{2+} showed no effect on the fluorescence intensity of YFP SAM in EOF (Figure 7.5). With Ca^{2+}, the fluorescence intensity increased to approximately three fold until a concentration of 15 mM, and it remained unchanged with further increase in Ca^{2+} concentrations. The studies showed that the YFP SAM in EOF can be sensitive enough even at micro molar concentrations of Ca^{2+}, with reasonably broad dynamic range of sensitivity between 0.025 and 10 mM. This response showed reasonable similarity to the response of EGFP based Ca^{2+} sensor in solution (Zou et al. 2007). This demonstrates a proof-of concept for the potential use of fluorescent proteins in *in vitro* sensor applications by conjugating the fluorescent proteins with optical fibers.

The fluorescent proteins are known to be resistant to proteases and highly stable to various denaturing agents and detergents in solutions (Alkaabi et al. 2005; Chiang et al. 2001). The stability of YFP SAM on EOF was analysed by immersing the EOF in corresponding solutions. Even though, YFP SAM showed an initial decrease in fluorescence intensity (13 % in 200 seconds) on treatment with proteases, it stabilized and remains further unchanged except for trypsin protease (Figure 7.5). In trypsin solution, reduction of fluorescence intensity with time was observed indicating cleavage of protein from the EOF. The exposure of the trypsin cleavage site (Lys238) at the C-terminal of the fluorescent protein due to insertion of the linker and the conjugation to the fiber surface could have resulted in the cleavage of the protein, leading to the loss of fluorescence. The high specificity of trypsin mediated cleavage at C-terminal lysine was

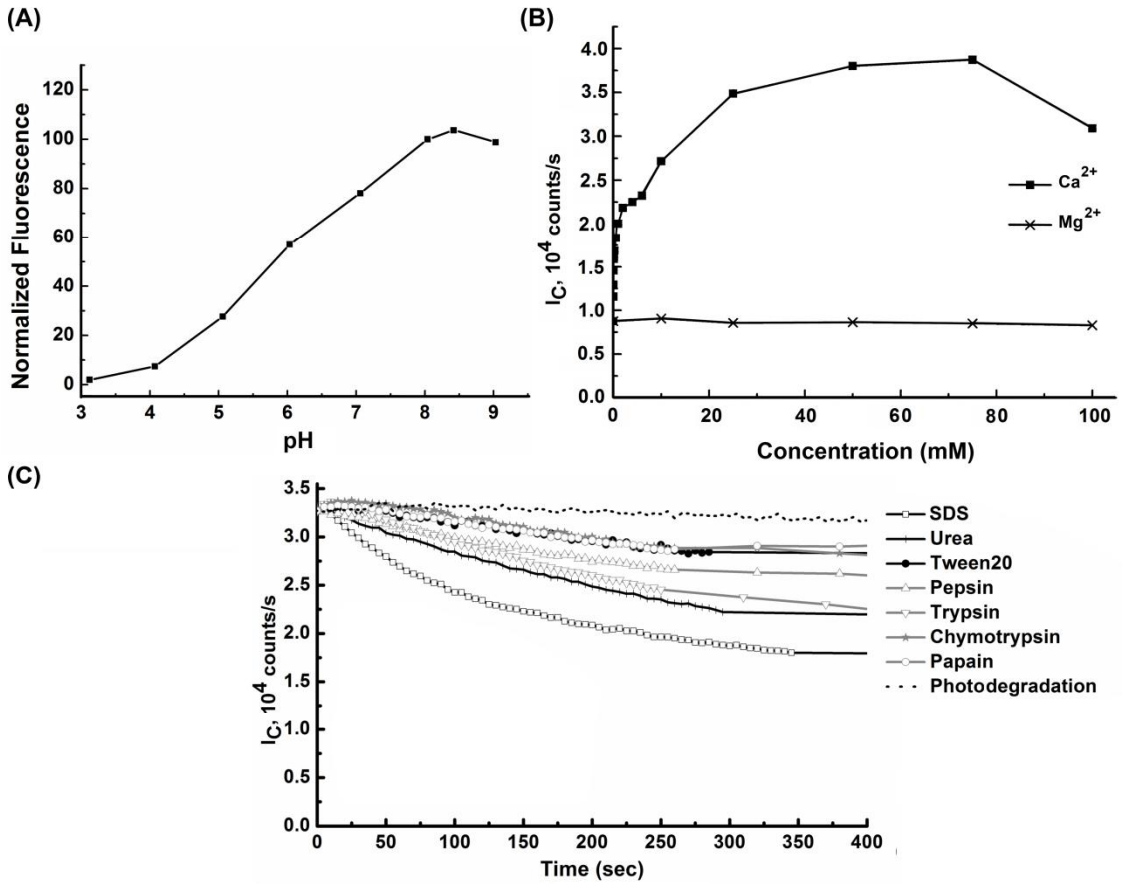

Figure 7.5 (*A*) pH dependence on fluorescence intensity of YFP SAM on EOF. (*B*) Effect of Ca2+ and Mg2+ on YFP SAM. (*C*) Effect of different proteases and denaturing agents (at pH 7.5) on the YFP SAM on EOF (modified from paper II)

reported previously (Olsen et al. 2004). However, with all other proteases tested, the YFP SAM showed reasonable stability even at high protease concentrations of 2 mg/ml.

The proteins also exhibited reasonable stability on treatment with high concentrations of denaturing agents which includes Urea (8 M), SDS (0.5 %) and Tween20, at physiological pH (Figure 7.5). At non-physiological pH conditions, reduction in fluorescence in EOF was observed for Tween 20 and SDS. This indicates either cleavage of proteins from EOF or protonation and conformational structural changes at chromophore of fluorescent proteins as reported previously (Alkaabi et al. 2005).

By this study, it was demonstrated that YFP SAMs can be deposited site-specifically and covalently on curved surfaces of EOFs and on the plane surfaces of glass plates. The treatment of YFP SAM on EOF with denaturing agents, proteases, ions and at varying pH conditions revealed that the bioconjugation has little or no effect on the fluorescence property of the fluorescent protein. To the best of our knowledge, this is the first study on development of SAM on the surface of EOF using fluorescent proteins. The covalent nature of conjugation without losing the fluorescence property and characteristics of the fluorescent proteins, when combined with the wide range of fluorescent protein based sensors, opens up new window in the design of *in vitro* biosensors. The ability of optical fibers to be tapered down to a few nanometers (Vo-

Dinh et al. 2006), and the possibility of SAM of fluorescent proteins in its surface (this study) can provide opportunities even in studying cell organelles in real-time, in future.

7.4. FRET based redox sensor

The first non-invasive ratiometric redox sensor developed for monitoring redox status in live cell was roGFP (redox-sensitive green fluorescent protein), and it was used to determine mitochondrial redox potential (Hanson et al. 2004). This probe was not sufficiently sensitive to measure the redox dynamics inside the cytoplasm (Yano et al. 2010) which prompted scientists in developing FRET based sensors using fluorescent proteins (Yano et al. 2010; Kolossov et al. 2011). In these sensors, the sensing domain (consisting of two or more cysteine residues) is present in the linker sequence joining the FRET pairs and was intended for *in vivo* assays in eukaryotic cells. However, they suffer limitations in the low FRET efficiency, in spite of modifications in the linker sequence (Kolossov et al. 2008). They also suffers from possibility of undesirable cross link formation due to the presence of more than two Cysteine residues exposed to the surface in the FRET constructs. In this study, we have developed a FRET based redox sensor to monitor redox status in bacterial cells (Paper **III**). To improve the FRET efficiency and to avoid the possibility of undesirable cross-link formations, we incorporated the cysteine residues on the fluorescent protein structure after removing all the native surface exposed cysteine residues as described in section 8.1. *In vitro* and intracellular fluorescence measurements were performed to analyze the working of the FRET based sensor.

7.4.1. *In vitro* fluorescence measurements

On donor excitation, the fluorescence emission spectrum of the FRET construct showed decrease in the Citrine (acceptor) emission with an increase in the Cerulean (donor) fluorescence peak on addition of reducing agent, and vice versa on addition of oxidizing agent (Figure 7.6). This change was not observed in the control FRET construct which lacks surface exposed cysteine residue. This suggests that the observed change in intensity ratio is due to the formation and dissociation of disulphide bonds between the cysteine residues in the FRET pairs. The formation and dissociation of disulphide bonds will alter the distance between the FRET pairs, which results in the change in FRET. This change in FRET accounts for the observed variation in intensity ratio.

The FRET efficiency was calculated using $(ratio)_A$ method (equation 7.2) which provides automatic correction of variations in sample to sample fluorophore concentration and automatically cancels changes occurring in fluorescence as a result of the microenvironment variations (Kolossov et al. 2008). The maximum FRET efficiency observed for the FRET redox construct was 0.55, which is higher than the

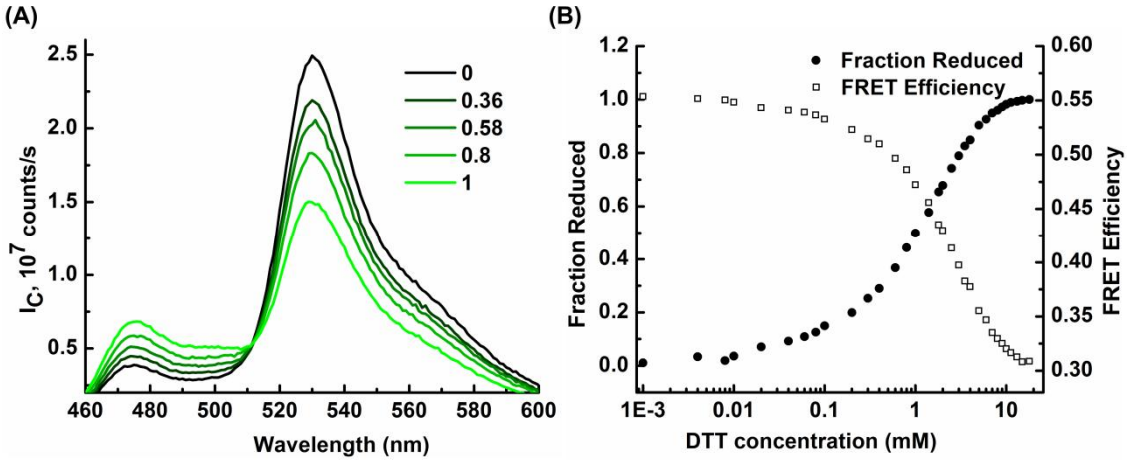

Figure 7.6 (*A*) Fluorescence emission spectra of the FRET sensor displaying variation in energy transfer at different relative fraction of reduced protein. Relative fraction '0' and '1' represents oxidized and reduced states, respectively. (*B*) The FRET efficiency determined $(ratio)_A$ method versus the fraction of reduced protein during titration of the oxidized protein with reducing agent (modified from paper **III)**.

FRET efficiencies reported for the previous FRET based redox sensors with maximum FRET efficiencies between 0.2 and 0.3 (Kolossov et al. 2008; Kolossov et al. 2011). The high FRET efficiency has also contributed to the larger dynamic range of the sensor response (Figure 7.6).

The reversibility of the sensor was validated by monitoring the variation in the fluorescence intensity ratio between the FRET pairs on treatment with alternating cycles of H_2O_2 and DTT. The alternating cycles of oxidation and reduction process was repeated for three cycles without losing the redox sensing property of the sensor displaying the reversibility of the sensor (Paper **III,** Figure 3). This proves that the Cysteine disulphide bond formed between the FRET pair is readily reversible and studies have demonstrated that the cysteine susceptible to reversible oxidation/reduction can be used in redox sensing (Hanson et al. 2004; Green & Paget 2004). The FRET sensor demonstrated good dynamic range in the pH range from 7 to 9 and even for pH 6 the change is still significant although it was less than for the 7 to 9 pH range (Paper **III,** Figure 5). However, variation in dynamic range was observed for different pH. This indicates that pH of the environment has to be considered when analyzing the redox status using the FRET sensor.

In this study, the sensing ability of the FRET based sensor after bioconjugation to solid surfaces was also analyzed. The biotinylation domain present in the linker between Cerulean and Citrine was used for conjugating to solid surfaces using streptavidin-biotin interaction. The bioconjugation was confirmed by fluorescence measurements. The non-biotinylated protein showed negligible surface binding, proving that the attachment of the biotinylated protein was site-specific through the biotinylated domain. Although, the bioconjugated FRET pair showed FRET variation on treatment with reducing and oxidizing agent, the dynamic range of the sensor was reduced as a result of

immobilization (Paper **III,** Figure 7). This is in contrary to the study from protein on EOF whereby the single fluorescent protein showed similar response in solution and after bioconjugation. Therefore, the variation in FRET before and after bioconjugation can be only due to the reduced flexibility of the linker domain between the fluorescent proteins as a result of attachment to solid surface. Nevertheless, this study provides a proof-of-concept for the use of fluorescent protein based FRET sensors for sensing applications by fabrication to solid surfaces. This is important, due to the fact that the bioconjugation of proteins to solid surfaces has become a promising tool in many areas of biosciences which includes biosensors, diagnostics and nanotechnology (Wong et al. 2009; Bilitewski 2006).

7.4.2. Intracellular measurements

The intracellular redox response of the sensor was analyzed by expressing the FRET sensor in *E.coli* BL21 cells. The FRET was analyzed from the live cells in culture as well as from single cells. Similar to *in vitro* measurements, the treatment of cells with the reducing agent (DTT) showed a steady increase in Cerulean fluorescence with a decrease in Citrine fluorescence and vice-versa on treatment with oxidizing agent (H_2O_2). This variation in the intensity ratio corresponds to FRET response verifying the functioning of the sensor in intracellular conditions. The dynamic range of the redox sensor reduced significantly in the measurements from culture. However, single cell measurements in microscope yielded better response with reduced background fluorescence and increased dynamic range (Figure 7.7). The high dynamic range observed in single cell measurements was comparable with the previous redox sensors used in mammalian systems (Table 7.2). The FRET response of the untreated cells showed reduced state compared to cells treated with either oxidizing or reducing agents. This is in accordance with the previous studies of the *E. coli* cytoplasm which demonstrates reducing environment (Green & Paget 2004; Beckwith 2007; Hatahet et al. 2010).

The sensor response in normal physiological condition of cells was analyzed by expressing the FRET pair in *E. coli* mutant strains - Origami B (trxB -, gor -) and BL21 (trxB+, gor+). The mutations in Origami will create oxidizing environment in the cytoplasm favoring disulphide bond formations (Derman et al. 1993). On the contrary, BL21 is its wild type without mutations for generating oxidizing environment and hence it is expected to have reduced cytoplasm (Hatahet et al. 2010). The fluorescence measurements from our study showed variation between the FRET ratios in both of the strains. As expected, the Origami tends to be at oxidizing state whereas BL21 cytoplasm showed reducing environment (Figure 7.7). This is in agreement with the published reports on disulfide bond formations in both the mutant strains (Hatahet et al. 2010; Xiong et al. 2005). These studies validate the working of the FRET based redox sensor

in intracellular environment. This sensor opens up possibility to study redox status in cells and cellular organelles with high dynamic range FRET efficiency.

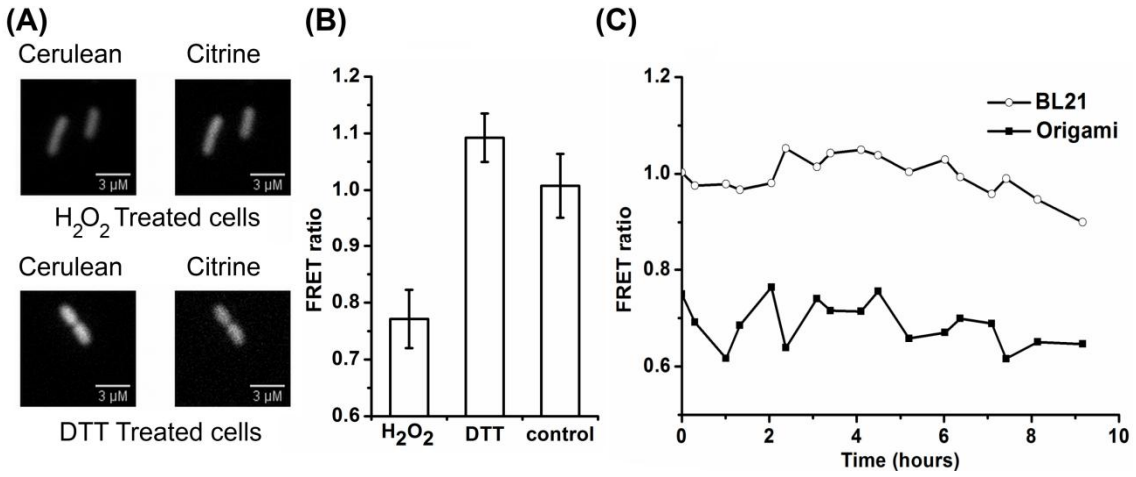

Figure 7.7 (*A*) Intensity Images (excitation 405 nm) of *E. coli* cells on treatment with oxidizing/reducing agents monitored through detection filters (483/35 nm for Cerulean and 535/30 nm for Citrine). The decrease in Cerulean emission with the increase in Citrine emission on treatment with H2O2 and vice-versa on treatment with DTT can be observed from the images. (*B*) Emission ratio of Cerulean/Citrine variation of cells (average of 20-25 single cells) (*C*) FRET variation in Origami and BL21 cells with respect to time during the cultivation time of 9 hours post induction (modified from paper **III).**

Table 7.2 Comparison of FRET efficiency and *in vivo* dynamic range of FRET based redox probes

Redox probe	***in vivo* FRET ratio**				**Reference**
	$\mathbf{r_{min}}$	$\mathbf{r_{max}}$	**Δr**	$\mathbf{E_{max}}$	
RL -5	28.0	40	30.0	25.20 %	(Kolossov et al. 2008)
HSP FRET	0.8	0.93	14.0	4.3 %	(Robin et al. 2007)
Redoxfluor	0.8	1.05	23.8	-	(Yano et al. 2010)
This Study	0.688	1.09	**36.9**	**56 %**	**This study (III)**
CY RL-7*****	0.35	0.6	41.6*	28.70 %	(Kolossov et al. 2011) (Lin et al. 2011)

E_{max} – Maximum FRET efficiency observed; Redoxfluor E_{max} is not reported to the best of our knowledge
$\Delta r = (r_{max} - r_{min}) / r_{max} \times 100\%$; r_{max} and r_{min} is approximated from the figures in original publications
***** Can be used only in relatively high oxidative environments

7.5. FRET pairs with improved dynamic range for fluorescence lifetime measurements

The traditional FRET based reporters used for live cell studies were developed using cyan and yellow variants of GFP's. However, with the development of orange and red variants of fluorescent proteins, the cyan-yellow FRET pairs are getting replaced as longer wavelength excitation and emission results in reduced cellular autofluorescence, decreased phototoxicity and lower light scattering (Amy et al. 2012; Shcherbakova & Verkhusha 2013). Together with the careful selection of FRET pairs, the selection of FRET detection method is also crucial in obtaining accurate results. For precise FRET analysis and detection, scientists are relying more on fluorescence lifetime based

methods rather than the traditional intensity based measurements. The fluorescence lifetime based measurements overcome the disadvantages of intensity based measurements which is affected by variations in probe concentration and optical path length (Dewitt et al. 2009; McGinty et al. 2009). Furthermore, complex calibration and correction procedures are needed to overcome the concentration changes, photobleaching, spectral bleed through and back-bleed through in intensity based FRET measurements (Piston & Kremers 2007; Gordon et al. 1998; Zal & Gascoigne 2004; Chang et al. 2009). The fluorescence lifetime based measurements are less susceptible to all these factors making it the most direct and robust way to measure FRET (Jares-Erijman & Jovin 2003; Suhling 2014; McGinty et al. 2009).

In this study (Paper **IV)**, the advantages of using fluorescent protein variants towards the red region of the spectrum, together with the advantages of using lifetime based measurements in FRET is combined to design novel FRET pairs. For this, we exploited the fluorescent protein with the longest reported fluorescence lifetime – NowGFP as donor, and screened for the best acceptor for FRET pair using various red fluorescent proteins as described in section 7.1. From steady-state fluorescence measurements, the spectral overlap integral *(*$J(\lambda)$) and the Förster radius (R_0) of the FRET pairs were calculated (Table 7.1). NowGFP-tdTomato and NowGFP-mRuby2 FRET pair demonstrates higher spectral overlap and R_0 values compared to the other FRET pairs analyzed. To the best of our knowledge, the R_0 of NowGFP-tdTomato (6.57 nm) is the largest R_0 value reported so far for any fluorescent protein based FRET pairs yet used in FRET studies. The previous highest R_0 value reported was for Clover-mRuby2 with an R_0 of 6.3 nm (Amy et al. 2012). With the NowGFP-mRuby2 pair, the R_0 (6.17 nm) obtained is the third highest value reported. The large R_0 value is crucial as the FRET efficiency increases when R_0 increases (Amy et al. 2012; Berney & Danuser 2003). The high R_0 values of NowGFP-tdTomato and NowGFP-mRuby2 was reflected in the FRET measurements as these two FRET pairs showed higher FRET efficiency compared to the other FRET pairs analyzed.

The FRET was analyzed by treating the protein with thrombin protease which cleaves the linker between the fluorescent proteins, thereby separating the FRET pairs. The fluorescence intensity and lifetime before and after the protease treatment was analyzed to study FRET. In steady-state spectroscopy measurements, on excitation at 483 nm, where only the donor (NowGFP) is excited, an enhanced acceptor fluorescence emission was observed for the different FRET pairs indicating energy transfer. After addition of thrombin, a decrease in the acceptor emission with an increase in donor emission was observed (at 515 nm) indicating reduced energy transfer as a result of cleavage of FRET pairs. Large FRET dynamic range was observed for NowGFP-tdTomato followed by NowGFP-mRuby2 and comparatively low FRET variation is detected in NowGFP-mOrange and NowGFP-TagRFP FRET pairs.

The fluorescence lifetime was studied using TCSPC technique. The donor decay was analyzed by exciting the samples at 483 nm and decay was monitored at 515 nm. At this monitoring wavelength, donor excited state lifetime can be analyzed selectively as none of the acceptors has noticeable emission at this wavelength. The single exponential decay of non-fused NowGFP showed lifetime of 5.00 ns ± 0.03 ns, similar to the lifetime obtained by Sarkisyan *et* al., (unpublished), and it is the highest lifetime reported so far for any GFP variant. The fluorescence lifetime of NowGFP in the FRET pairs after thrombin treatment displayed lifetime of ~4.8-5.0 ns for different FRET pairs indicating complete cleavage of the FRET pairs on protease action. The decay of the donor undergoing FRET showed decrease in the lifetime with the largest decrease for NowGFP-tdTomato followed by NowGFP-mRuby2, NowGFP-mOrange and NowGFP-TagRFP FRET pairs. The donor lifetime reduction observed in NowGFP-tdTomato FRET pair was more than 2.6 fold and this is the highest lifetime dynamic change reported so far for any fluorescent protein based FRET pairs. The longest fluorescent lifetime previously reported was for mTurquoise with 4.0 ns (Goedhart et al. 2012) and the donor lifetime change on FRET for mTurquoise was only 1.6 fold (Klarenbeek et al. 2011). The decrease in donor lifetime as a result of FRET is shown in Figure 7.8. The FRET efficiency determined from the fluorescence lifetimes showed high FRET efficiency for NowGFP-tdTomato and NowGFP-mRuby2 FRET pairs (Table 7.3). Both of these FRET pairs have FRET efficiency close to 0.5 which is advantageous in the development of FRET reporters with high dynamic range (Amy et al. 2012).

Intracellular FRET analysis was performed using FLIM by comparing *E. coli* cells expressing donor alone with the cells expressing FRET pair. The donor fluorescence lifetime was captured selectively using donor emission filter (510/20 nm). The *in vivo*

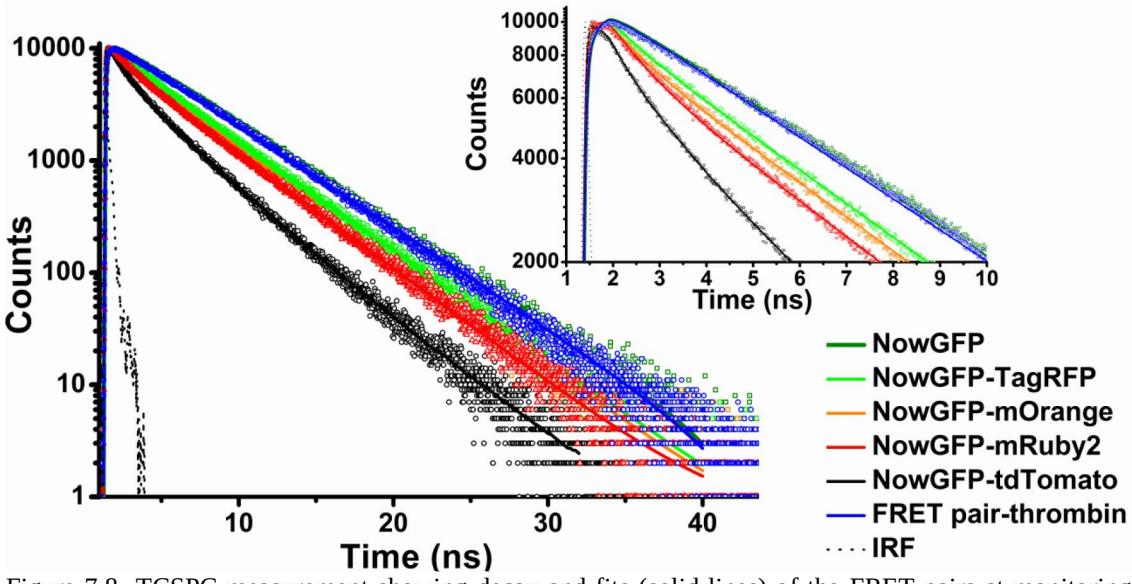

Figure 7.8 TCSPC measurement showing decay and fits (solid lines) of the FRET pairs at monitoring wavelength of 515 nm, to selectively analyze donor decay. NowGFP denotes the lifetime decay of the donor alone and FRET pair-thrombin denotes the lifetime of the donor after proteolytic cleavage. The inset shows the same data with shorter timescale to differentiate the variation in FRET (modified from paper **IV**).

Table 7.3 Fluorescence lifetime and FRET efficiency of the FRET pairs (paper **IV**)

Fluorescent protein / FRET pairs	τ_{ave}	χ^2	**E**
NowGFP (Donor alone)	5.00 ± 0.03	1.42	-
NowGFP-mOrange	3.42 ± 0.05	1.18	0.30
NowGFP-TagRFP	3.74 ± 0.07	1.13	0.25
NowGFP-mRuby2	2.84 ± 0.05	1.20	0.43
NowGFP-tdTomato	2.02 ± 0.02	1.01	0.59
FRET pairs after proteolytic cleavage*	4.88 ± 0.02	1.37	-

* Average from all the FRET pairs after thrombin treatment
E - FRET efficiency (calculated according to eq.4.9)
$\chi 2$ - calculated standard weighted least squares to assess the goodness of the fit

fluorescence lifetime of NowGFP was found to be 4.03 ns. The reduction in the lifetime in comparison with *in vitro* measurements can be attributed to the intracellular microenvironment which affects the fluorescence lifetime (Borst et al. 2005; Pliss et al. 2012). Obvious variation in fluorescence lifetime of NowGFP was observed in the presence of an acceptor (Figure 7.9). The lifetime of NowGFP was reduced to 3.14 ns in NowGFP-mRuby2 FRET pair and 2.80 ns in NowGFP-tdTomato FRET pair displaying very high *in vivo* dynamic ranges for the FRET pairs. The high fluorescence lifetime dynamic change of the FRET pair is on higher side relative to the lifetime changes previously reported for red fluorescent protein based FRET pairs (van et al. 2008; Shcherbo et al. 2009; Lleres et al. 2007). The large change in FRET lifetime for the novel FRET pairs is advantageous in the development of improved FRET based sensors and FRET reporters which switches between well-defined ON and OFF states.

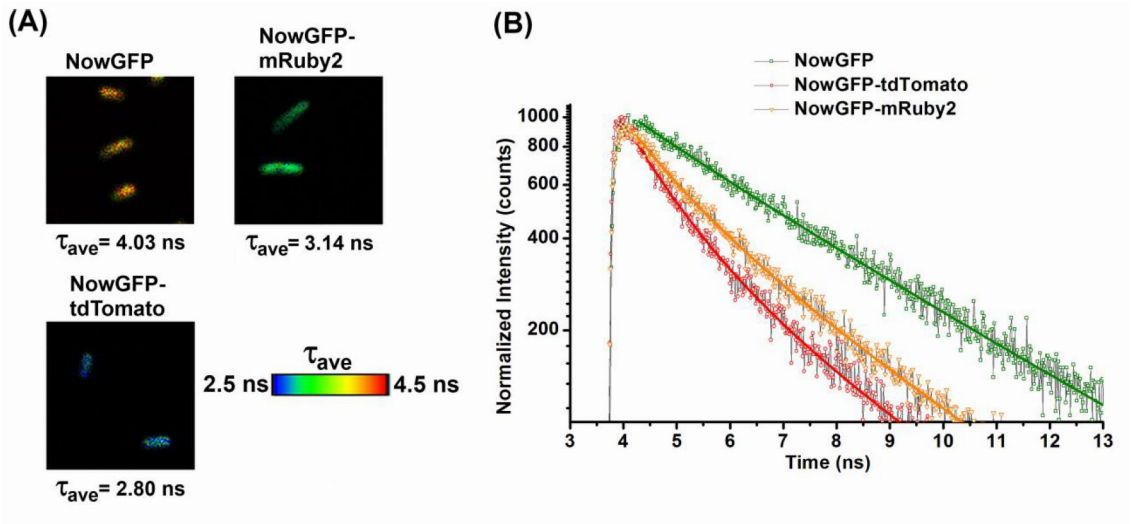

Figure 7.9 (*A*) Intracellular FLIM of E. coli cells showing fluorescence lifetime image displaying FRET. The cells expressing fluorescent proteins were excited at of 483 nm and donor lifetime was captured selectively through band pass filter (510/20 nm). NowGFP donor alone cells and the variation in lifetime as a result of FRET can be observed from the cells expressing the FRET pairs. Image size - 10 µm × 10 µm. (*B*) Fluorescence decay curve and fits (solid lines) from the cells showing decrease in the fluorescence lifetime due to FRET (modified from paper **IV**).

8. CONCLUSION

The intramolecular FRET in fluorescent protein was demonstrated by conjugating chemical fluorophores to different sites in the fluorescent protein (Paper **I**). This was done by studying the FRET from conjugated chemical fluorophore to the fluorescent protein and from the protein to the chemical label using novel FRET pairs MDCC-YFP and YFP-Alexafluor 568, respectively. The high FRET efficiency observed, together with the bidirectional FRET approach used in this study is expected to open up new possibilities in studying protein-protein interactions, protein flexibility, macromolecule dynamics, and in design of FRET based sensors. To the best of our knowledge, this is the first study on bidirectional intramolecular FRET in florescent proteins. This study also demonstrates the potential of cysteine sites in the protein structure for protein modification, as thiol-reactive fluorophores can be covalently attached to it.

The engineered cysteine sites in the protein structure was further exploited in the bioconjugation of fluorescent protein to solid surfaces offering future prospects in the development of *in vitro* sensors (Paper **II**). The fluorescent proteins were deposited on the surface of etched optical fiber using self-assembled monolayer method. The fluorescence measurements revealed that the conjugation is site-specific and covalent in nature. The conjugated fluorescent protein was found to be stable on treatment with denaturing agents and proteases even at non-physiological conditions. The treatment with divalent cations and in varying pH conditions indicated that the conjugated fluorescent proteins retain its spectral and photochemical properties on comparison to similar proteins in solution. We presume that the ability of optical fibers to provide excellent light delivery at high sensitivity and to fabricate them into nanoscale size, when combined with the inherent ability of the fluorescent proteins to act as sensors - can pave way to novel biosensors with lower detection limit and sensitivity.

The genetically incorporated site-specific cysteine residues exposed on the surface of fluorescent proteins was used to develop FRET based redox sensor (Paper **III**). The presence of sensing domain on the protein structure brings the FRET pairs in close proximity, exhibiting high FRET efficiency, compared to the previous FRET based redox sensors where the sensing domain is located inside the linker connecting FRET pairs. Along with the high FRET efficiency, fluorescence measurements also revealed improved dynamic range and reversible nature of the sensor. Even though the FRET efficiency was reduced on expressing in *E. coli* cytoplasm, the sensor could respond to changes in the redox status inside the bacteria at the single-cell level. However, the

limited fluorescence lifetime dynamic range still remains a limitation for FLIM studies in the sensors employing the CFP-YFP FRET pairs.

Novel red-shifted FRET pairs were developed with improved fluorescence lifetime dynamic range and high FRET efficiency (Paper **IV**). The incorporation of a thrombin protease cleavage site in the linker connecting FRET pairs enabled the study of FRET variations in the analyzed FRET pairs. The long fluorescence lifetime of the FRET donor - NowGFP is exploited in obtaining large FRET lifetime dynamic range. Among the red fluorescent protein acceptors screened, tdTomato has demonstrated the highest FRET efficiency and dynamic range with NowGFP as donor. NowGFP-tdTomato and NowGFP-mRuby2 FRET pairs were found to have the highest and third highest Förster radius respectively, for any fluorescent protein based FRET pairs yet reported. This is reflected in obtaining high FRET efficiency for both the FRET pairs. TagRFP and mOrange were not found to be optimal for FRET pair design with NowGFP. NowGFP-tdTomato and NowGFP-mRuby2 were observed to be superior FRET pairs which could replace the traditional CFP-YFP FRET pairs in FRET based FLIM studies and sensors.

To conclude, by this study we have developed novel FRET based redox sensor with improved FRET efficiency and high dynamic range to detect redox status in bacterial cells at single cell level, novel FRET pairs with the highest reported lifetime dynamic range and Förster distance, and a novel platform comprised of fluorescent protein in optical fiber for development of *in vitro* sensor. In this study, we have also conducted chemical coupling with fluorescent protein and small molecular weight fluorophores, and studied their interplay by FRET measurements. To this best of our knowledge this is the first and only study describing bidirectional FRET between fluorescent protein and conjugated chemical label. We believe that the tools developed in this thesis could be useful for the scientists around the world in expanding the knowledge on cellular biochemistry and dynamics and in the development of novel biosensors.

9. REFERENCES

Abraham, B.G., Tkachenko, N.V., Santala, V., Lemmetyinen, H. & Karp, M. (2011). Bidirectional Fluorescence Resonance Energy Transfer (FRET) in Mutated and Chemically Modified Yellow Fluorescent Protein (YFP), Bioconjugate chemistry, Vol. 22(2), pp. 227-234.

Abraham, B., Santala, V., Tkachenko, N. & Karp, M. (2014). Fluorescent protein-based FRET sensor for intracellular monitoring of redox status in bacteria at single cell level, Analytical and Bioanalytical Chemistry, Vol. 406(28), pp. 7195-7204.

Adkins, E.M., Samuvel, D.J., Fog, J.U., Eriksen, J., Jayanthi, L.D., Vaegter, C.B., Ramamoorthy, S. & Gether, U. (2007). Membrane mobility and microdomain association of the dopamine transporter studied with fluorescence correlation spectroscopy and fluorescence recovery after photobleaching, Biochemistry, Vol. 46(37), pp. 10484-10497.

Ai, H.-., Hazelwood, K.L., Davidson, M.W. & Campbell, R.E. (2008). Fluorescent protein FRET pairs for ratiometric imaging of dual biosensors, Nature Methods, Vol. 5(5), pp. 401-403.

Ai, H.-., Shaner, N.C., Cheng, Z., Tsien, R.Y. & Campbell, R.E. (2007). Exploration of new chromophore structures leads to the identification of improved blue fluorescent proteins, Biochemistry, Vol. 46(20), pp. 5904-5910.

Akerboom, J., Calderón, N.C., Tian, L., Wabnig, S., Prigge, M., Tolö, J., Gordus, A., Orger, M.B., Severi, K.E., Macklin, J.J., Patel, R., Pulver, S.R., Wardill, T.J., Fischer, E., Schüler, C., Chen, T.-., Sarkisyan, K.S., Marvin, J.S., Bargmann, C.I., Kim, D.S., Kügler, S., Lagnado, L., Hegemann, P., Gottschalk, A., Schreiter, E.R. & Looger, L.L. (2013). Genetically encoded calcium indicators for multi-color neural activity imaging and combination with optogenetics, Frontiers in Molecular Neuroscience, (FEB), .

Albert Pan, Y., Freundlich, T., Weissman, T.A., Schoppik, D., Cindy Wang, X., Zimmerman, S., Ciruna, B., Sanes, J.R., Lichtman, J.W. & Schier, A.F. (2013). Zebrabow: Multispectral cell labeling for cell tracing and lineage analysis in zebrafish, Development (Cambridge), Vol. 140(13), pp. 2835-2846.

Alkaabi, K.M., Yafea, A. & Ashraf, S.S. (2005). Effect of pH on thermal- and chemical-induced denaturation of GFP, Applied Biochemistry and Biotechnology, Vol. 126(2), pp. 149-156.

Amy, J.L., François, S., Gong, Y., Jesse, D.M., Paula, J.C., Michelle, A.B., Michael, R.M., Wiedenmann, J., Michael, W.D., Mark, J.S., Roger, Y.T. & Michael, Z.L. (2012). Improving FRET dynamic range with bright green and red fluorescent proteins, Nature Methods, Vol. 9(10), pp. 1005-1012.

Ando, R., Hama, H., Yamamoto-Hino, M., Mizuno, H. & Miyawaki, A. (2002). An optical marker based on the UV-induced green-to-red photoconversion of a fluorescent protein, Proceedings of the National Academy of Sciences of the United States of America, Vol. 99(20), pp. 12651-12656.

Awais, M., Sato, M., Lee, X. & Umezawa, Y. (2006). A Fluorescent Indicator To Visualize Activities of the Androgen Receptor Ligands in Single Living Cells, Angewandte Chemie International Edition, Vol. 45(17), pp. 2707-2712.

Bagorda, A., Das, S., Rericha, E.C., Chen, D., Davidson, J. & Parent, C.A. (2009). Real-time measurements of cAMP production in live Dictyostelium cells, Journal of cell science, Vol. 122(21), pp. 3907-3914.

Baird, G.S., Zacharias, D.A. & Tsien, R.Y. (1999). Circular permutation and receptor insertion within green fluorescent proteins, Proceedings of the National Academy of Sciences, Vol. 96(20), pp. 11241-11246.

Barbieri, C.M., Thomson, C.M. & Ward, W.W. (2001). Heterodimerization between blue and green forms of *Aequorea Victoria* GFP, in: Case, J.F., Herring, P.J., Robison, B.H., Haddock, S.H.D., Kricka, L.J. & Stanley, P.E. (ed.), Bioluminescence and Chemiluminescence, World Scientific Publishing Co. Pte. Ltd, Singapore, pp. 13-16.

Bayle, V., Nussaume, L. & Bhat, R.A. (2008). Combination of novel green fluorescent protein mutant TSapphire and DsRed variant mOrange to set up a versatile in planta FRET-FLIM assay, Plant Physiology, Vol. 148(1), pp. 51-60.

Beckwith, J. (2007). What Lies Beyond Uranus?: Preconceptions, Ignorance, Serendipity and Suppressors in the Search for Biology's Secrets, Genetics, Vol. 176(2), pp. 733-740.

Belousov, V.V., Fradkov, A.F., Lukyanov, K.A., Staroverov, D.B., Shakhbazov, K.S., Terskikh, A.V. & Lukyanov, S. (2006). Genetically encoded fluorescent indicator for intracellular hydrogen peroxide, Nature Methods, Vol. 3(4), pp. 281-286.

Berezin, M.Y. & Achilefu, S. (2010). Fluorescence lifetime measurements and biological imaging, Chemical reviews, Vol. 110(5), pp. 2641-2684.

Berney, C. & Danuser, G. (2003). FRET or no FRET: A quantitative comparison, Biophysical journal, Vol. 84(6), pp. 3992-4010.

Betzig, E., Patterson, G.H., Sougrat, R., Lindwasser, O.W., Olenych, S., Bonifacino, J.S., Davidson, M.W., Lippincott-Schwartz, J. & Hess, H.F. (2006). Imaging Intracellular Fluorescent Proteins at Nanometer Resolution, Science, Vol. 313(5793), pp. 1642-1645.

Bilitewski, U. (2006). Protein-sensing assay formats and devices, Analytica Chimica Acta, Vol. 568(1–2), pp. 232-247.

Borst, J.W., Hink, M.A., Van Hoek, A. & Visser, A.J.W.G. (2005). Effects of refractive index and viscosity on fluorescence and anisotropy decays of enhanced cyan and yellow fluorescent proteins, Journal of Fluorescence, Vol. 15(2), pp. 153-160.

Bregestovski, P., Waseem, T. & Mukhtarov, M. (2009). Genetically encoded optical sensors for monitoring of intracellular chloride and chloride-selective channel activity, Frontiers in Molecular Neuroscience, Vol. 2(DEC), .

Campbell, R.E., Tour, O., Palmer, A.E., Steinbach, P.A., Baird, G.S., Zacharias, D.A. & Tsien, R.Y. (2002). A monomeric red fluorescent protein, Proceedings of the National Academy of Sciences of the United States of America, Vol. 99(12), pp. 7877-7882.

Campbell, T.N. & Choy, F.Y.M. (2001). The effect of pH on green fluorescent protein: A brief review, Molecular Biology Today, Vol. 2(1), pp. 1-4.

Cava, F., De Pedro, M.A., Blas-Galindo, E., Waldo, G.S., Westblade, L.F. & Berenguer, J. (2008). Expression and use of superfolder green fluorescent protein at high temperatures in vivo: a tool to study extreme thermophile biology, Environmental microbiology, Vol. 10(3), pp. 605-613.

Chalfie, M., Tu, Y., Euskirchen, G., Ward, W. & Prasher, D. (1994). Green fluorescent protein as a marker for gene expression, Science, Vol. 263(5148), pp. 802-805.

Chalfie, M. (1995). GREEN FLUORESCENT PROTEIN, Photochemistry and photobiology, Vol. 62(4), pp. 651-656.

Chang, C., Wu, M., Merajver, S.D. & Mycek, M. (2009). Physiological fluorescence lifetime imaging microscopy improves Förster resonance energy transfer detection in living cells, Journal of Biomedical Optics, Vol. 14(6), pp. 060502.

Chang, H., Tang, L., Wang, Y., Jiang, J. & Li, J. (2010). Graphene fluorescence resonance energy transfer aptasensor for the thrombin detection, Analytical Chemistry, Vol. 82(6), pp. 2341-2346.

Chiang, C., Okou, D.T., Griffin, T.B., Verret, C.R. & Williams, M.N.V. (2001). Green Fluorescent Protein Rendered Susceptible to Proteolysis: Positions for Protease-Sensitive Insertions, Archives of Biochemistry and Biophysics, Vol. 394(2), pp. 229-235.

Chu, J., Zhang, Z., Zheng, Y., Yang, J., Qin, L., Lu, J., Huang, Z.-, Zeng, S. & Luo, Q. (2009). A novel far-red bimolecular fluorescence complementation system that allows for efficient visualization of protein interactions under physiological conditions, Biosensors and Bioelectronics, Vol. 25(1), pp. 234-239.

Chuang, W.-, Chen, B.-, Chen, K.-, Hsieh, C.-. & Chou, P.-. (2009). Fluorescent protein red Kaede chromophore; One-step, high-yield synthesis and potential application for solar cells, Chemical Communications, (45), pp. 6982-6984.

Chudakov, D.M., Matz, M.V., Lukyanov, S. & Lukyanov, K.A. (2010). Fluorescent proteins and their applications in imaging living cells and tissues, Physiological Reviews, Vol. 90(3), pp. 1103-1163.

Cicchetti, G., Biernacki, M., Farquharson, J. & Allen, P.G. (2004). A Ratiometric Expressible FRET Sensor for Phosphoinositides Displays a Signal Change in Highly Dynamic Membrane Structures in Fibroblasts, Biochemistry, Vol. 43(7), pp. 1939-1949.

Clegg, R.M. (2009). Chapter 1 Förster resonance energy transfer-FRET what is it, why do it, and how it's done, in: Laboratory Techniques in Biochemistry and Molecular Biology, pp. 1-57.

Clegg, R.M. (1992). Fluorescence resonance energy transfer and nucleic acids, Vol. Volume 211pp. 353-388.

Cormack, B.P., Valdivia, R.H. & Falkow, S. (1996). FACS-optimized mutants of the green fluorescent protein (GFP), Gene, Vol. 173(1), pp. 33-38.

Cubitt, A.B., Woollenweber, L.A., Heim, R. (1999) Understanding structure - Function relationships in the Aequorea victoria green fluorescent protein . 19-30 p.

Cubitt, A.B., Heim, R., Adams, S.R., Boyd, A.E., Gross, L.A. & Tsien, R.Y. (1995). Understanding, improving and using green fluorescent proteins, Trends in biochemical sciences, Vol. 20(11), pp. 448-455.

Dale, R.E., Eisinger, J. & Blumberg, W.E. (1979). The orientational freedom of molecular probes. The orientation factor in intramolecular energy transfer. Biophysical journal, Vol. 26(2), pp. 161-193.

Damelin, M. & Silver, P.A. (2000). Mapping Interactions between Nuclear Transport Factors in Living Cells Reveals Pathways through the Nuclear Pore Complex, Molecular cell, Vol. 5(1), pp. 133-140.

Davis, S. & Vierstra, R. (1998). Soluble, highly fluorescent variants of green fluorescent protein (GFP) for use in higher plants, Plant Molecular Biology, Vol. 36(4), pp. 521-528.

Day, R.N. & Davidson, M.W. (2009). The fluorescent protein palette: tools for cellular imaging, Chemical Society Reviews, Vol. 38(10), pp. 2887-2921.

De Michele, R., Carimi, F. & Frommer, W.B. (2014). Mitochondrial biosensors, The international journal of biochemistry & cell biology, Vol. 48(0), pp. 39-44.

De, S., Macara, I.G. & Lannigan, D.A. (2005). Novel biosensors for the detection of estrogen receptor ligands, The Journal of steroid biochemistry and molecular biology, Vol. 96(3–4), pp. 235-244.

Del Pozo, M.A., Kiosses, W.B., Alderson, N.B., Meller, N., Hahn, K.M. & Schwartz, M.A. (2002). Integrins regulate GTP-Rac localized effector interactions through dissociation of Rho-GDI, Nature cell biology, Vol. 4(3), pp. 232-239.

Derman, A.I., Prinz, W.A., Belin, D. & Beckwith, J. (1993). Mutations that allow disulfide bond formation in the cytoplasm of Escherichia coli, Science (New York, N.Y.), Vol. 262(5140), pp. 1744-1747.

Detert Oude Weme, R.,G.J., Kovacs, A.,T., de Jong, S.,J.G., Veening, J., Siebring, J. & Kuipers, O.P. (2015). Single Cell FRET Analysis for the Identification of Optimal FRET-Pairs in Bacillus subtilis Using a Prototype MEM-FLIM System, PLoS ONE, Vol. 10(4), pp. e0123239.

Dewitt, S., Darley, R.L. & Hallett, M.B. (2009). Translocation or just location? Pseudopodia affect fluorescent signals, The Journal of cell biology, Vol. 184(2), pp. 197-203.

Dexter, D.L. (1953). A theory of sensitized luminescence in solids, The Journal of chemical physics, Vol. 21(5), pp. 836-850.

Dickenson, N.E. & Picking, W.D. (2012). Förster resonance energy transfer (FRET) as a tool for dissecting the molecular mechanisms for maturation of the Shigella type III secretion needle tip complex, International Journal of Molecular Sciences, Vol. 13(11), pp. 15137-15161.

Ding, Y., Ai, H.-., Hoi, H. & Campbell, R.E. (2011). Förster resonance energy transfer-based biosensors for multiparameter ratiometric imaging of Ca 2+ dynamics and caspase-3 activity in single cells, Analytical Chemistry, Vol. 83(24), pp. 9687-9693.

Domingo, B., Sabariegos, R., Picazo, F. & Llopis, J. (2007). Imaging FRET standards by steady-state fluorescence and lifetime methods, Microscopy research and technique, Vol. 70(12), pp. 1010-1021.

Dopf, J. & Horiagon, T.M. (1996). Deletion mapping of the Aequorea victoria green fluorescent protein, Gene, Vol. 173(1), pp. 39-44.

Duncan, R.R., Bergmann, A., Cousin, M.A., Apps, D.K. & Shipston, M.J. (2004). Multi-dimensional time-correlated single photon counting (TCSPC) fluorescence lifetime imaging microscopy (FLIM) to detect FRET in cells, Journal of microscopy, Vol. 215(1), pp. 1-12.

Evdokimov, A.G., Pokross, M.E., Egorov, N.S., Zaraisky, A.G., Yampolsky, I.V., Merzlyak, E.M., Shkoporov, A.N., Sander, I., Lukyanov, K.A. & Chudakov, D.M. (2006). Structural basis for the fast maturation of Arthropoda green fluorescent protein, EMBO reports, Vol. 7(10), pp. 1006-1012.

Evers, T.H., Appelhof, M.A.M., de Graaf-Heuvelmans, P.T.H.M., Meijer, E.W. & Merkx, M. (2007). Ratiometric Detection of Zn(II) Using Chelating Fluorescent Protein Chimeras, Journal of Molecular Biology, Vol. 374(2), pp. 411-425.

Evers, T.H., Van Dongen, E.M.W.M., Faesen, A.C., Meijer, E.W. & Merkx, M. (2006). Quantitative understanding of the energy transfer between fluorescent proteins connected via flexible peptide linkers, Biochemistry, Vol. 45(44), pp. 13183-13192.

Fehr, M., Frommer, W.B. & Lalonde, S. (2002). Visualization of maltose uptake in living yeast cells by fluorescent nanosensors, Proceedings of the National Academy of Sciences, Vol. 99(15), pp. 9846-9851.

Fehr, M., Lalonde, S., Lager, I., Wolff, M.W. & Frommer, W.B. (2003). In Vivo Imaging of the Dynamics of Glucose Uptake in the Cytosol of COS-7 Cells by Fluorescent Nanosensors, Journal of Biological Chemistry, Vol. 278(21), pp. 19127-19133.

Fernández-Suárez, M. & Ting, A.Y. (2008). Fluorescent probes for super-resolution imaging in living cells, Nature Reviews Molecular Cell Biology, Vol. 9(12), pp. 929-943.

Förster, T. (2012). Energy migration and fluorescence, Journal of Biomedical Optics, Vol. 17(1), .

Forster, T. (1946). Energiewanderung und Fluoreszenz, Die Naturwissenschaften, Vol. 33(6), pp. 166-175.

Fron, E., Van Der Auweraer, M., Hofkens, J. & Dedecker, P. (2013). Excited state dynamics of photoswitchable fluorescent protein padron, Journal of Physical Chemistry B, Vol. 117(51), pp. 16422-16427.

Fyk-Kolodziej, B., Hellmer, C.B. & Ichinose, T. (2014). Marking cells with infrared fluorescent proteins to preserve photoresponsiveness in the retina, BioTechniques, Vol. 57(5), pp. 245-253.

Gather, M.C. & Yun, S.H. (2011). Single-cell biological lasers, Nature Photonics, Vol. 5(7), pp. 406-410.

Gavet, O. & Pines, J. (2010). Activation of cyclin B1–Cdk1 synchronizes events in the nucleus and the cytoplasm at mitosis, The Journal of cell biology, Vol. 189(2), pp. 247-259.

Genevieve Park, J., Qin, Y., Galati, D.F. & Palmer, A.E. (2012). New sensors for quantitative measurement of mitochondrial Zn 2+sup, ACS Chemical Biology, Vol. 7(10), pp. 1636-1640.

Giordano, L., Jovin, T.M., Irie, M. & Jares-Erijman, E.A. (2002). Diheteroarylethenes as thermally stable photoswitchable acceptors in photochromic fluorescence resonance energy transfer (pcFRET), Journal of the American Chemical Society, Vol. 124(25), pp. 7481-7489.

Goedhart, J., von Stetten, D., Noirclerc-Savoye, M., Lelimousin, M., Joosen, L., Hink, M.A., van Weeren, L., Gadella, T.W.J., & Royant, A. (2012). Structure-guided evolution of cyan fluorescent proteins towards a quantum yield of 93%, Nat Commun, Vol. 3pp. 751.

Gordon, G.W., Berry, G., Liang, X.H., Levine, B. & Herman, B. (1998). Quantitative Fluorescence Resonance Energy Transfer Measurements Using Fluorescence Microscopy, Biophysical journal, Vol. 74(5), pp. 2702-2713.

Graham, D.L., Lowe, P.N. & Chalk, P.A. (2001). A Method to Measure the Interaction of Rac/Cdc42 with Their Binding Partners Using Fluorescence Resonance Energy Transfer between Mutants of Green Fluorescent Protein, Analytical Biochemistry, Vol. 296(2), pp. 208-217.

Green, J. & Paget, M.S. (2004). Bacterial redox sensors, Nature reviews.Microbiology, Vol. 2(12), pp. 954-966.

Griesbeck, O., Baird, G.S., Campbell, R.E., Zacharias, D.A. & Tsien, R.Y. (2001). Reducing the environmental sensitivity of yellow fluorescent protein. Mechanism and applications, Journal of Biological Chemistry, Vol. 276(31), pp. 29188-29194.

Gu, H., Lalonde, S., Okumoto, S., Looger, L.L., Scharff-Poulsen, A.M., Grossman, A.R., Kossmann, J., Jakobsen, I. & Frommer, W.B. (2006). A novel analytical method for in vivo phosphate tracking, FEBS letters, Vol. 580(25), pp. 5885-5893.

Gu, Y., Di, W.L., Kelsell, D.P. & Zicha, D. (2004). Quantitative fluorescence resonance energy transfer (FRET) measurement with acceptor photobleaching and spectral unmixing, Journal of microscopy, Vol. 215(2), pp. 162-173.

Gurskaya, N.G., Fradkov, A.F., Pounkova, N.I., Staroverov, D.B., Bulina, M.E., Yanushevich, Y.G., Labas, Y.A., Lukyanov, S. & Lukyanov, K.A. (2003). A colourless green fluorescent protein homologue from the non-fluorescent hydromedusa Aequorea coerulescens and its fluorescent mutants, Biochemical Journal, Vol. 373(2), pp. 403-408.

Gurskaya, N.G., Verkhusha, V.V., Shcheglov, A.S., Staroverov, D.B., Chepurnykh, T.V., Fradkov, A.F., Lukyanov, S. & Lukyanov, K.A. (2006). Engineering of a monomeric green-to-red photoactivatable fluorescent protein induced by blue light, Nature biotechnology, Vol. 24(4), pp. 461-465.

Hägglöf, P., Bergström, F., Wilczynska, M., Johansson, L.B.-. & Ny, T. (2004). The reactive-center loop of active PAI-1 is folded close to the protein core and can be partially inserted, Journal of Molecular Biology, Vol. 335(3), pp. 823-832.

Hanson, G.T., Aggeler, R., Oglesbee, D., Cannon, M., Capaldi, R.A., Tsien, R.Y. & Remington, S.J. (2004). Investigating Mitochondrial Redox Potential with Redox-sensitive Green Fluorescent Protein Indicators, Journal of Biological Chemistry, Vol. 279(13), pp. 13044-13053.

Hanson, G.T., McAnaney, T.B., Park, E.S., Rendell, M.E.P., Yarbrough, D.K., Chu, S., Xi, L., Boxer, S.G., Montrose, M.H. & Remington, S.J. (2002). Green fluorescent protein variants as ratiometric dual emission ph sensors. 1. Structural characterization and preliminary application, Biochemistry, Vol. 41(52), pp. 15477-15488.

Hatahet, F., Nguyen, V.D., Salo, K. & Ruddock, L. (2010). Disruption of reducing pathways is not essential for efficient disulfide bond formation in the cytoplasm of E. coli, Microbial Cell Factories, Vol. 9(1), pp. 67.

Heikal, A.A., Hess, S.T., Baird, G.S., Tsien, R.Y. & Webb, W.W. (2000). Molecular spectroscopy and dynamics of intrinsically fluorescent proteins: Coral red (dsRed) and yellow (Citrine), Proceedings of the National Academy of Sciences of the United States of America, Vol. 97(22), pp. 11996-12001.

Heim, R., Cubitt, A.B. & Tsien, R.Y. (1995). Improved green fluorescence [4], Nature, Vol. 373(6516), pp. 663-664.

Heim, R., Prasher, D.C. & Tsien, R.Y. (1994). Wavelength mutations and posttranslational autoxidation of green fluorescent protein, Proceedings of the National Academy of Sciences of the United States of America, Vol. 91(26), pp. 12501-12504.

Hein, B., Willig, K.I. & Hell, S.W. (2008). Stimulated emission depletion (STED) nanoscopy of a fluorescent protein-labeled organelle inside a living cell, Proceedings of the National Academy of Sciences, Vol. 105(38), pp. 14271-14276.

Hell, S.W. & Wichmann, J. (1994). Breaking the diffraction resolution limit by stimulated emission: stimulated-emission-depletion fluorescence microscopy, Optics Letters, Vol. 19(11), pp. 780-782.

Hink, M.A., Visser, N.V., Borst, J.W., Van Hoek, A. & Visser, A.J.W.G. (2003). Practical Use of Corrected Fluorescence Excitation and Emission Spectra of Fluorescent Proteins in Förster Resonance Energy Transfer (FRET) Studies, Journal of Fluorescence, Vol. 13(2), pp. 185-188.

Ho, S.N., Hunt, H.D., Horton, R.M., Pullen, J.K. & Pease, L.R. (1989). Site-directed mutagenesis by overlap extension using the polymerase chain reaction, Gene, Vol. 77(1), pp. 51-59.

Hoff, B. & Kück, U. (2005). Use of bimolecular fluorescence complementation to demonstrate transcription factor interaction in nuclei of living cells from the filamentous fungus Acremonium chrysogenum, Current genetics, Vol. 47(2), pp. 132-138.

Hoi, H., Ding, Y. & Campbell, R.E. (2013). FRET with Fluorescent Proteins, in: Medintz, I.L. & Hildebrandt, N. (ed.), FRET - Förster Resonance Energy Transfer: From Theory to Applications, Wiley-VCH Verlag GmbH & Co. KGaA, pp. 431-473.

Hoppe, A., Christensen, K. & Swanson, J.A. (2002). Fluorescence Resonance Energy Transfer-Based Stoichiometry in Living Cells, Biophysical journal, Vol. 83(6), pp. 3652-3664.

Howarth, M., Takao, K., Hayashi, Y. & Ting, A.Y. (2005). Targeting quantum dots to surface proteins in living cells with biotin ligase, Proceedings of the National Academy of Sciences of the United States of America, Vol. 102(21), pp. 7583-7588.

Huang, B., Wang, W., Bates, M. & Zhuang, X. (2008). Three-Dimensional Super-Resolution Imaging by Stochastic Optical Reconstruction Microscopy, Science, Vol. 319(5864), pp. 810-813.

Hung, Y., Albeck, J., Tantama, M. & Yellen, G. (2011). Imaging Cytosolic NADH-NAD+ Redox State with a Genetically Encoded Fluorescent Biosensor, Cell Metabolism, Vol. 14(4), pp. 545-554.

Imamura, H., Huynh Nhat, K.P., Togawa, H., Saito, K., Iino, R., Kato-Yamada, Y., Nagai, T. & Noji, H. (2009). Visualization of ATP levels inside single living cells with fluorescence resonance energy transfer-based genetically encoded indicators, Proceedings of the National Academy of Sciences, Vol. 106(37), pp. 15651-15656.

Iqbal, A., Arslan, S., Okumus, B., Wilson, T.J., Giraud, G., Norman, D.G., Ha, T. & Lilley, D.M.J. (2008). Orientation dependence in fluorescent energy transfer between Cy3 and Cy5 terminally attached to double-stranded nucleic acids, Proceedings of the National Academy of Sciences of the United States of America, Vol. 105(32), pp. 11176-11181.

Ishikawa-Ankerhold, H.C., Ankerhold, R. & Drummen, G.P.C. (2012). Advanced fluorescence microscopy techniques-FRAP, FLIP, FLAP, FRET and FLIM, Molecules, Vol. 17(4), pp. 4047-4132.

Jäger, M., Michalet, X. & Weiss, S. (2005). Protein-protein interactions as a tool for site-specific labeling of proteins, Protein Science, Vol. 14(8), pp. 2059-2068.

Jäger, M., Nir, E. & Weiss, S. (2006). Site-specific labeling of proteins for single-molecule FRET by combining chemical and enzymatic modification, Protein Science, Vol. 15(3), pp. 640-646.

Janetopoulos, C., Jin, T. & Devreotes, P. (2001). Receptor-Mediated Activation of Heterotrimeric G-Proteins in Living Cells, Science, Vol. 291(5512), pp. 2408-2411.

Jares-Erijman, E.A. & Jovin, T.M. (2003). FRET imaging, Nature biotechnology, Vol. 21(11), pp. 1387-1395.

Jin, Z. & Hildebrandt, N. (2012). Semiconductor quantum dots for in vitro diagnostics and cellular imaging, Trends in biotechnology, Vol. 30(7), pp. 394-403.

Jung, J.,Hwan, Cheon, D.,Sung, Liu, F., Lee, K.,Bum & Seo, T.,Seok (2010). A Graphene Oxide Based Immuno-biosensor for Pathogen Detection, Angewandte Chemie International Edition, Vol. 49(33), pp. 5708-5711.

Kandhavelu, M., Lloyd-Price, J., Gupta, A., Muthukrishnan, A., Yli-Harja, O. & Ribeiro, A.S. (2012). Regulation of mean and noise of the in vivo kinetics of transcription under the control of the lac/ara-1 promoter, FEBS letters, Vol. 586(21), pp. 3870-3875.

Karasawa, S., Araki, T., Nagai, T., Mizuno, H. & Miyawaki, A. (2004). Cyan-emitting and orange-emitting fluorescent proteins as a donor/acceptor pair for fluorescence resonance energy transfer, Biochemical Journal, Vol. 381(1), pp. 307-312.

Karasawa, S., Araki, T., Yamamoto-Hino, M. & Miyawaki, A. (2003). A Green-emitting Fluorescent Protein from Galaxeidae Coral and Its Monomeric Version for Use in Fluorescent Labeling, Journal of Biological Chemistry, Vol. 278(36), pp. 34167-34171.

Karolin, J., Fa, M., Wilczynska, M., Ny, T. & Johansson, L.B.-. (1998). Donor-donor energy migration for determining intramolecular distances in proteins: I. Application of a model to the latent plasminogen activator inhibitor-1 (PAI-1), Biophysical journal, Vol. 74(1), pp. 11-21.

Kawai, Y., Sato, M. & Umezawa, Y. (2004). Single color fluorescent indicators of protein phosphorylation for multicolor imaging of intracellular signal flow dynamics, Analytical Chemistry, Vol. 76(20), pp. 6144-6149.

Kerppola, T.K. (2006). Design and implementation of bimolecular fluorescence complementation (BiFC) assays for the visualization of protein interactions in living cells, Nature Protocols, Vol. 1(3), pp. 1278-1286.

Kettling, U., Koltermann, A., Schwille, P. & Eigen, M. (1998). Real-time enzyme kinetics monitored by dual-color fluorescence cross-correlation spectroscopy, Proceedings of the National Academy of Sciences, Vol. 95(4), pp. 1416-1420.

Kim, S.A., Heinze, K.G., Waxham, M.N. & Schwille, P. (2004). Intracellular calmodulin availability accessed with two-photon cross-correlation, Proceedings of the National Academy of Sciences, Vol. 101(1), pp. 105-110.

Kim, S.A. & Schwille, P. (2003). Intracellular applications of fluorescence correlation spectroscopy: prospects for neuroscience, Current opinion in neurobiology, Vol. 13(5), pp. 583-590.

Klarenbeek, J.B., Goedhart, J., Hink, M.A., Gadella, T.W.J. & Jalink, K. (2011). A mTurquoise-based cAMP sensor for both FLIM and ratiometric read-out has improved dynamic range, PLoS ONE, Vol. 6(4), .

Kleemola, M., Toivonen, M., Mykkänen, J., Simell, O., Huoponen, K. & Heiskanen, K.M. (2007). Heterodimerization of y+LAT-1 and 4F2hc visualized by acceptor photobleaching FRET microscopy, Biochimica et Biophysica Acta (BBA) - Biomembranes, Vol. 1768(10), pp. 2345-2354.

Kneen, M., Farinas, J., Li, Y. & Verkman, A.S. (1998). Green fluorescent protein as a noninvasive intracellular pH indicator, Biophysical journal, Vol. 74(3), pp. 1591-1599.

Knöpfel, T., Tomita, K., Shimazaki, R. & Sakai, R. (2003). Optical recordings of membrane potential using genetically targeted voltage-sensitive fluorescent proteins, Methods, Vol. 30(1), pp. 42-48.

Kolossov, V.L., Spring, B.Q., Clegg, R.M., Henry, J.J., Sokolowski, A., Kenis, P.J.A. & Gaskins, H.R. (2011). Development of a high-dynamic range, GFP-based FRET probe sensitive to oxidative microenvironments, Experimental biology and medicine, Vol. 236(6), pp. 681-691.

Kolossov, V.L., Spring, B.Q., Sokolowski, A., Conour, J.E., Clegg, R.M., Kenis, P.J.A. & Gaskins, H.R. (2008). Engineering Redox-Sensitive Linkers for Genetically Encoded FRET-Based Biosensors, Experimental biology and medicine, Vol. 233(2), pp. 238-248.

Köster, M., Frahm, T. & Hauser, H. (2005). Nucleocytoplasmic shuttling revealed by FRAP and FLIP technologies, Current opinion in biotechnology, Vol. 16(1), pp. 28-34.

Krasel, C., Vilardaga, J.-., Bünemann, M. & Lohse, M.J. (2004). Kinetics of G-protein-coupled receptor signalling and desensitization, Biochemical Society transactions, Vol. 32(6), pp. 1029-1031.

Krebber, A., Bornhauser, S., Burmester, J., Honegger, A., Willuda, J., Bosshard, H.R. & Plückthun, A. (1997). Reliable cloning of functional antibody variable domains from hybridomas and spleen cell repertoires employing a reengineered phage display system, Journal of immunological methods, Vol. 201(1), pp. 35-55.

Kredel, S., Oswald, F., Nienhaus, K., Deuschle, K., Röcker, C., Wolff, M., Heilker, R., Nienhaus, G.U. & Wiedenmann, J. (2009). mRuby, a bright monomeric red fluorescent protein for labeling of subcellular structures, PLoS ONE, Vol. 4(2), .

Kremers, G.-., Goedhart, J., Van Den Heuvel, D.J., Gerritsen, H.C. & Gadella Jr., T.W.J. (2007). Improved green and blue fluorescent proteins for expression in bacteria and mammalian cells, Biochemistry, Vol. 46(12), pp. 3775-3783.

Kremers, G.-., Goedhart, J., Van Munster, E.B. & Gadella Jr., T.W.J. (2006). Cyan and yellow super fluorescent proteins with improved brightness, protein folding, and FRET förster radius, Biochemistry, Vol. 45(21), pp. 6570-6580.

Kukolka, F., Schoeps, O., Woggon, U. & Niemeyer, C.M. (2007). DNA-directed assembly of supramolecular fluorescent protein energy transfer systems, Bioconjugate chemistry, Vol. 18(3), pp. 621-627.

Kuner, T. & Augustine, G.J. (2000). A Genetically Encoded Ratiometric Indicator for Chloride: Capturing Chloride Transients in Cultured Hippocampal Neurons, Neuron, Vol. 27(3), pp. 447-459.

Kwon, Y., Coleman, M.A. & Camarero, J.A. (2006). Selective Immobilization of Proteins onto Solid Supports through Split-Intein-Mediated Protein Trans-Splicing, Angewandte Chemie International Edition, Vol. 45(11), pp. 1726-1729.

Lager, I., Fehr, M., Frommer, W.B. & Lalonde, S. (2003). Development of a fluorescent nanosensor for ribose, FEBS letters, Vol. 553(1–2), pp. 85-89.

Lakowicz, J.R. (1999). Energy Transfer, in: Principles of Fluorescence Spectroscopy, 2nd ed., Springer Science+Business Media, LLC, New York, USA, pp. 367-394.

Lakowicz, J.R. (2006a). Introduction to fluorescence, in: Principles of Fluorescence Spectroscopy, 3rd ed., Springer Science+Business Media, LLC, New York, USA, pp. 1.

Lakowicz, J.R. (2006b). Mechanisms and Dynamics of Fluorescence Quenching, in: Principles of Fluorescence Spectroscopy, 3rd ed., Springer Science+Business Media, LLC, New York, USA, pp. 331-351.

Lakowicz, J.R. (2006c). Time-domain lifetime measurements, in: Principles of Fluorescence Spectroscopy, 3rd ed., Springer Science+Business Media, LLC, New York, USA, pp. 97.

Leray, A., Riquet, F.B., Richard, E., Spriet, C., Trinel, D. & Héliot, L. (2009). Optimized protocol of a frequency domain fluorescence lifetime imaging microscope for FRET measurements, Microscopy research and technique, Vol. 72(5), pp. 371-379.

Lin, C., Kolossov, V.L., Tsvid, G., Trump, L., Henry, J.J., Henderson, J.L., Rund, L.A., Kenis, P.J., Schook, L.B., Gaskins, H.R. & Timp, G. (2011). Imaging in real-time with FRET the redox response of tumorigenic cells to glutathione perturbations in a microscale flow, Integrative biology : quantitative biosciences from nano to macro, Vol. 3(3), pp. 208-217.

Lin, M.Z., McKeown, M.R., Ng, H., Aguilera, T.A., Shaner, N.C., Campbell, R.E., Adams, S.R., Gross, L.A., Ma, W., Alber, T. & Tsien, R.Y. (2009). Autofluorescent Proteins with Excitation in the Optical Window for Intravital Imaging in Mammals, Chemistry & biology, Vol. 16(11), pp. 1169-1179.

Lin, P., Ueng, S., Tseng, M., Ko, J., Huang, K., Yu, S., Adak, A.K., Chen, Y. & Lin, C. (2006). Site-Specific Protein Modification through CuI-Catalyzed 1,2,3-Triazole Formation and Its Implementation in Protein Microarray Fabrication, Angewandte Chemie International Edition, Vol. 45(26), pp. 4286-4290.

Lindenburg, L.H., Vinkenborg, J.L., Oortwijn, J., Aper, S.J.A. & Merkx, M. (2013). MagFRET: The first genetically encoded fluorescent Mg2+ sensor, PLoS ONE, Vol. 8(12), .

Livet, J., Weissman, T.A., Kang, H., Draft, R.W., Lu, J., Bennis, R.A., Sanes, J.R. & Lichtman, J.W. (2007). Transgenic strategies for combinatorial expression of fluorescent proteins in the nervous system, Nature, Vol. 450(7166), pp. 56-62.

Lleres, D., Swift, S. & Lamond, A.I. (2007). Detecting protein-protein interactions in vivo with FRET using multiphoton fluorescence lifetime imaging microscopy (FLIM), Current protocols in cytometry / editorial board, J.Paul Robinson, managing editor ...[et al.], Vol. Chapter 12pp. Unit12.10.

Llopis, J., McCaffery, J.M., Miyawaki, A., Farquhar, M.G. & Tsien, R.Y. (1998). Measurement of cytosolic, mitochondrial, and Golgi pH in single living cells with green fluorescent proteins, Proceedings of the National Academy of Sciences of the United States of America, Vol. 95(12), pp. 6803-6808.

Llopis, J., Westin, S., Ricote, M., Wang, J., Cho, C.Y., Kurokawa, R., Mullen, T., Rose, D.W., Rosenfeld, M.G., Tsien, R.Y. & Glass, C.K. (2000). Ligand-dependent interactions of coactivators steroid receptor coactivator-1 and peroxisome proliferator-activated receptor binding protein with nuclear hormone receptors can be imaged in live cells and are required for transcription, Proceedings of the National Academy of Sciences, Vol. 97(8), pp. 4363-4368.

Loura, L.M.S. & Prieto, M. (2011). FRET in membrane biophysics: An overview, Frontiers in Physiology, Vol. 2 NOV.

Lundby, A., Mutoh, H., Dimitrov, D., Akemann, W. & Knöpfel, T. (2008). Engineering of a genetically encodable fluorescent voltage sensor exploiting fast Ci-VSP voltage-sensing movements, PLoS ONE, Vol. 3(6), .

Majoul, I., Straub, M., Hell, S.W., Duden, R. & Soeling, H. (2001). KDEL-Cargo Regulates Interactions between Proteins Involved in COPI Vesicle Traffic: Measurements in Living Cells Using FRET, Developmental Cell, Vol. 1(1), pp. 139-153.

Maniatis, T., Fritsch, E.F. & Sambrook, J. (1989). Molecular cloning: a laboratory manual, 2nd ed. Cold Spring Harbor Laboratory Press, Cold Spring Harbor, N.Y., .

Mank, M., Reiff, D.F., Heim, N., Friedrich, M.W., Borst, A. & Griesbeck, O. (2006). A FRET-based calcium biosensor with fast signal kinetics and high fluorescence change, Biophysical journal, Vol. 90(5), pp. 1790-1796.

Manley, S., Gillette, J.M., Patterson, G.H., Shroff, H., Hess, H.F., Betzig, E. & Lippincott-Schwartz, J. (2008). High-density mapping of single-molecule trajectories with photoactivated localization microscopy, Nature Methods, Vol. 5(2), pp. 155-157.

Markwardt, M.L., Kremers, G., Kraft, C.A., Ray, K., Cranfill, P.J.C., Wilson, K.A., Day, R.N., Wachter, R.M., Davidson, M.W. & Rizzo, M.A. (2011). An Improved Cerulean Fluorescent Protein with Enhanced Brightness and Reduced Reversible Photoswitching, PLoS ONE, Vol. 6(3), pp. e17896.

Marras, S.A., Kramer, F.R. & Tyagi, S. (2002). Efficiencies of fluorescence resonance energy transfer and contact-mediated quenching in oligonucleotide probes. Nucleic acids research, Vol. 30(21), .

Matz, M.V., Fradkov, A.F., Labas, Y.A., Savitsky, A.P., Zaraisky, A.G., Markelov, M.L. & Lukyanov, S.A. (1999). Fluorescent proteins from nonbioluminescent Anthozoa species, Nature biotechnology, Vol. 17(10), pp. 969-973.

McGinty, J., Dunsby, C., Auksorius, E., Benninger, R.K.P., De Beule, P., Elson, D.S., Galletly, N., Grant, D., Hofmann, O., Kennedy, G., Kumar, S., Lanigan, P.M.P., Manning, H., Munro, I., Önfelt, B., Owen, D., Requejo-Isidro, J., Suhling, K., Talbot, C.B., Soutter, P., Lever, M.J., deMello, A.J., Stamp, G.S., Neil, M.A.A. & French, P.M.W. (2009). Chapter 4 Multidimensional fluorescence imaging, Laboratory Techniques in Biochemistry and Molecular Biology, Vol. 33(0), pp. 133-169.

Meile, J.-., Wu, L.J., Ehrlich, S.D., Errington, J. & Noirot, P. (2006). Systematic localisation of proteins fused to the green fluorescent protein in Bacillus subtilis: Identification of new proteins at the DNA replication factory, Proteomics, Vol. 6(7), pp. 2135-2146.

Mena, M.A., Treynor, T.P., Mayo, S.L. & Daugherty, P.S. (2006). Blue fluorescent proteins with enhanced brightness and photostability from a structurally targeted library, Nature biotechnology, Vol. 24(12), pp. 1569-1571.

Merzlyak, E.M., Goedhart, J., Shcherbo, D., Bulina, M.E., Shcheglov, A.S., Fradkov, A.F., Gaintzeva, A., Lukyanov, K.A., Lukyanov, S., Gadella, T.W.J. & Chudakov, D.M. (2007). Bright monomeric red fluorescent protein with an extended fluorescence lifetime, Nature Methods, Vol. 4(7), pp. 555-557.

Mitra, R.D., Silva, C.M. & Youvan, D.C. (1996). Fluorescence resonance energy transfer between blue-emitting and red-shifted excitation derivatives of the green fluorescent protein, Gene, Vol. 173(1), pp. 13-17.

Miyawaki, A., Llopis, J., Heim, R., Michael McCaffery, J., Adams, J.A., Ikura, M. & Tsien, R.Y. (1997). Fluorescent indicators for Ca2+ based on green fluorescent proteins and calmodulin, Nature, Vol. 388(6645), pp. 882-887.

Morgner, F., Stufler, S., Geißler, D., Medintz, I.L., Algar, W.R., Susumu, K., Stewart, M.H., Blanco-Canosa, J.B., Dawson, P.E. & Hildebrandt, N. (2011). Terbium to quantum dot FRET bioconjugates for clinical diagnostics: Influence of human plasma on optical and assembly properties, Sensors, Vol. 11(10), pp. 9667-9684.

Morise, H., Shimomura, O., Johnson, F.H. & Winant, J. (1974). Intermolecular energy transfer in the bioluminescent system of Aequorea, Biochemistry, Vol. 13(12), pp. 2656-2662.

Morozova, K.S., Piatkevich, K.D., Gould, T.J., Zhang, J., Bewersdorf, J. & Verkhusha, V. (2010). Far-Red Fluorescent Protein Excitable with Red Lasers for Flow Cytometry and Superresolution STED Nanoscopy, Biophysical journal, Vol. 99(2), pp. L13-L15.

Müller, S.M., Galliardt, H., Schneider, J., George Barisas, B. & Seidel, T. (2013). Quantification of Förster resonance energy transfer by monitoring sensitized emission in living plant cells, Frontiers in Plant Science, Vol. 4(OCT), .

Nagai, T., Ibata, K., Park, E.S., Kubota, M., Mikoshiba, K. & Miyawaki, A. (2002). A variant of yellow fluorescent protein with fast and efficient maturation for cell-biological applications, Nature biotechnology, Vol. 20(1), pp. 87-90.

Nagai, T., Yamada, S., Tominaga, T., Ichikawa, M. & Miyawaki, A. (2004). Expanded dynamic range of fluorescent indicators for Ca2+ by circularly permuted yellow fluorescent proteins, Proceedings of the National Academy of Sciences of the United States of America, Vol. 101(29), pp. 10554-10559.

Nguyen, A.W. & Daugherty, P.S. (2005). Evolutionary optimization of fluorescent proteins for intracellular FRET, Nature biotechnology, Vol. 23(3), pp. 355-360.

Nikolaev, V.O., Gambaryan, S. & Lohse, M.J. (2006). Fluorescent sensors for rapid monitoring of intracellular cGMP, Nature Methods, Vol. 3(1), pp. 23-25.

Nitsche, A., Steuer, N., Schmidt, C.A., Landt, O. & Siegert, W. (1999). Different real-time PCR formats compared for the quantitative detection of human cytomegalovirus DNA, Clinical chemistry, Vol. 45(11), pp. 1932-1937.

O'Connor, D.V., Ware, W.R. & Andre, J.C. (1979). Deconvolution of fluorescence decay curves. A critical comparison of techniques, Journal of Physical Chemistry, Vol. 83(10), pp. 1333-1342.

Okumoto, S., Looger, L.L., Micheva, K.D., Reimer, R.J., Smith, S.J. & Frommer, W.B. (2005). Detection of glutamate release from neurons by genetically encoded surface-displayed FRET nanosensors, Proceedings of the National Academy of Sciences of the United States of America, Vol. 102(24), pp. 8740-8745.

Oliveira, A.F. & Yasuda, R. (2013). An Improved Ras Sensor for Highly Sensitive and Quantitative FRET-FLIM Imaging, PLoS ONE, Vol. 8(1), .

Olofsson, M., Kalinin, S., Zdunek, J., Oliveberg, M. & Johansson, L.B.-. (2006). Tryptophan-BODIPY: A versatile donor-acceptor pair for probing generic changes of intraprotein distances, Physical Chemistry Chemical Physics, Vol. 8(26), pp. 3130-3140.

Olsen, J.V., Ong, S. & Mann, M. (2004). Trypsin Cleaves Exclusively C-terminal to Arginine and Lysine Residues, Molecular & Cellular Proteomics, Vol. 3(6), pp. 608-614.

Ormö, M., Cubitt, A.B., Kallio, K., Gross, L.A., Tsien, R.Y. & Remington, S.J. (1996). Crystal structure of the Aequorea victoria green fluorescent protein, Science, Vol. 273(5280), pp. 1392-1395.

Patterson, G.H., Piston, D.W. & Barisas, B.G. (2000). Forster distances between green fluorescent protein pairs, Analytical Biochemistry, Vol. 284(2), pp. 438-440.

Pedelacq, J.D., Cabantous, S., Tran, T., Terwilliger, T.C. & Waldo, G.S. (2006). Engineering and characterization of a superfolder green fluorescent protein, Nature biotechnology, Vol. 24(1), pp. 79-88.

Pelet, S., Previte, M.J.R. & So, P.T.C. (2006). Comparing the quantification of Förster resonance energy transfer measurement accuracies based on intensity, spectral, and lifetime imaging, Journal of Biomedical Optics, Vol. 11(3), .

Pepperkok, R., Squire, A., Geley, S. & Bastiaens, P.I.H. (1999). Simultaneous detection of multiple green fluorescent proteins in live cells by fluorescence lifetime imaging microscopy, Current Biology, Vol. 9(5), pp. 269-272.

Phillips Jr., G.N. (1997). Structure and dynamics of green fluorescent protein, Current opinion in structural biology, Vol. 7(6), pp. 821-827.

Piston, D.W. & Kremers, G. (2007). Fluorescent protein FRET: the good, the bad and the ugly, Trends in biochemical sciences, Vol. 32(9), pp. 407-414.

Pletneva, N.V., Pletnev, V.Z., Souslova, E., Chudakov, D.M., Lukyanov, S., Martynov, V.I., Arhipova, S., Artemyev, I., Wlodawer, A., Dauter, Z. & Pletnev, S. (2013). Yellow fluorescent protein phiYFPv (Phialidium): Structure and structure-based mutagenesis, Acta Crystallographica Section D: Biological Crystallography, Vol. 69(6), pp. 1005-1012.

Pliss, A., Zhao, L., Ohulchanskyy, T.Y., Qu, J. & Prasad, P.N. (2012). Fluorescence lifetime of fluorescent proteins as an intracellular environment probe sensing the cell cycle progression, ACS chemical biology, Vol. 7(8), pp. 1385-1392.

Porcelli, A.M., Ghelli, A., Zanna, C., Pinton, P., Rizzuto, R. & Rugolo, M. (2005). pH difference across the outer mitochondrial membrane measured with a green fluorescent protein mutant, Biochemical and biophysical research communications, Vol. 326(4), pp. 799-804.

Prasher, D.C., Eckenrode, V.K., Ward, W.W., Prendergast, F.G. & Cormier, M.J. (1992). Primary structure of the Aequorea victoria green-fluorescent protein, Gene, Vol. 111(2), pp. 229-233.

Proudnikov, D. & Mirzabekov, A. (1996). Chemical Methods of DNA and RNA Fluorescent Labeling, Nucleic acids research, Vol. 24(22), pp. 4535-4542.

Reddy, D.V., Shenoy, B.C., Carey, P.R. & Sonnichsen, F.D. (2000). High resolution solution structure of the 1.3S subunit of transcarboxylase from Propionibacterium shermanii, Biochemistry, Vol. 39(10), pp. 2509-2516.

Reid, B.G. & Flynn, G.C. (1997). Chromophore formation in green fluorescent protein, Biochemistry, Vol. 36(22), pp. 6786-6791.

Reits, E.A.J. & Neefjes, J.J. (2001). From fixed to FRAP: Measuring protein mobility and activity in living cells, Nature cell biology, Vol. 3(6), pp. E145-E147.

Remus, T.P., Zima, A.V., Bossuyt, J., Bare, D.J., Martin, J.L., Blatter, L.A., Bers, D.M. & Mignery, G.A. (2006). Biosensors to Measure Inositol 1,4,5-Trisphosphate Concentration in Living Cells with Spatiotemporal Resolution, Journal of Biological Chemistry, Vol. 281(1), pp. 608-616.

Rizvi, S., Ghaderi, S., Keshtgar, M. & Seifalian, A. (2010). Semiconductor quantum dots as fluorescent probes for in vitro and in vivo bio-molecular and cellular imaging, Nano Reviews, Vol. 1(0), .

Rizzo, M.A., Springer, G.H., Granada, B. & Piston, D.W. (2004). An improved cyan fluorescent protein variant useful for FRET, Nature biotechnology, Vol. 22(4), pp. 445-449.

Robin, E., Guzy, R.D., Loor, G., Iwase, H., Waypa, G.B., Marks, J.D., Hoek, T.L.V. & Schumacker, P.T. (2007). Oxidant Stress during Simulated Ischemia Primes Cardiomyocytes for Cell Death during Reperfusion, Journal of Biological Chemistry, Vol. 282(26), pp. 19133-19143.

Rosenow, M.A., Huffman, H.A., Phail, M.E. & Wachter, R.M. (2004). The Crystal Structure of the Y66L Variant of Green Fluorescent Protein Supports a Cyclization-Oxidation-Dehydration Mechanism for Chromophore Maturation, Biochemistry, Vol. 43(15), pp. 4464-4472.

Roy, R., Hohng, S. & Ha, T. (2008). A practical guide to single-molecule FRET, Nature Methods, Vol. 5(6), pp. 507-516.

Sakai, R., Repunte-Canonigo, V., Raj, C.D. & Knöpfel, T. (2001). Design and characterization of a DNA-encoded, voltage-sensitive fluorescent protein, European Journal of Neuroscience, Vol. 13(12), pp. 2314-2318.

Santala, V. & Lamminmäki, U. (2004). Production of a biotinylated single-chain antibody fragment in the cytoplasm of Escherichia coli, Journal of immunological methods, Vol. 284(1-2), pp. 165-175.

Sarkar, P., Koushik, S.V., Vogel, S.S., Gryczynski, I. & Gryczynski, Z. (2009). Photophysical properties of Cerulean and Venus fluorescent proteins, Journal of Biomedical Optics, Vol. 14(3), pp. 034047.

Sarkisyan, K.S., Yampolsky, I.V., Solntsev, K.M., Lukyanov, S.A., Lukyanov, K.A. & Mishin, A.S. (2012). Tryptophan-based chromophore in fluorescent proteins can be anionic, Scientific reports, Vol. 2pp. 608.

Schneider, C.A., Rasband, W.S. & Eliceiri, K.W. (2012). NIH Image to ImageJ: 25 years of image analysis, Nature Methods, Vol. 9(7), pp. 671-675.

Schuler, B. (2013). Single-molecule FRET of protein structure and dynamics - a primer. Journal of nanobiotechnology, Vol. 11 Suppl 1.

Schwarzländer, M., Logan, D.C., Fricker, M.D. & Sweetlove, L.J. (2011). The circularly permuted yellow fluorescent protein cpYFP that has been used as a superoxide probe is highly responsive to pH but not superoxide in mitochondria: Implications for the existence of superoxide 'flashes', Biochemical Journal, Vol. 437(3), pp. 381-387.

Sekar, R.B. & Periasamy, A. (2003a). Fluorescence resonance energy transfer (FRET) microscopy imaging of live cell protein localizations, Journal of Cell Biology, Vol. 160(5), pp. 629-633.

Sekar, R.B. & Periasamy, A. (2003b). Fluorescence resonance energy transfer (FRET) microscopy imaging of live cell protein localizations, The Journal of cell biology, Vol. 160(5), pp. 629-633.

Shagin, D.A., Barsova, E.V., Yanushevich, Y.G., Fradkov, A.F., Lukyanov, K.A., Labas, Y.A., Semenova, T.N., Ugalde, J.A., Meyers, A., Nunez, J.M., Widder, E.A., Lukyanov, S.A. & Matz, M.V.

(2004). GFP-like Proteins as Ubiquitous Metazoan Superfamily: Evolution of Functional Features and Structural Complexity, Molecular biology and evolution, Vol. 21(5), pp. 841-850.

Shaner, N.C., Campbell, R.E., Steinbach, P.A., Giepmans, B.N., Palmer, A.E. & Tsien, R.Y. (2004). Improved monomeric red, orange and yellow fluorescent proteins derived from Discosoma sp. red fluorescent protein, Nature biotechnology, Vol. 22(12), pp. 1567-1572.

Shaner, N.C., Lin, M.Z., McKeown, M.R., Steinbach, P.A., Hazelwood, K.L., Davidson, M.W. & Tsien, R.Y. (2008). Improving the photostability of bright monomeric orange and red fluorescent proteins, Nature Methods, Vol. 5(6), pp. 545-551.

Shaner, N.C., Steinbach, P.A. & Tsien, R.Y. (2005). A guide to choosing fluorescent proteins, Nature Methods, Vol. 2(12), pp. 905-909.

Shcherbakova, D.M. & Verkhusha, V.V. (2013). Near-infrared fluorescent proteins for multicolor in vivo imaging, Nature Methods, Vol. 10(8), pp. 751-754.

Shcherbakova, D.M., Subach, O.M. & Verkhusha, V.V. (2012). Red Fluorescent Proteins: Advanced Imaging Applications and Future Design, Angewandte Chemie International Edition, Vol. 51(43), pp. 10724-10738.

Shcherbo, D., Merzlyak, E.M., Chepurnykh, T.V., Fradkov, A.F., Ermakova, G.V., Solovieva, E.A., Lukyanov, K.A., Bogdanova, E.A., Zaraisky, A.G., Lukyanov, S. & Chudakov, D.M. (2007). Bright far-red fluorescent protein for whole-body imaging, Nature Methods, Vol. 4(9), pp. 741-746.

Shcherbo, D., Murphy, C.S., Ermakova, G.V., Solovieva, E.A., Chepurnykh, T.V., Shcheglov, A.S., Verkhusha, V.V., Pletnev, V.Z., Hazelwood, K.L., Roche, P.M., Lukyanov, S., Zaraisky, A.G., Davidson, M.W. & Chudakov, D.M. (2009). Far-red fluorescent tags for protein imaging in living tissues, Biochemical Journal, Vol. 418(3), pp. 567-574.

Shcherbo, D., Shemiakina, I.I., Ryabova, A.V., Luker, K.E., Schmidt, B.T., Souslova, E.A., Gorodnicheva, T.V., Strukova, L., Shidlovskiy, K.M., Britanova, O.V., Zaraisky, A.G., Lukyanov, K.A., Loschenov, V.B., Luker, G.D. & Chudakov, D.M. (2010). Near-infrared fluorescent proteins, Nature methods, Vol. 7(10), pp. 827-829.

Shcherbo, D., Souslova, E., Goedhart, J., Chepurnykh, T., Gaintzeva, A., Shemiakina, I., Gadella, T., Lukyanov, S. & Chudakov, D. (2009). Practical and reliable FRET/FLIM pair of fluorescent proteins, BMC Biotechnology, Vol. 9(1), pp. 24.

Shi, X., Abbyad, P., Shu, X., Kallio, K., Kanchanawong, P., Childs, W., Remington, S.J. & Boxer, S.G. (2007a). Ultrafast excited-state dynamics in the green fluorescent protein variant S65T/H148D. 2. Unusual photophysical properties, Biochemistry, Vol. 46(43), pp. 12014-12025.

Shi, X., Basran, J., Seward, H.E., Childs, W., Bagshaw, C.R. & Boxer, S.G. (2007b). Anomalous negative fluorescence anisotropy in Yellow Fluorescent Protein (YFP 10C): Quantitative analysis of FRET in YFP dimers, Biochemistry, Vol. 46(50), pp. 14403-14417.

Shigeto, H., Ikeda, T., Kuroda, A. & Funabashi, H. (2015). A BRET-Based Homogeneous Insulin Assay Using Interacting Domains in the Primary Binding Site of the Insulin Receptor, Analytical Chemistry, .

Shih, W.M., Gryczynski, Z., Lakowicz, J.R. & Spudich, J.A. (2000). A FRET-Based Sensor Reveals Large ATP Hydrolysis–Induced Conformational Changes and Three Distinct States of the Molecular Motor Myosin, Cell, Vol. 102(5), pp. 683-694.

Shimomura, O. (1979). Structure of the chromophore of Aequorea green fluorescent protein, FEBS letters, Vol. 104(2), pp. 220-222.

Shimomura, O., Johnson, F.H. & Saiga, Y. (1962). Extraction, Purification and Properties of Aequorin, a Bioluminescent Protein from the Luminous Hydromedusan, Aequorea, Journal of Cellular and Comparative Physiology, Vol. 59(3), pp. 223-239.

Shimozono, S., Iimura, T., Kitaguchi, T., Higashijima, S.-. & Miyawaki, A. (2013). Visualization of an endogenous retinoic acid gradient across embryonic development, Nature, Vol. 496(7445), pp. 363-366.

Shu, X., Royant, A., Lin, M.Z., Aguilera, T.A., Lev-Ram, V., Steinbach, P.A. & Tsien, R.Y. (2009). Mammalian Expression of Infrared Fluorescent Proteins Engineered from a Bacterial Phytochrome, Science, Vol. 324(5928), pp. 804-807.

Sprague, B.L. & McNally, J.G. (2005). FRAP analysis of binding: proper and fitting, Trends in cell biology, Vol. 15(2), pp. 84-91.

Sridharan, R., Zuber, J., Connelly, S.M., Mathew, E. & Dumont, M.E. (2014). Fluorescent approaches for understanding interactions of ligands with G protein coupled receptors, Biochimica et Biophysica Acta - Biomembranes, Vol. 1838(1 PARTA), pp. 15-33.

Stepanenko, O.V., Stepanenko, O.V., Shcherbakova, D.M., Kuznetsova, I.M., Turoverov, K.K. & Verkhusha, V.V. (2011). Modern fluorescent proteins: From chromophore formation to novel intracellular applications, BioTechniques, Vol. 51(5), pp. 313-327.

Strack, R.L., Hein, B., Bhattacharyya, D., Hell, S.W., Keenan, R.J. & Glick, B.S. (2009). A rapidly maturing far-red derivative of DsRed-Express2 for whole-cell labeling, Biochemistry, Vol. 48(35), pp. 8279-8281.

Subach, F.V., Subach, O.M., Gundorov, I.S., Morozova, K.S., Piatkevich, K.D., Cuervo, A.M. & Verkhusha, V.V. (2009). Monomeric fluorescent timers that change color from blue to red report on cellular trafficking, Nature Chemical Biology, Vol. 5(2), pp. 118-126.

Subach, O.M., Gundorov, I.S., Yoshimura, M., Subach, F.V., Zhang, J., Grüenwald, D., Souslova, E.A., Chudakov, D.M. & Verkhusha, V.V. (2008). Conversion of Red Fluorescent Protein into a Bright Blue Probe, Chemistry and Biology, Vol. 15(10), pp. 1116-1124.

Suhling, K., French, P.M.W. & Phillips, D. (2005). Time-resolved fluorescence microscopy, Photochemical and Photobiological Sciences, Vol. 4(1), pp. 13-22.

Suhling, K. (2014). Photophysics of fluorescence, in: Marcu, L., French, P.M.W. & Elson, D.S. (ed.), Fluorescence Lifetime Spectroscopy and Imaging- Principles and Applications in Biomedical Diagnostics, CRC Press, pp. Chapter 2, 23-46.

Sun, Y., Day, R.N. & Periasamy, A. (2011a). Investigating protein-protein interactions in living cells using fluorescence lifetime imaging microscopy, Nature Protocols, Vol. 6(9), pp. 1324-1340.

Sun, Y., Wallrabe, H., Seo, S.-. & Periasamy, A. (2011b). FRET microscopy in 2010: The legacy of Theodor Förster on the 100th anniversary of his birth, ChemPhysChem, Vol. 12(3), pp. 462-474.

Terskikh, A., Fradkov, A., Ermakova, G., Zaraisky, A., Tan, P., Kajava, A.V., Zhao, X., Lukyanov, S., Matz, M., Kim, S., Weissman, I. & Siebert, P. (2000). "Fluorescent Timer": Protein That Changes Color with Time, Science, Vol. 290(5496), pp. 1585-1588.

Thaler, C., Koushik, S.V., Blank, P.S. & Vogel, S.S. (2005). Quantitative multiphoton spectral imaging and its use for measuring resonance energy transfer, Biophysical journal, Vol. 89(4), pp. 2736-2749.

Tian, L., Hires, S.A., Mao, T., Huber, D., Chiappe, M.E., Chalasani, S.H., Petreanu, L., Akerboom, J., McKinney, S.A., Schreiter, E.R., Bargmann, C.I., Jayaraman, V., Svoboda, K. & Looger, L.L. (2009). Imaging neural activity in worms, flies and mice with improved GCaMP calcium indicators, Nature Methods, Vol. 6(12), pp. 875-881.

Tkachenko, N. & Lemmetyinen, H. (2008). Time-Resolved Fluorometry: Typical Methods, Challenges, Applications and Standards, in: Resch-Genger, U. (ed.), Springer Berlin Heidelberg, pp. 195-214.

Tomosugi, W., Matsuda, T., Tani, T., Nemoto, T., Kotera, I., Saito, K., Horikawa, K. & Nagai, T. (2009). An ultramarine fluorescent protein with increased photostability and pH insensitivity, Nature Methods, Vol. 6(5), pp. 351-353.

Topell, S., Hennecke, J. & Glockshuber, R. (1999). Circularly permuted variants of the green fluorescent protein, FEBS letters, Vol. 457(2), pp. 283-289.

Tramier, M., Sanvitto, D., Emiliani, V., Durieux, C. & Coppey-Moisan, M. (2005). FRET and fluorescence lifetime imaging microscopy, in: Goldman, R.D. & Spector, D.L. (ed.), Live Cell Imaging: A Laboratory Manual**.**, 1st ed., Cold Spring Harbor Press, Cold Spring Harbor, New York, pp. 127.

Truong, K., Sawano, A., Mizuno, H., Hama, H., Tong, K.I., Mal, T.K., Miyawaki, A. & Ikura, M. (2001). FRET-based in vivo Ca2+ imaging by a new calmodulin-GFP fusion molecule, Nature structural biology, Vol. 8(12), pp. 1069-1073.

Tsien, R.Y. (1998). The green fluorescent protein, Annual Review of Biochemistry, Vol. 67pp. 509-544.

Tsutsui, H., Karasawa, S., Okamura, Y. & Miyawaki, A. (2008). Improving membrane voltage measurements using FRET with new fluorescent proteins, Nature Methods, Vol. 5(8), pp. 683-685.

van der Meer, B.W., van der Meer, D.M. & Vogel, S.S. (2013). Optimizing the Orientation Factor Kappa-Squared for More Accurate FRET Measurements, in: FRET ? Förster Resonance Energy Transfer, Wiley-VCH Verlag GmbH & Co. KGaA, pp. 63-104.

Van Dongen, E.M.W.M., Evers, T.H., Dekkers, L.M., Meijer, E.W., Klomp, L.W.J. & Merkx, M. (2007). Variation of linker length in ratiometric fluorescent sensor proteins allows rational tuning of Zn(II) affinity in the picomolar to femtomolar range, Journal of the American Chemical Society, Vol. 129(12), pp. 3494-3495.

Van Munster, E.B., Kremers, G.J., Adjobo-Hermans, M.J.W. & Gadella, T.W.J. (2005). Fluorescence resonance energy transfer (FRET) measurement by gradual acceptor photobleaching, Journal of microscopy, Vol. 218(3), pp. 253-262.

van Rheenen, J., Langeslag, M. & Jalink, K. (2004). Correcting Confocal Acquisition to Optimize Imaging of Fluorescence Resonance Energy Transfer by Sensitized Emission, Biophysical journal, Vol. 86(4), pp. 2517-2529.

van, d.K., Ogink, J., Ponsioen, B. & Jalink, K. (2008). A Comparison of Donor-Acceptor Pairs for Genetically Encoded FRET Sensors: Application to the Epac cAMP Sensor as an Example, PLoS ONE, Vol. 3(4), pp. e1916.

VanEngelenburg, S.B. & Palmer, A.E. (2008). Fluorescent biosensors of protein function, Current opinion in chemical biology, Vol. 12(1), pp. 60-65.

Veetil, J.V., Jin, S. & Ye, K. (2012). Fluorescence lifetime imaging microscopy of intracellular glucose dynamics, Journal of Diabetes Science and Technology, Vol. 6(6), pp. 1276-1285.

Verkhusha, V.V. & Sorkin, A. (2005). Conversion of the Monomeric Red Fluorescent Protein into a Photoactivatable Probe, Chemistry & biology, Vol. 12(3), pp. 279-285.

Veselov, A.A., Abraham, B.G., Lemmetyinen, H., Karp, M.T. & Tkachenko, N.V. (2012). Photochemical properties and sensor applications of modified yellow fluorescent protein (YFP) covalently attached to the surfaces of etched optical fibers (EOFs), Analytical and bioanalytical chemistry, Vol. 402(3), pp. 1149-1158.

Vinkenborg, J.L., Evers, T.H., Reulen, S.W.A., Meijer, E.W. & Merkx, M. (2007). Enhanced sensitivity of FRET-based protease sensors by redesign of the GFP dimerization interface, ChemBioChem, Vol. 8(10), pp. 1119-1121.

Vo-Dinh, T., Kasili, P. & Wabuyele, M. (2006). Nanoprobes and nanobiosensors for monitoring and imaging individual living cells, Nanomedicine: Nanotechnology, Biology and Medicine, Vol. 2(1), pp. 22-30.

Vogel, S.S., van der Meer, B.W. & Blank, P.S. (2014). Estimating the distance separating fluorescent protein FRET pairs, Methods, Vol. 66(2), pp. 131-138.

Wachter, R.M., Elsliger, M.A., Kallio, K., Hanson, G.T. & Remington, S.J. (1998). Structural basis of spectral shifts in the yellow-emission variants of green fluorescent protein, Structure (London, England : 1993), Vol. 6(10), pp. 1267-1277.

Wallrabe, H. & Periasamy, A. (2005). Imaging protein molecules using FRET and FLIM microscopy, Current opinion in biotechnology, Vol. 16(1), pp. 19-27.

Wang, L., Jackson, W.C., Steinbach, P.A. & Tsien, R.Y. (2004). Evolution of new nonantibody proteins via iterative somatic hypermutation, Proceedings of the National Academy of Sciences of the United States of America, Vol. 101(48), pp. 16745-16749.

Weissman, T.A. & Pan, Y.A. (2015). Brainbow: New Resources and Emerging Biological Applications for Multicolor Genetic Labeling and Analysis, Genetics, Vol. 199(2), pp. 293-306.

Wlodarczyk, J., Woehler, A., Kobe, F., Ponimaskin, E., Zeug, A. & Neher, E. (2008). Analysis of FRET signals in the presence of free donors and acceptors, Biophysical journal, Vol. 94(3), pp. 986-1000.

Wong, F.H., Banks, D.S., Abu-Arish, A. & Fradin, C. (2007). A molecular thermometer based on fluorescent protein blinking, Journal of the American Chemical Society, Vol. 129(34), pp. 10302-10303.

Wong, L.S., Khan, F. & Micklefield, J. (2009). Selective covalent protein immobilization: Strategies and applications, Chemical reviews, Vol. 109(9), pp. 4025-4053.

Wouters, F.S., Bastiaens, P.I.H., Wirtz, K.W.A. & Jovin, T.M. (1998). FRET microscopy demonstrates molecular association of non-specific lipid transfer protein (nsL-TP) with fatty acid oxidation enzymes in peroxisomes, EMBO Journal, Vol. 17(24), pp. 7179-7189.

Wu, B., Piatkevich, K.D., Lionnet, T., Singer, R.H. & Verkhusha, V.V. (2011). Modern fluorescent proteins and imaging technologies to study gene expression, nuclear localization, and dynamics, Current opinion in cell biology, Vol. 23(3), pp. 310-317.

Wüstner, D., Solanko, L.M., Lund, F.W., Sage, D., Schroll, H.J. & Lomholt, M.A. (2012). Quantitative fluorescence loss in photobleaching for analysis of protein transport and aggregation, BMC Bioinformatics, Vol. 13(1), .

Xia, N.-., Luo, W.-., Zhang, J., Xie, X.-., Yang, H.-., Li, S.-., Chen, M. & Ng, M.-. (2002). Bioluminescence of Aequorea macrodactyla, a common jellyfish species in the East China Sea, Marine Biotechnology, Vol. 4(2), pp. 155-162.

Xiong, S., Wang, Y.F., Ren, X.R., Li, B., Zhang, M.Y., Luo, Y., Zhang, L., Xie, Q.L. & Su, K.Y. (2005). Solubility of disulfide-bonded proteins in the cytoplasm of Escherichia coli and its "oxidizing" mutant, World journal of gastroenterology : WJG, Vol. 11(7), pp. 1077-1082.

Yan, Y. & Marriott, G. (2003). Analysis of protein interactions using fluorescence technologies, Current opinion in chemical biology, Vol. 7(5), pp. 635-640.

Yang, F., Moss, L.G. & Phillips, G.N.,Jr (1996a). The molecular structure of green fluorescent protein, Nature biotechnology, Vol. 14(10), pp. 1246-1251.

Yang, T., Cheng, L. & Kain, S.R. (1996b). Optimized Codon Usage and Chromophore Mutations Provide Enhanced Sensitivity with the Green Fluorescent Protein, Nucleic acids research, Vol. 24(22), pp. 4592-4593.

Yang, T., Sinai, P., Green, G., Kitts, P.A., Chen, Y., Lybarger, L., Chervenak, R., Patterson, G.H., Piston, D.W. & Kain, S.R. (1998). Improved Fluorescence and Dual Color Detection with Enhanced Blue and Green Variants of the Green Fluorescent Protein, Journal of Biological Chemistry, Vol. 273(14), pp. 8212-8216.

Yano, T., Oku, M., Akeyama, N., Itoyama, A., Yurimoto, H., Kuge, S., Fujiki, Y. & Sakai, Y. (2010). A novel fluorescent sensor protein for visualization of redox states in the cytoplasm and in peroxisomes, Molecular and cellular biology, Vol. 30(15), pp. 3758-3766.

Zacharias, D.A., Violin, J.D., Newton, A.C. & Tsien, R.Y. (2002). Partitioning of lipid-modified monomeric GFPs into membrane microdomains of live cells, Science, Vol. 296(5569), pp. 913-916.

Zal, T. & Gascoigne, N.R.J. (2004). Photobleaching-Corrected FRET Efficiency Imaging of Live Cells, Biophysical journal, Vol. 86(6), pp. 3923-3939.

Zapata-Hommer, O. & Griesbeck, O. (2003). Efficiently folding and circularly permuted variants of the Sapphire mutant of GFP, BMC Biotechnology, Vol. 3.

Zhang, J., Campbell, R.E., Ting, A.Y. & Tsien, R.Y. (2002). Creating new fluorescent probes for cell biology, Nature Reviews Molecular Cell Biology, Vol. 3(12), pp. 906-918.

Zhang, L., Patel, H.N., Lappe, J.W. & Wachter, R.M. (2006). Reaction progress of chromophore biogenesis in green fluorescent protein, Journal of the American Chemical Society, Vol. 128(14), pp. 4766-4772.

Zilian, E. & Maiss, E. (2011). An optimized mRFP-based bimolecular fluorescence complementation system for the detection of protein-protein interactions in planta, Journal of virological methods, Vol. 174(1-2), pp. 158-165.

Zou, J., Hofer, A.M., Lurtz, M.M., Gadda, G., Ellis, A.L., Chen, N., Huang, Y., Holder, A., Ye, Y., Louis, C.F., Welshhans, K., Rehder, V. & Yang, J.J. (2007). Developing sensors for real-time measurement of high Ca2+ concentrations, Biochemistry, Vol. 46(43), pp. 12275-12288.

I

BIDIRECTIONAL FLUORESCENCE RESONANCE ENERGY TRANSFER (FRET) IN MUTATED AND CHEMICALLY MODIFIED YELLOW FLUORESCENT PROTEIN (YFP)

by

Bobin George Abraham, Nikolai V. Tkachenko, Ville Santala, Helge Lemmetyinen, and Matti Karp (2011)

Bioconjugate Chemistry, 22 (2), pp 227–234

II

PHOTOCHEMICAL PROPERTIES AND SENSOR APPLICATIONS OF MODIFIED YELLOW FLUORESCENT PROTEIN (YFP) COVALENTLY ATTACHED TO THE SURFACES OF ETCHED OPTICAL FIBERS (EOFS)

by

Alexey A. Veselov*, Bobin George Abraham*, Helge Lemmetyinen, Matti Karp and Nikolai V. Tkachenko (2012)

* - Equal contribution

Analytical and Bioanalytical Chemistry, 402 (3), pp 1149–1158

III

FLUORESCENT PROTEIN-BASED FRET SENSOR FOR INTRACELLULAR MONITORING OF REDOX STATUS IN BACTERIA AT SINGLE CELL LEVEL

by

Bobin George Abraham, Ville Santala, Nikolai V. Tkachenko and Matti Karp
(2014)

Analytical and Bioanalytical Chemistry, 406 (28), pp 7195-7204

IV

FLUORESCENT PROTEIN BASED FRET PAIRS WITH IMPROVED DYNAMIC RANGE FOR FLUORESCENCE LIFETIME MEASUREMENTS

by

Bobin George Abraham, Karen S. Sarkisyan, Alexander S. Mishin, Ville Santala, Nikolai V. Tkachenko and Matti Karp (2015)

PLOS ONE, 2015; 10(8): e0134436.

Tampereen teknillinen yliopisto
PL 527
33101 Tampere

Tampere University of Technology
P.O.B. 527
FI-33101 Tampere, Finland

ISBN 978-952-15-3635-9
ISSN 1459-2045